The delay interval of electric breakdown in gases

by
Keith Lawrence Wilson

1957

University of London, Northern Polytechnic

THE DELAY INTERVAL OF ELECTRICAL BREAKDOWN IN GASES.

ABSTRACT

A survey is given of the time required, and the physical processes which occur, during the delay interval between the application across two cold electrodes of a uniform electric field of sufficient magnitude to produce breakdown and the actual instant of breakdown.

The ionisation processes are described in terms of the first and second Townsend ionisation coefficients and the Townsend breakdown criterion derived. Experimental techniques are reviewed for study of the initial electron avalanche.

The statistical time lag is defined, experimental techniques for its study described, and a review given of the effect of various experimental conditions on the value measured. The theory of statistical time lag is given in detail for the case of secondary emission from the cathode and shown to agree well with experiment.

Measurements of formative time lag at a pressure of a few millimetres of mercury are explained by secondary ionisation at the cathode due to positive ion impact. A survey of early measurements of formative time lag in air at atmospheric pressure is discussed together with additional evidence and shown to indicate that the low pressure mechanism does not apply at high pressure. The reasons for the

proposal of an alternative "Streamer" mechanism are then reviewed and the Streamer theory described and compared with experiment.

Subsequent experimental investigations, described in detail, are shown to conflict with the Streamer theory and support the Townsend theory of secondary ionisation at the cathode due to positive ion and photon impact.

Finally, the two theories are reconciled by the proposal that although the magnitude of the delay interval may be calculated on the basis of the Townsend theory, the filamentary spark which occurs in some cases is explained by a transition of the current build-up process to the Streamer mechanism in the final stage of the delay interval.

CONTENTS

A. INTRODUCTION.

A.1. Definition of Electrical Breakdown and Delay Interval.

A.1.1. Electrical breakdown of a gas is an irreversible transient process, which marks the transition from one stable state to another more stable state under an applied potential difference.

A.1.2. In the initial stable state, which exists before breakdown, the current is usually within the range 10^{-20} Amp to 10^{-10} Amp, and is due to the transport of a comparatively small number of electrons and ionised atoms or molecules existing within the gap, probably by the action of cosmic radiation. This current will be referred to as the priming current i_o.

A.1.3. In the final stable state, the current has increased by several orders of magnitude, and is independent of the original source of ionised particles. The actual value of the current is limited by the impedance of the external circuit, and has a stable value such that the sum of the potential differences across the external resistance and discharge gap is equal to the applied emf.

A.1.4. The potential difference across the electrodes below which this transition cannot occur is herein referred to as the breakdown voltage.

A.1.5. Breakdown does not occur as soon as the breakdown voltage is applied. The time interval which elapses between the instant of application of the breakdown voltage and the occurrence of breakdown is referred to in the title as the "delay interval".

A.1.6. The magnitude or duration of the delay interval is defined as the "time lag". The expression "delay interval" was chosen since it is intended to discuss, in addition to this duration, the physical processes which occur between the application of the breakdown voltage and the occurrence of breakdown. This is necessary in order to assess theoretically the reasons for the varied values of time lag obtained by different investigators under different conditions of electrode geometry and gas pressure.

A.1.7. The time zero of the time lag is defined as the instant when the applied voltage becomes equal to the breakdown voltage.

A.1.8. The end of the time lag, i.e. the instant of breakdown, has been defined in different ways by different investigators in accordance with the technique of measurement which has been used by them. The principal definitions which have been used are:-

(a) The instant when the applied voltage across the gap starts to fall to the value characteristic of the second stable state.

(b) The instant when the current flowing across the inter-electrode gap reaches a certain value which is always many orders of magnitude greater than the priming current.

(c) The instant when intense light is emitted from the inter-electrode gap.

A.1.9. Fortunately, the value of time delay obtained is virtually the same, whichever definition is used, but care will be taken to point out any differences in definition when comparison is made between the results

obtained by different investigators.

A.2. Outline of the Physical Processes which produce Breakdown.

A.2.1. Electrical breakdown of the gas between the electrodes involves a rapid increase in the number of charged particles (electrons and positive ions) in that region. It is the rate at which these are produced which determines the time lag.

A.2.2. This process is briefly as follows:-

During the first stage, external ionising agents such as cosmic rays produce electrons which move towards the anode, and positive ions which move towards the cathode, under the action of an applied voltage between the electrodes. If the applied voltage is increased, both electrons and positive ions are accelerated, and at a certain value of applied voltage, the electrons receive sufficient energy in each free path from the applied field to ionise neutral gas atoms or molecules by collision. The current between the electrodes is increased, but nevertheless would be reduced to zero if the source of primary ionisation were removed.

A.2.3. This is often called the "first ionisation process". Since the electron density increases with distance from the cathode owing to ionisation, the distribution of charged particles is often called an "electron avalanche".

A.2.4. This electron avalanche alone is insufficient to cause breakdown for which an additional "second stage" or "secondary ionisation process" is essential.

A.2.5. When breakdown occurs, the current is self-maintained, i.e. independent of the source of primary ionisation. The secondary ionisation process must be such that an electron which leaves the cathode can start a first ionisation process, the products of which are capable of liberating at some future time at least one more electron.

A.2.6. This second ionisation process may consist of any or all of the following principal mechanisms:

(a) The emission of electrons from the cathode by the impact of (1) positive ions, (2) photons, or (3) metastable atoms, or a combination thereof, which have been produced in the inter-electrode gap by the first ionisation process.

(b) The ionisation of neutral gas atoms or molecules by collisions with (1) positive ions, (2) photons, (3) electrons or (4) metastable atoms produced by the first ionisation process.

(c) An increase in the rate of the first ionisation process and of (a) and (b) caused by a change in the potential distribution across the gap, resulting from an accumulation of space charges within it.

A.2.7. The type of secondary ionisation process active depends on the gas pressure, electrode geometry, and applied voltage, and the assessment of which of these is the most important, is necessary before a theoretical reason for the value of time lag can be provided.

A.2.8. In as much as the particular process determines the value of the breakdown voltage, and the

rate of increase of current with applied field, the measurement of these two quantities is essential to explain the observed values of time lag.

A.2.9. The type of secondary ionisation process also affects the time lag in the following way: The rate of ionisation is a function of:-

(a) The efficiency of the secondary ionisation process, i.e. the average number of electrons $_p$roduced per ionising agent. This depends on the electric field in the region of ionising impacts.

(b) The time which elapses between the liberation of the secondary ionising agent from its parent atom or molecule and an ionising collision with an atom of the cathode (case (a)) or the gas (case (b)). This is a function of the mean free path, velocity, and ionisation cross section of the ionising agent in the gas considered.

A.2.10. In general, it can be assumed that:

(a) the transit time of an electron between the electrodes is negligible compared with the transit time of a positive ion.

(b) the transit time of a photon between the electrodes is negligible compared with the transit of an electron.

A.2.11. Consequently, the value of time lag in many cases provides a good indication of the secondary ionisation agent(s) acting.

A.2.12. From this brief introduction, it will be seen that the title chosen does in fact cover a field

which involves the understanding of the basic principles of electrical breakdown in gases, although this paper will deal specifically with the interpretation of the observed values of time lag in terms of first and second ionisation processes.

A.3. The Statistical Lag and Formative Lag.

A.3.1. The magnitude of the delay interval or alternatively the time lag is the sum of the "Statistical Lag" and the "Formative Lag", the magnitudes of which are mutually independent.

A.3.2. The occurrence of breakdown depends on two independent factors. As already described, breakdown occurs when a combination of the first and second ionisation processes ensures that the current is independent of the source of primary ionisation. One initial electron only is sufficient to start this process, and the Formative Time Lag is the time between the beginning of the electron avalanche started by this particular electron, and the instant of breakdown, which may be defined in any of the ways given above, in Section A.1.8.

A.3.3. As will be explained in more details later, the first and secondary ionisation processes are governed by the random nature of the motion of the gas atoms due to their thermal energy. Consequently, each electron which is a potential ionising agent follows a zig-zag path. Its energy varies from impact to impact owing to the fact that the time between impacts and the direction of motion with respect to the direction of the applied field vary from impact to impact. The effect of this is that not every electron starts an

avalanche which eventually leads to breakdown. In addition, if the supply of primary electrons is small, owing for example to a low primary current from the cathode, some time may elapse between the application of the breakdown voltage and the arrival of a suitable electron in the gap.

A.3.4. Both these factors produce a "Statistical Lag" which is defined as the time interval between the application of the breakdown voltage and the formation of a free electron which will start an electron avalanche which in combination with secondary ionisation processes subsequently produces breakdown.

A.4. The Scope of This Dissertation.

A.4.1. Only cold cathode discharges under uniform field conditions will be considered. This is because of mathematical complications which arise by the treatment of the non-uniform field case and which tend to make more difficult an interpretation of the basic principles of the phenomena observed.

A.4.2. The range of gas pressures studied is from the order of microns of mercury to approximately atmospheric pressure. The best way to specify the range is to refer to Paschen's Law, which states that the breakdown voltage is a function only of the product of gas pressure p and electrode separation d. The upper limit of pd considered will be of the order of 10^3 mm Hg x cm which is equivalent to a gap of a few centimetres at atmospheric pressure.

A.4.3. Most experimental results given relate to air, which of all gases has been by far the most extensively

studied in view of its commercial importance and availability. Data for nitrogen and the noble gases are also presented.

A.4.4. Details of experimental techniques will be given where applicable with special reference to their reliability for comparison of theory with experiment.

A.5. Mode of Presentation.

A.5.1. A description will first of all be given of the electron avalanche together with a survey of experimental methods of studying it, which have given essential information leading to a better theoretical interpretation of time lag values.

A.5.2. The existing knowledge of the types of ionising agent which occur during the second stage is next described, with particular reference to Townsend's second Ionisation Coefficient and the results of early measurements of it which to some extent have retarded the understanding of the breakdown process at high gas pressure.

A.5.3. The random nature of collisions within the gas is then described in a study of the statistical time lag with reference to the effect of cathode material, irradiation and gas pressure on the magnitude of the lag.

A.5.4. The subject of formative time lag will be introduced by a survey of the different measurement techniques which have been used. Details of early methods will then be given, and a description given of the experimental observations on which the Streamer Theory of breakdown at high pressure was based. The

manner in which subsequent experiments have discredited the Streamer theory will then be described and analysed. Evidence will be given to support the view that the Formative Time Lag may be calculated on the basis of the Townsend Theory of breakdown at both low and high gas pressure.

B. BASIC IONISATION PROCESSES.

B.1. The Electron Avalanche and Townsend's First Ionisation Coefficient.

B.1.1. Consider two plane parallel electrodes separated by a distance d, between which a voltage V is applied. If the applied voltage is increased, the variation of current up to the point of breakdown is approximately as shown in Fig. B.1.1. The priming current first of all increases linearly and then reaches a saturation value i_o at A. When the voltage is increased beyond B the electron density increases owing to the action of the first ionisation process and later in combination with the secondary ionisation process breakdown occurs at C.

B.1.2. Townsend investigated the region BC by measuring the value of current i for various values of electrode separation for a fixed value of applied field. He found that for a given applied field the current i increased with electrode separation and that a linear plot was obtained if log i is plotted against x.

$$\text{i.e. } \log i = \alpha x + \log i_o \qquad \text{B.1.2.1.}$$

By differentiation

$$\frac{di}{i} = \alpha\, dx \qquad \text{B.1.2.2.}$$

$$\text{or} \qquad \frac{di}{dx} = \alpha i \qquad \text{B.1.2.3.}$$

Townsend defined α as the First Ionisation Coefficient which is equivalent to the average number of new electrons liberated by one electron in travelling

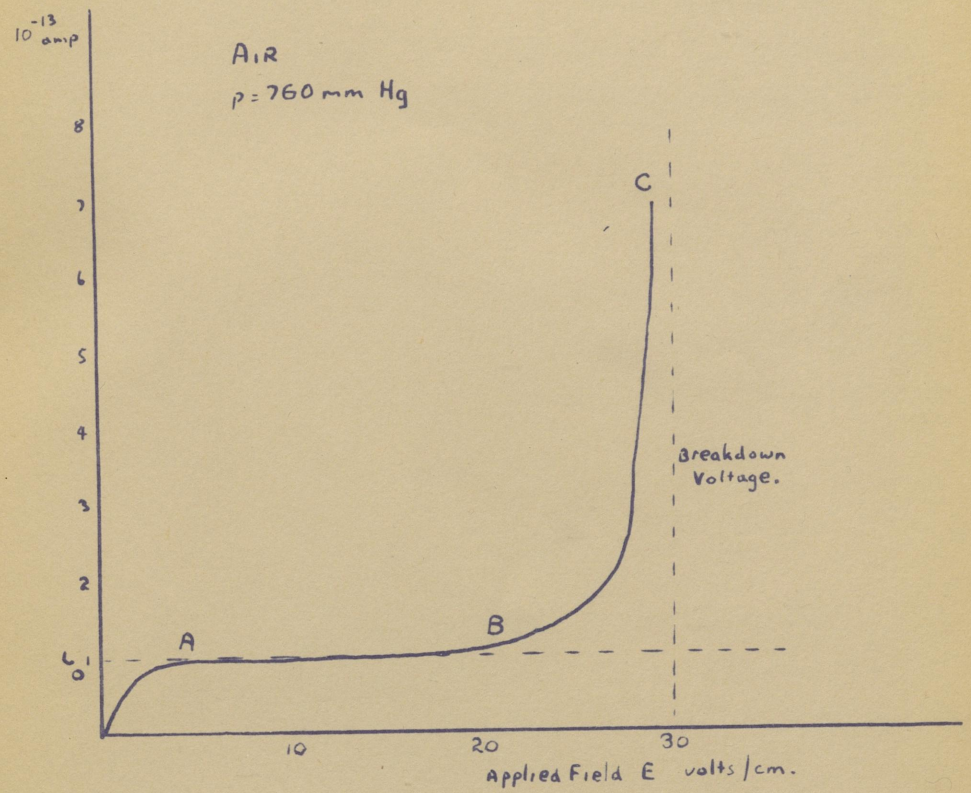

Current as a function of applied field E at constant pressure

FIG B 1·1

unit distance in the direction of the applied field. The average number of collisions per cm. is equal to the average number of collisions per second divided by the drift velocity of the electrons in the direction of the field E. The electron drift velocity is a function of the energy gained between impacts and therefore a function of $E\lambda$ or a function of $\frac{E}{p}$. Since the number of impacts per second is proportional to the pressure for a given electron energy we may write:

$$\frac{\alpha}{p} = f(\frac{E}{p}) \qquad \text{B.1.2.4.}$$

B.1.3. Townsend repeated the experiment just described for various values of applied field and gas pressure and found that $\frac{\alpha}{p}$ is the following unique function of $\frac{E}{p}$:

$$\frac{\alpha}{p} = A \exp. -\frac{B}{\frac{E}{p}} \qquad \text{B.1.3.1.}$$

where A and B are experimental constants for a given gas. This relationship applies only to a limited range of $\frac{E}{p}$ and a satisfactory theoretical basis has not yet been given. Nevertheless, equation B.1.3.1. has been used with success in the theory of formative time lag.

B.1.4. It is important to remember that α is an average, and not a fixed quantity for every individual electron. The electrons move along a zig-zag path to the anode, with a velocity which is termed their thermal velocity v, the mean value of which also determines the electron temperature Te.

B.1.5. The mean velocity measured in the direction of the field is called the drift velocity u. As a result

of their high thermal velocity v >>u the electrons diffuse sideways on their way to the anode.

B.1.6. Because of their much greater mass, the drift velocity of the ions back to the cathode is about one hundredth of the drift velocity of the electrons.

B.2. The Cloud Chamber Method of Detecting an Electron Avalanche.

B.2.1. The above theoretical concept of the nature of the electron avalanche has been confirmed by the experiments of Raether and his collaborators 1941-1949 who have perfected the use of the Wilson Cloud Chamber for this purpose.

B.2.2. The cloud chamber consists essentially of two parallel electrodes contained in an expansible chamber as shown in Fig. B.2.1. The chamber contains the gas to be studied mixed with water vapour which is brought into a super saturated condition by the expansion of the bellows, shown at A. The cathode is usually irradiated by ultra violet light which produces sufficient numbers of photoelectrons at the cathode surface to reduce the statistical lag to a negligible value. A voltage pulse, applied to the electrodes immediately before the expansion, attracts an electron from the cathode to the anode and this produces an electron avalanche by impact ionisation on its way. This electron avalanche is arrested before it reaches the anode by the use of a voltage pulse with a flat top of duration less than the transit time of the electron avalanche between cathode and anode. When the chamber expands immediately after the application of the pulse

the vapour condenses on the charged particles in preference to the neutral atoms. It is then possible to photograph the avalanche by a camera synchronised with the expansion mechanism of the bellows.

B.2.3. The profile of an avalanche recorded by such a photograph is usually as shown in Fig. B.2.2., which also shows an approximate diagrammatic representation of the distribution of the charged particles. The arrows show the direction of the resultant electric field surrounding the avalanche.

B.2.4. This technique has been applied by Raether 1941-49 to air at high pressure for which the time of formation of the electron avalanche is of the order of 10^{-7} sec.

B.2.5. By measuring the length of the avalanche for various values of pulse duration, the drift velocity of the electrons can be measured.

B.2.6. For example, Raether found that in air with $\frac{E}{p} = 27$ volt/cm/Hg the drift velocity u was 1.3 x 10^7 cm/sec.

B.2.7. This method is unique in that it supplies a visual check of the theoretical proposals. It is also extremely sensitive and may be applied to a large range of applied voltages. For instance, although at high gas pressure breakdown occurs when $\alpha d = 20$, individual avalanches may be observed for applied voltages which correspond to values of αd of about two. Of course, as the breakdown voltage is reached, the photograph also contains the products of the secondary ionisation process as well as the first.

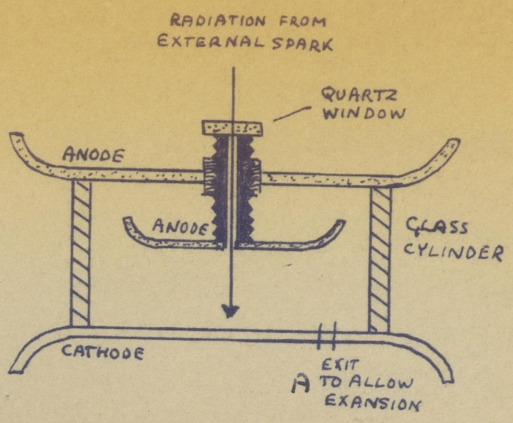

SKETCH OF RAETHER'S CLOUDCHAMBER

FIG B2·1

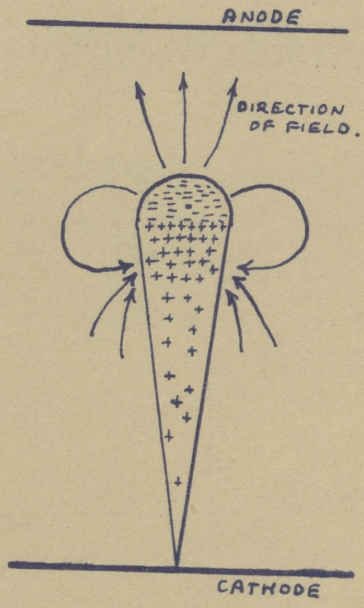

DIAGRAMATIC REPRESENTION OF AN
ELECTRON AVALANCHE

FIG B2·2

B.2.8. On the other hand, although this experimental technique does provide an extremely valuable insight into the nature of the current build-up process, the quantitative analyses based on the values of the avalanche diameter and avalanche velocity must be treated with caution. The principal errors involved are (a) the observed width of the streamer depends on the expansion ratio of the cloud chamber, (b) since the electron and positive ion density will only gradually decrease with distance from the avalanche axis the observed breadth will also depend on the sensitivity of the photographic plate and (c) avalanche velocity can only be computed from measurements on a number of independent avalanches which may not necessarily be identical.

B.3. The Electrical Method of Detecting an Electron Avalanche.

B.3.1. Whereas Raether's cloud chamber technique demonstrates the shape of the initial avalanche, it does not detect the random nature of the individual avalanches. A demonstration of this latter effect has been obtained by the following electrical method also developed by Raether 1955.

B.3.2. The apparatus consists of plane parallel electrodes of capacity C connected in the circuit as shown in Fig. B.3.1. When the avalanche is formed the current produced by the motion of electrons and positive ions causes a voltage drop across the external resistance R. The temporal variation of this voltage can be observed via a wide band amplifier on the screen of the oscillograph.

B.3.3. In the case of zero series resistance the

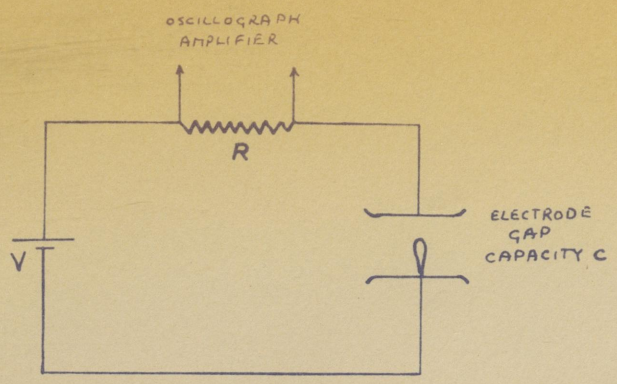

CIRCUIT DIAGRAM FOR ELECTRICAL METHOD OF DETECTING AN ELECTRON AVALANCHE.

FIG B3·1

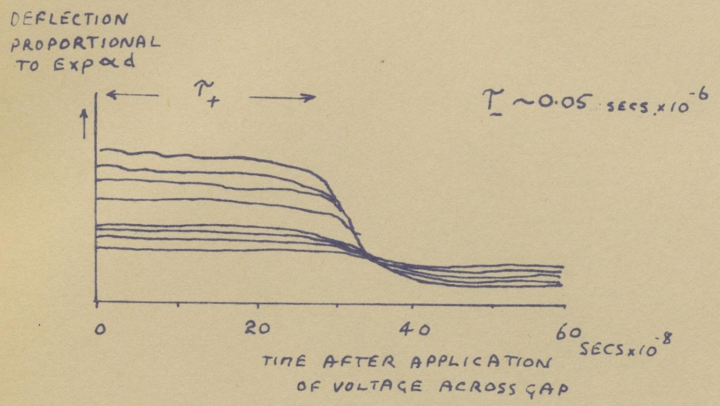

TYPICAL OSCILLOGRAPH RECORDS SUPERIMPOSED ON ONE ANOTHER.

FIG B3·2

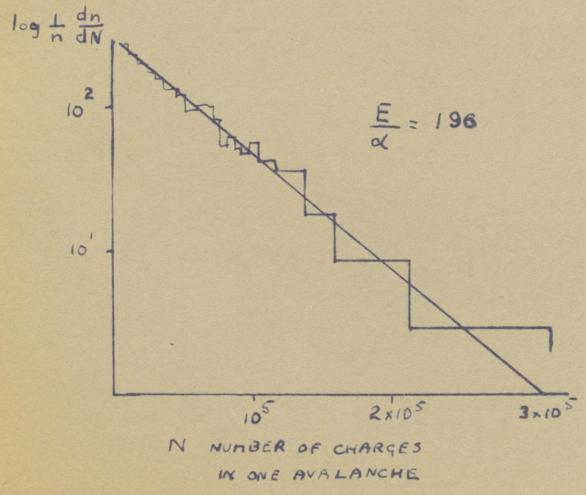

DISTRIBUTION OF PULSE HEIGHTS OF INDIVIDUAL ELECTRON AVALANCHES

FIG B3·3

energy required by the charge carriers to drive them through the gas is derived exclusively from the electrical energy of the condenser. In the latter case a potential drop would be produced across the discharge track, which would take place in two stages:-

(a) A rapid potential fall within the very short duration of the transit time Te of approximately

$$Ve = \frac{1}{\alpha d} \frac{e}{C} \exp.\alpha d \qquad \text{B.3.3.1.}$$

This is due to the motion of the electrons.

(b) A slow linear voltage drop within the ion transit time Tp approximately

$$Vp = \frac{e}{C}\left(1 - \frac{1}{\alpha d}\right)\exp.\alpha d \qquad \text{B.3.3.2.}$$

This is due to the motion of the positive ions.

These relationships have been derived by Schmidt 1954.

B.3.4. Since e exp.α d is the total charge transferred, the total voltage drop across the condenser is

$$V = \frac{e}{C} \exp.\alpha d \qquad \text{B.3.4.1.}$$

which agrees with the sum of Ve and Vp represented by equations B.3.3.1. and B.3.3.2.

B.3.5. If it is desired to study the electron current only, the value of R may be adjusted so that the energy supplied to the battery during the avalanche is just sufficient to cancel out the slow voltage drop caused by the ion current within the long transit time.

B.3.6. The sensitivity of the apparatus is limited by the noise at the input of the amplifier which is about 20×10^{-6} volt. Unfortunately, this limits the avalanches which can be studied to those with amplification above a critical amount. For example, if the input capacity including the capacity of the discharge track is about 1×10^{-11} farad, the avalanche must have an amplification exp. α d of 10^4 in order to raise itself as a rectangular pulse above the noise level.

B.3.7. Until this difficulty can be overcome, it will not be possible to use this technique for the study of gases with a strong secondary ionisation process. In fact, in all pure gases the secondary ionisation is so great that breakdown occurs before the critical amplification of 10^4 is reached.

B.3.8. Nevertheless, this technique is useful for obtaining a better understanding of the avalanche processes, and has been applied successfully by Raether 1955, to the case of a gas mixed with organic vapours to inhibit the secondary ionisation process. If the value of γ is decreased in this way, the value of exp. α d necessary for breakdown will be increased, and by this technique amplifications of 10^7 could be obtained which were readily detectable above the noise level.

B.3.9. It is essential for the ionisation potential of the gas to be greater than the ionisation potential of the vapour. It is then possible for vapour ions to be produced by charge-transfer on impact with gas ions. These vapour ions do not release electrons at the cathode owing to the fact that their knietic energy is

low because of their high mass and low mobility.

B.3.10. The random nature of the processes within the electron avalanche has been demonstrated by this technique, in the following manner:- Several oscillograph records are superimposed as shown in Fig. B.3.2. The electron component of each avalanche is so rapid that it does not give any photographic record with the oscillograph time base used. τ_- was calculated to be about 0.05 μsec. The length of the rectangular pulse gives the ion transit time τ_+, which therefore enables the ion velocity to be calculated for a particular gas filling and field strength. The vertical height of the pulse is proportional to the total number of charge carriers produced. It is found that in spite of the discharge conditions being carefully kept constant the amplification factor is subject to large fluctuations. As already discussed this spread is due to large variations in the first ionising impacts.

The distribution of pulse heights of the individual electron avalanches in a uniform field is shown in Fig. B.3.3. In Section C.2.10. a mathematical analysis will be given, the result of which confirms this experimental observation.

B.4. The Optical Method of Detecting an Electron Avalanche.

B.4.1. A third method of observing the electron avalanche has been developed by W. Legler 1955, by detecting the light quanta formed in the avalanche by electronic impact. Excitation is always present with ionisation and the light emitted is produced when the

excited atoms fall to the ground state.

B.4.2. The sensitivity of the apparatus was largely dependent on the output of the photo-cathode and the proportion of the light emitted by the avalanche which can fall upon it. The wavelength of the light which could be detected was limited to values of 2200°A by the window of the multiplier and it was found that for this range of wavelength the light emitted was equivalent to approximately one quantum for every two ionic pairs.

B.4.3. The sensitivity of this technique compares favourably with the electrical method. Up to the present 10^{8} of avalanches with an amplification exp.α d of 4×10^{3} have been detected. It should be possible by the use of different geometry and improved photo-cathodes to increase the sensitivity by 10^{2}, which them compares with the cloud chamber technique. However, unless the avalanche can be arrested by the use of a flat topped pulse as in the cloud chamber technique, it is necessary to inhibit the secondary mechanisms as in the electrical method.

B.4.4. These techniques have demonstrated the nature of the electron avalanche which agrees with Townsend's theoretical concept. In particular the random nature of the collision processes has been emphasized. A description will next be given of the secondary processes which form the second stage of the delay interval.

B.5. The Second Ionisation Stage and Townsend's Second Ionisation Coefficient.

B.5.1. As described in section B.1.2. Townsend

found that for a given applied field the logarithm of the current was proportional to the electrode separation. However, when he extended the work to higher values of applied voltage he found that the current increased beyond the extrapolated linear curve. This increase was attributed to additional ionisation produced by the second ionisation stage.

B.5.2. Sanders 1933 examined the problem in greater detail and his results are given in Fig. B.5.1. It will be observed that for values of $\frac{E}{p}$ less than 110, the plots are strictly linear up to the point of breakdown. This observation has greatly influenced the theory of electrical breakdown, since it implies that breakdown may occur without secondary ionisation. First of all, it was ascribed to voltage fluctuations in the H.T. source, but repeat experiments made by Posin 1936 and later by Bowls 1938 and Hale 1939 who claimed that their voltage sources were stable appeared to confirm the result.

B.5.3. Recently, F. Llewellyn Jones and his associates have succeeded in developing a voltage source sufficiently stable to demonstrate that secondary ionisation does in fact occur in all cases of breakdown. This will be dealt with in more detail in section D.5.9. onwards.

B.5.4. Townsend first of all attributed the upcurving to additional ionisation produced by the impact of negative ions and neutral atoms or molecules. After about 1915 it was realised that the negative charge carriers are not negative ions but free electrons and the extra ionisation was then attributed to the impact of positive ions and neutral atoms. Of course all ionisation by electron - neutral atoms impacts are

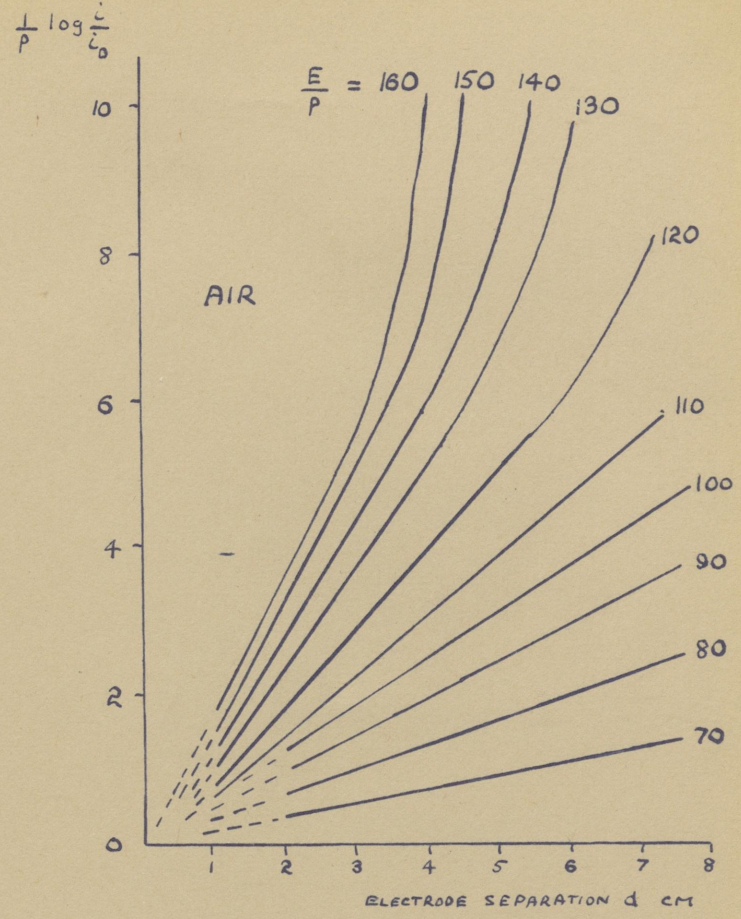

SANDERS' EXPERIMENT VALUES OF THE GROWTH OF CURRENT WITH ELECTRODE SEPARATION FOR VARIOUS VALUES OF $\frac{E}{p}$

FIG B5·1

classified as the first ionisation process.

B.5.5. Townsend assumed by analogy with α, a secondary ionisation coefficient β, which was defined as the number of electrons produced by a positive ion in unit distance in the direction of the anode.

Consider a slab of gas of thickness dx situated x cm. from the cathode.

Let it contain p positive ions per sq. cm. of area between the cathode and the slab, and let the number of positive ions generated per sq. cm. of area in the distance d-x between the slab and the anode be represented by q.

Then the number of electrons reaching the anode per cm^2 is given by

$$N = N_0 + p + q \qquad \text{B.5.5.1.}$$

where N_0 is the number of electrons leaving the cathode $/cm^2$.

The number of ions produced/cm^2 in a distance dx is

$$(N_0 + p)\,\alpha\,dx + q\beta\,dx \qquad \text{B.5.5.2.}$$

Hence from equation B.5.5.1.:

$$\frac{dp}{dx} = (N_0 + p)\alpha + (N-N_0-p)\beta$$

$$= (N_0 + p)(\alpha-\beta) + N\beta \qquad \text{B.5.5.3.}$$

By separating the variable and integrating

$$N = N_0 \frac{(\alpha-\beta)\exp.\,(\alpha-\beta)x}{\alpha-\beta\exp.\,(\alpha-\beta)x} \qquad \text{B.5.5.4.}$$

or, $$i = i_0 \frac{(\alpha - \beta)\exp.(\alpha - \beta)x}{\alpha - \beta \exp.(\alpha - \beta)x} \qquad \text{B.5.5.5.}$$

This equation represents the curved parts of Fig. B.5.1., and is the basic equation for the action of first and second ionisation coefficients. α may be obtained from the gradient of the linear portions for which β is zero.

B.5.6. Townsend 1915 demonstrated that for a limited range of $\frac{E}{p}$, $\frac{\beta}{p}$ was the following unique function of $\frac{E}{p}$:-

$$\frac{\beta}{p} = C \exp. \; D\frac{E}{p} \qquad \text{B.5.6.1.}$$

where C and D are constant for a particular gas.

B.5.7. The criterion for which i becomes infinitely great is:

$$0 = \alpha - \beta \exp.(\alpha - \beta)x \qquad \text{B.5.7.1.}$$

Townsend used this criterion for the threshold of breakdown.

B.5.8. If the values of $\frac{\alpha}{p}$ and $\frac{\beta}{p}$ are known as functions of $\frac{E}{p}$ the value of $\frac{E}{p}$ for which equation B.5.7.1. applies may be determined, which gives the value of the breakdown voltage. This theoretical value may then be compared with experimental values obtained in the same apparatus as used to measure α and β.

B.5.9. Townsend showed that good agreement is obtained for air at low pressure.

B.5.10. Since Townsend's original supposition, it has been established that the probability of ionisation by impacts between positive ions and neutral atoms is

very small. In the case of many gases, especially helium, there is a high probability of charge transfer on impact between a positive ion and neutral atom. The effect of this is to reduce the mobility of the ions within their parent gas. The coulomb forces applied to the solid sphere model of a gas must in this case be replaced by wave-mechanically defined exchange forces, whose net effect is to increase the collision cross section of positive ions within their parent gas. The energy of positive ions is thereby kept so low that the probability of producing ionisation of a neutral atom on impact is negligible.

B.5.11. Later, instead of using β Townsend proposed an alternative secondary coefficient γ_p defined as the probability that a new electron will be created at the cathode by each impacting positive ion:-

Consider plane parallel electrodes, and let

N_o = number of electrons leaving the cathode due to external sources.

N = number of electrons reaching the anode.

N_o' = total number of electrons leaving the cathode.

Then the number of new electrons liberated in the gap which is equal to the number of positive ions liberated in the gas is $N - N_o'$, so that:-

$$N_o' = N_o + \gamma_p(N - N_o') \qquad \text{B.5.11.1.}$$

Therefore,

$$N_o' = \frac{N_o + \gamma_p N}{1 + \gamma_p} \qquad \text{B.5.11.2.}$$

But,

$$N = N_o' \exp.\alpha x \qquad \text{B.5.11.3.}$$

Therefore,

$$N = \frac{N_o + \gamma_p N \exp.\alpha x}{1 + \gamma_p} \qquad \text{B.5.11.4.}$$

From which,

$$N = N_o \frac{\exp.\alpha x}{1 - \gamma_p(\exp.\alpha x - 1)} \qquad \text{B.5.11.5.}$$

or,

$$i = i_o \frac{\exp.\alpha x}{1 - \gamma_p(\exp.\alpha x - 1)} \qquad \text{B.5.11.6.}$$

If γ_p is set equal to $\frac{\beta'}{\alpha - \beta'}$, where β' is a constant

$$i = i_o \frac{(\alpha - \beta') \exp.\alpha x}{\alpha - \beta' \exp.\alpha x} \qquad \text{B.5.11.7.}$$

If β is small compared with α so that $\alpha - \beta \doteq \alpha$ equation B.5.11.7. may be compared with equation B.5.5.5.

Also, it may be assumed that

$$\gamma_p \doteq \frac{\beta'}{\alpha} \doteq \frac{\beta}{\alpha} \qquad \text{B.5.11.8.}$$

Hence an alternative expression for the breakdown criterion is

$$\gamma_p(\exp.\alpha d - 1) = 1 \qquad \text{B.5.11.9.}$$

and this is referred to below as the Townsend Breakdown Criterion.

B.5.12. This result is significant because it demonstrates that although ionisation by positive ions in the gas is very unlikely, the equation which represents it is so like the equation for electron emission at the cathode by positive bombardment that measurement of growth of current or breakdown voltage would not easily

distinguish between the two.

B.5.13. Photons produced during the first electron avalanche may also release electrons from the cathode. γ_r may be defined as the probability that an electron will be liberated at the cathode by a photon produced within the gap. Whereas all positive ions reach the cathode, photons are radiated in random directions so that it is necessary to define a fraction f_r of the photons produced which reach the cathode. If N_r represents the number of photons produced for every positive ion produced in the electron avalanche, the number of electrons emitted at the cathode by this process per positive ion in the gap is:

$$\gamma_r N_r f_r \qquad \text{B.5.13.1.}$$

B.5.14. Photons are also subject to attenuation by absorption and re-emission.

B.5.15. In some cases, it is possible for electrons to be released at the cathode by the impact of metastable atoms or molecules. By analogy with the previous case, the number of electrons produced at the cathode by metastables per positive ion in the gap is:

$$\gamma_m N_m f_m \qquad \text{B.5.15.1.}$$

B.5.16. In conclusion, it is seen to be likely that the three principal secondary mechanisms are:

(a) Positive ion bombardment of the cathode,
(b) Photon bombardment of the cathode,
(c) Metastable combardment of the cathode.

These may be combined to produce a generalized secondary coefficient

$$\gamma = \gamma_p + \gamma_r f_r N_r + \gamma_m f_m N_m \qquad \text{B.5.16.1.}$$

C. THE STATISTICAL TIME LAG.

C.1. Introduction.

C.1.1. As outlined in section A.3.2. the magnitude of the statistical time lag depends essentially on two factors:-

(a) The availability of initiatory electrons e.g. the magnitude of the priming current.

(b) The dependence of the ability of each potential initiatory electron to produce breakdown, upon the random nature of the ionisation process in addition to the magnitude of the applied field, gas pressure and geometry.

The source of primary electrons may be either the cathode or the gas. Electrons can be released from the cathode if the energy of the ionisation agent exceeds the work function of the cathode which is usually within the range 4 - 7 electrons volts. For ionisation within the gas a higher energy is generally required, equivalent to the ionisation energy of the constituent atoms or molecules which may be roughly within the range 4 to 24 volts.

C.2. The Theory of Statistical Time Lag.

C.2.1. The theory of statistical time lag when the gas acts as the source of primary electrons is complicated by the fact that the magnitude of the lag is dependent upon the position of the electron when liberated. Consequently, very little successful theoretical analysis has been made up to the present time, although Heymann 1950 has made an attempt to do so.

C.2.2. On the other hand, the theory of statistical time lag when the cathode acts as the source of primary electrons is well established and will next be described. As described in section B.1.2., an electron emitted at the cathode will on average produce on its way to the anode an avalanche of exp.α d electrons. The number of positive ions produced is exp. α d - 1, and if it is assumed that all of them reach the cathode, the number of new electrons produced at the cathode due to this single avalanche is

$$\gamma (\exp. \alpha d - 1) \qquad \text{C.2.2.1.}$$

This expression will be called the multiplication factor M. The breakdown criterion is:

$$M = 1$$

as shown by equation B.5.11.9.

If it is assumed that the space charge formation is negligible and that the electric field between the electrodes is uniform, it is possible to calculate the probability P that the statistical time lag will be greater than a certain time t.

C.2.3. The following analysis is due to Hertz 1937. The value of M is governed by the random nature of the motion of electrons and positive ions. The breakdown criterion must therefore be applied to the average of a number of consecutive avalanches. For instance, if after the first avalanche due to one electron no further electrons are emitted from the cathode, then breakdown will not occur. Alternatively one, two, three or more electrons may be released after the first avalanche. Each of these starts another avalanche, the products of

which may or may not produce another electron at the cathode. If after a number of such avalanches it happens that no electron is released at the cathode then breakdown still does not occur, i.e. the net value of M is still zero.

C.2.4. Consider the case when an electron from the cathode produces an avalanche which contains N ions. Let u_ν represent the probability that these N ions will liberate from the cathode ν electrons. Each of these electrons may originate an electron avalanche. Let the probability that no subsequent electron is produced at the cathode as a result of a single avalanche be Q, i.e. Q is the probability that the avalanche sequence will stop. Each avalanche is independent of the others. Hence, from the theory of probability for independent variables, the probability that an avalanche of ν positive ions does not produce breakdown is

$$u_\nu Q^\nu \qquad \text{C.2.4.1.}$$

Then according to Loeb & Meek 1941

$$Q = \sum_{\nu=0}^{\nu=N} u^\nu Q^\nu \qquad \text{C.2.4.2.}$$

The probability of the liberation of an electron from the cathode by a particular positive ion is α_p^ν. Then u_ν the probability that N ions will liberate from the cathode ν electrons is the product of the following terms:-

(a) The probability of ν positive ions producing ν electrons = α_p^ν. This assumes that the positive ions are mutually independent.

(b) The probability of $N - \nu$ positive ions not producing an electron at the cathode $= (1 - \alpha_p)^{N-\nu}$

(c) The number of ways of choosing ν positive ions from N positive ions = ${}^{N}C_{\nu}$.

$$\text{i.e. } u_{\nu} = \alpha_p (1-\alpha_p)^{N-\nu} {}^{N}C_{\nu} \qquad \text{C.2.4.3.}$$

$$= (1-\alpha_p)^{N} \left(\frac{\alpha_p}{1-\alpha_p}\right)^{\nu} {}^{N}C_{\nu} \qquad \text{C.2.4.4.}$$

Combining equation C.1.4.2. with equation C.1.4.3.:

$$Q = (1-\alpha_p)^{N} \sum_{\nu=0}^{\nu=N} \left(\frac{\alpha_p}{1-\alpha_p}\right)^{\nu} {}^{N}C_{\nu} Q^{\nu} \qquad \text{C.2.4.5.}$$

$$\therefore Q = (1-\alpha_p)^{N} \left(1 + \frac{Q\alpha_p}{1-\alpha_p}\right)^{N} \qquad \text{C.2.4.6.}$$

$$\therefore Q = (1-\alpha_p + \alpha_p Q)^{N} \qquad \text{C.2.4.7.}$$

Let P represent the probability of breakdown produced by one initiatory electron,

$$\text{Since } Q = 1-P \qquad \text{C.2.4.8.}$$

$$1-P = (1-\alpha_p P)^{N} \qquad \text{C.2.4.9.}$$

$$\text{i.e. } N = \frac{\log(1-P)}{\log(1-\alpha_p P)} \qquad \text{C.2.4.10.}$$

$$\text{Since } N = (\exp.\alpha d - 1) \therefore M = N\gamma \qquad \text{C.2.4.11.}$$

$$\text{and } M = \gamma_p \frac{\log(1-P)}{\log(1-\alpha_p P)} \qquad \text{C.2.4.12.}$$

The full line of Fig. C.2.1. shows the dependence of P on M.

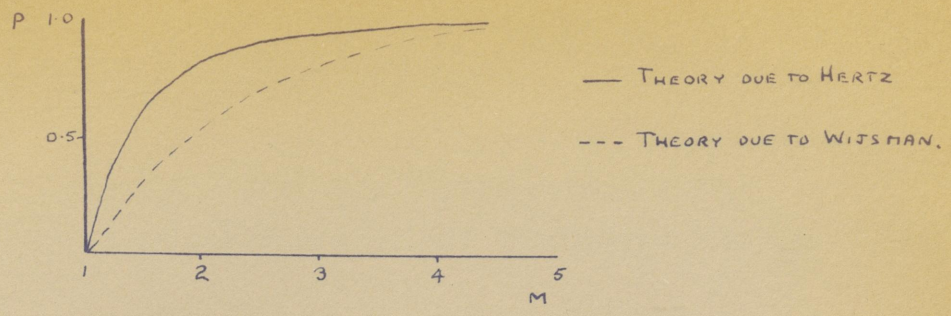

THEORETICAL RELATIONSHIP BETWEEN PROBABILITY P THAT A PRIMARY ELECTRON IS MULTIPLIED INTO A STEADY CURRENT AND THE MULTIPLICATION FACTOR M

FIG C2·1

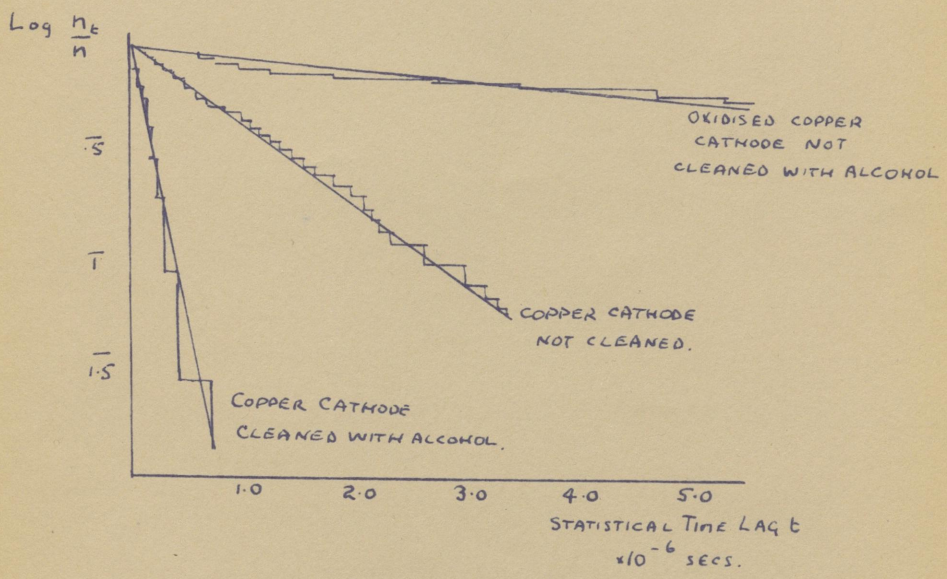

DISTRIBUTION OF STATISTICAL TIME LAGS. FOR VARIOUS STATES OF CATHODE SURFACE.

FIG C2·2

C.2.5. A relationship between t_s and N_o may be obtained in the following manner:

If N_o represents the number of electrons leaving the cathode per second, then $N_o P \Delta t$ represents the probability of the occurrence of breakdown within the time interval Δt.

Then the probability of a time lag which exceeds t is equal to the probability of the non-occurrence of breakdown between t = 0 and t = t. Let this interval be divided into s intervals of duration Δt.

Then the probability of breakdown after t = t is:

$$(1 - PN_o \Delta t)^s \qquad \text{C.2.5.1.}$$

or

$$(1 - \frac{PN_o t}{s})^s \qquad \text{C.2.5.2.}$$

$$\rightarrow \quad \exp.(-PN_o t) \quad \text{as } s \rightarrow \infty \qquad \text{C.2.5.3.}$$

The probability of a time lag between t and t+dt is therefore:

$$\exp.(-PN_o t) \times PN_o dt \qquad \text{C.2.5.4.}$$

Therefore the mean statistical time lag ts is given by:

$$ts = \frac{\int_o^\infty PN_o t \exp.(-PN_o t)dt}{\int_o^\infty PN_o \exp.(-PN_o t)dt} \qquad \text{C.2.5.5.}$$

$$\therefore \quad ts = \frac{1}{PN_o} \qquad \text{C.2.5.6.}$$

C.2.6. If experimental investigation is to be made of the statistical time lag, a high overvoltage is necessary to reduce the formative time lag to as small a value as

possible together with a small value of i_o. Usually the probability of breakdown P may be regarded as unity in such an investigation, whereupon equation C.1.5.6. becomes:

$$ts = \frac{1}{N_o} \qquad \text{C.2.6.1.}$$

C.2.7. Consider an experiment in which a large number of measurements of statistical time lag are made. Let the number of measurements made be n.
Let the number of measurements for which the observed statistical time lag is longer than t secs. be n_t.
Then the probability of breakdown after t secs. is:

$$\frac{\text{Number of lags longer than t}}{\text{Total number of measurements}} = \frac{n_t}{n} \qquad \text{C.2.7.1.}$$

which from equation C.2.5.3. is equal to $\exp.(-PN_o t)$. If, as described in the previous section, the experimental conditions are such that P = 1, we have

$$\log_e \frac{n_t}{n} = -N_o t \qquad \text{C.2.7.2.}$$

Hence, by plotting $\log_e \frac{n_t}{n}$ against t, N_o can be derived from the gradient of the straight line graph. Such a plot is shown in Fig. C.2.2.

C.2.8. It is convenient at this point to return to the analysis of Hertz, and in particular the expression for u_ν denoted by equation C.2.4.3. In order to obtain this equation, it was assumed that an ionising electron produces N electrons and N - 1 ions. The positive ions in turn produce ν more electrons at the cathode. But by the very random nature of the collision processes one electron from the cathode will not always produce N - 1 positive ions. In fact, this has been

demonstrated by Raether as described in section B.3. Equation C.2.4.3. is therefore not strictly correct and neither is equation C.2.4.12., which is derived from it.

C.2.9. In the following analysis due to Wijsmann 1949 more correct versions of these equations will be derived. First of all it is necessary to calculate the probability p (N,x) that one particular electron leaving the cathode has become an avalanche of N electrons and N - 1 positive ions after a distance x. p (1,x) is the probability that an electron does not ionise an atom at all in travelling a distance x.

$$p(1,x) = \exp.(-\alpha x) \qquad \text{C.2.9.1.}$$

p(N-1, x') is the probability that one electron from the cathode has become an avalanche of N-1 electrons at x'. Consider the interval x' to x' + dx, and let us suppose that during this interval one more electron is released by an ionising collision. The probability of such an occurrence is the product of the three following quantities:-

(a) The chance that one electron will ionise a neutral atom = $\alpha\, dx'$.

(b) The number of ways of choosing that one electron from N-1 electrons = N-1.

(c) The chance that each of the other N - 2 electrons will not have an ionising collision $= (1 - \alpha\, dx')^{N-2}$.

i.e. the probability that N-1 electrons at x' become N electrons at x' + dx' is:

$$\alpha\, dx' (N-1)(1-\alpha\, dx')^{N-2} \qquad \text{C.2.9.2.}$$

As $dx' \rightarrow 0$ equation C.2.9.2. becomes

$$(N - 1) \alpha \, dx' \qquad \text{C.2.9.3.}$$

Therefore the probability that there are N electrons at $x' + dx'$ is:

$$p\,(N - 1, x')(N - 1) \alpha \, dx' \qquad \text{C.2.9.4.}$$

The probability that none of these N electrons ionises between $x' + dx'$ and x is:

$$\exp.(-\alpha N(x-x')) \qquad \text{C.2.9.5.}$$

Therefore the probability of N electrons at x is the product of expressions C.2.9.4. and C.2.9.5.,

i.e. $p(N-1, x')(N-1)(\alpha) \exp.(-\alpha N(x-x'))$ C.2.9.6.

Therefore,

$$p(N,x) = \int_0^x p(N-1, x')(N-1)(\alpha)\exp.(-\alpha N(x-x'))dx' \qquad \text{C.2.9.7.}$$

From which

$$p(N,x) = \exp.(-N\alpha x)(\exp.\alpha x-1)^{N-1} \qquad \text{C.2.9.8.}$$

At the anode

$$p(N,d) = \exp.(-N\alpha d)(\exp.\alpha d-1)^{N-1} \qquad \text{C.2.9.9.}$$

Let $\overline{N}$ = expectation value of N

$$\overline{N} = \sum_{N=1}^{\infty} N \; p(n,d) = \exp.\alpha d \qquad \text{C.2.9.10.}$$

$$\therefore \; p(N,d) = \frac{1}{(\overline{N})^N}(\overline{N}-1)^{N-1} \qquad \text{C.2.9.11.}$$

$$= \frac{1}{\bar{N}} \left(1 - \frac{1}{\bar{N}}\right)^{N-1} \qquad \text{C.2.9.12.}$$

Usually $\bar{N} \gg 1$ and $N \gg 1$,

Therefore,

$$p(N,d) = \frac{1}{\bar{N}} \exp.\left(-\frac{N}{\bar{N}}\right) \qquad \text{C.2.9.13.}$$

C.2.10. This equation has been confirmed by the experiments of Raether 1955, described in section B.3.10. In these experiments, the height h of the oscillogram was a measure of the number of electrons N produced. By studying the results on a total number of oscillograms n Raether counted the number dn with a number of electrons between N and dN. Then the probability that the number of electrons produced in the avalanche shall be between N and N + dN is $\frac{dn}{n}$. But from equation C.2.9.13., this probability given by $p(Nd)dN$ is given by $\frac{1}{\bar{N}} \exp.\left(-\frac{N}{\bar{N}}\right)dN$,

Hence
$$\frac{dn}{n} = \frac{1}{\bar{N}} \exp.\left(-\frac{N}{\bar{N}}\right)dN \qquad \text{C.2.10.1.}$$

or
$$\log_e\left(\frac{1}{n}\frac{dn}{dN}\right) = \log \frac{1}{\bar{N}} - \frac{N}{\bar{N}} \qquad \text{C.2.10.2.}$$

Raether plotted the value of $\log \left(\frac{1}{n}\frac{dn}{dN}\right)$ against N, and found that a straight line was obtained, as shown in Fig. B.3.3. The gradient gives the value of $\bar{N} = \exp.\alpha d$, which agreed well with the experimental values of α obtained by other methods.

C.2.11. Once the value of $p(N,d)$ has been derived, we may continue to derive a more correct expression for Q than derived by Hertz in the following manner which is due to Wijsmann 1949. As before, we use the equation:

$$Q = \sum_{\nu=0}^{\nu=\infty} u_\nu Q^\nu \qquad \text{C.2.4.2.}$$

The value of u_ν is now derived:

$p(N,d)$ represents the probability that the avalanche due to an initial electron from the cathode contains N-1 positive ions. We require the probability that these N-1 will produce ν secondary electrons when they reach the cathode, i.e. "the probability that ν positive ions liberate electrons at the cathode 'multiplied by' the probability that N-1-ν do not 'multiplied by' the number of ways of selecting them."

i.e. $$\gamma_p^{\nu}(1-\gamma_p)^{N-1-\nu}\,({}^{N-1}C_{\nu}) \qquad \text{C.2.11.1.}$$

Therefore, $$u_\nu = \sum_{N-1}^{\infty} p(N,d)\;{}^{N-1}C_{\nu}\;\gamma_p^{\nu}\,(1-\gamma_p)^{N-1-\nu} \qquad \text{C.2.11.2.}$$

Substitute for $p(N,d)$ from above and we obtain

$$u_\nu = \frac{q^{\nu}}{(q+1)^{\nu+1}}$$

where $$q = \gamma_p(\bar{N}-1) \qquad \text{C.2.11.3.}$$

i.e. q is the average number of secondary electrons eventually emitted from the cathode by an initial electron.

$$q = \gamma_p \exp.\left(\int_0^d \alpha\,dx' - 1\right) \qquad \text{C.2.11.4.}$$

If equation C.2.11.3. is now subetituted in equation C.2.11.4.

$$Q = \sum_{\nu=0}^{N} \frac{(qQ)^{\nu}}{(q+1)^{\nu+1}} \qquad \text{C.2.11.5.}$$

i.e. $$Q = \frac{1}{q+1-qQ} \qquad \text{C.2.11.6.}$$

There are two solutions to this equation, namely:

$Q = 1$ $\qquad$ $Q = \frac{1}{q}$ $\qquad$ C.2.11.7.

$P = 0$ $\qquad$ $P = 1 - \frac{1}{q}$ $\qquad$ C.2.11.8.

for $V < V_s$ $\qquad$ for $V > V_s$

This solution is compared with that of Hertz in Fig. C.2.1. It should be noted that the above calculation applies only when the formation of space charge before breakdown is negligible.

C.3. The Theory of Statistical Lag of Impulse Breakdown.

C.3.1. The probability of breakdown after time t, viz $\exp.(-PN_o t)$, derived for the case of a constant applied voltage in section C.2.5., must be modified to $\exp.(-\int_o^t PN_o dt)$ for the case of impulse breakdown due to the application of a voltage which increases with time. C.3.1.1.

Then P is a function of time, since M the multiplication factor is a function of time.

In order to express P as a function of time, the relationship between P and M given by equation C.2.4.12. must first be simplified. Provided the overvoltage is small $\gamma_p P$ is small compared with unity.

$$M \doteq \gamma_p \frac{\log(1 - P)}{-\gamma_p P} \qquad \text{C.3.1.2.}$$

$$\therefore \quad M \doteq 1 + \frac{P}{2} \qquad \text{C.3.1.3.}$$

$$\therefore \quad \frac{P}{2} \doteq M - 1 \qquad \text{C.3.1.4.}$$

M may now be replaced by C.2.2.1. and the value of unity equated to $\gamma_p(\exp. \alpha_o d - 1)$ from the Townsend breakdown criterion.

$$\therefore \quad \frac{P}{2} \doteq \gamma_p[\exp.(\alpha_o + \Delta\alpha)d - 1] - \gamma_p[\exp. \alpha_o d - 1] \qquad \text{C.3.1.5.}$$

where α_o denotes the value of α at the breakdown voltage, and $\Delta\alpha$ denotes the increase in α due to the applied overvoltage at which breakdown occurs.

Rearranging

$$\frac{P}{2} = \gamma_p \exp.\ \alpha_o d(\exp.\Delta\alpha\, d - 1) \qquad C.3.1.6.$$

Since

$$\frac{P}{2} = \gamma_p(\exp.\alpha d - 1) - 1 \qquad C.3.1.7.$$

$$\frac{1}{2}\frac{\partial P}{\partial t} = 2\gamma_p d \exp.\alpha d \frac{\partial \alpha}{\partial t} \qquad C.3.1.8.$$

Substituting in equation C.3.1.6.

$$\frac{P}{2} = \frac{1}{2}\frac{\partial P}{\partial t} d\,(\exp.\Delta\alpha\, d - 1) \qquad C.3.1.9.$$

Simplifying

$$P = \frac{\partial P}{\partial t}\frac{\partial t}{\partial \alpha}\Delta\alpha \qquad C.3.1.10.$$

Since $\Delta\alpha$ is the change in α during the time lag t, we write

$$P = \frac{\partial P}{\partial t} t \qquad C.3.1.11.$$

Then substituting in C.3.1.1.

The probability of breakdown in time t is:-

$$\exp. -\int_o^t \frac{\partial P}{\partial t} t\, dt \qquad C.3.1.12.$$

Heywood assumed that $\frac{\partial P}{\partial t}$ is independent of t and obtained by integration the following expression for the probability of breakdown after time t with the applied voltage rising linearly with time.

$$\exp. \left\{ -\frac{1}{2}\left(\frac{t}{t_n}\right)^2 \right\} \qquad C.3.1.13.$$

This expression is only valid for small values of over-voltage.

Whereas there is little experimental evidence to support the above the static breakdown theory is well-established.

C.4. Experimental Studies of Statistical Time Lag.

C.4.1. A study of the statistical time lag has usually been made for one of the two following reasons:-

1. The need to eliminate the statistical time lag in measurements of formative time lag.
2. The use of measurements of statistical time lag for the determination of the rate of electron emission from a cathode surface.

The practical aspects of these two problems will next be considered.

C.4.2. The effect on the statistical time lag of cathode irradiation.

The statistical time lag may be reduced by irradiation of the cathode to release additional primary electrons. Three principal types of irradiation are used, namely, (a) Carbon Arc, (b) Mercury Vapour Lamp, (c) Spark discharge across electrodes in air at atmospheric pressure. All produce a high intensity of ultra violet illumination.

The priming current produced for most cathodes by this method is of the order of 10^{-11} amps per sq.cm. This value may be increased by placing the source at the side of the gap, the radiation being applied at normal incidence to the cathode through holes in the anode.

The efficiency of the cathode irradiator is dependent upon the work function of the cathode surface. Consequently, the nature of the irradiated cathode surface affects the statistical time lag. An example of this is shown in Fig. C.2.2., which is taken from the experiments of

Strigel 1939. Clean copper electrodes (work function 3.9 ev) provide much lower statistical time lags than oxidised copper electrodes (work function 5.3 ev).

$\frac{n_t}{n}$ represents the number of lags greater than a value of t secs divided by the total number of lags measured. It will be noted that log $\frac{n_t}{n}$ is approximately proportional to t. The applied voltage was such that P could be assumed equal to unity and the linearity of Fig. C.2.2. confirms equation C.2.7.2., derived in section C.2.7.

C.4.3. The effect of the state of the cathode surface.

The presence of particles of insulating material on the cathode surface may also affect the statistical time lag, because of the increased electron emission, at points where the applied field is distorted at the non-uniform cathode surface. The size of the particle is critical and the biggest reduction was found by experiment to be produced by a particle of linear dimensions within the range 0.002 to 0.015 cm. The nature of the dielectric particle is of secondary importance. If the applied voltage is in the form of a rapidly rising pulse, the effect of the reduction in statistical time lag is to reduce also the breakdown voltage. A 20% reduction in impulse breakdown voltage has been observed by Berkeley & Slepian 1940 by the presence of alumina particles.

C.4.4. The effect of the preceding discharge.

Paetow 1939 has shown that the passage of a discharge across electrodes on which an insulating oxide layer is present produces a reduction in the statistical time

lag of subsequent discharges. The explanation proposed is that the first discharge causes the particles of the insulating layer to become charged so that highly localized fields are formed which increase the emission.

The reduction in statistical time lag produced by a previous discharge decreases roughly exponentially with the interval between the cessation of the first discharge and the attempt to initiate the succeeding discharge. The time constant of this decay may be of the order of minutes.

C.4.5. The use of statistical time lag measurement to determine the rate of electron emission from the cathode.

An example of the use of statistical time lag measurement for the determination of the rate of electron emission from the cathode is the work of Llewellyn Jones 1949, who studied the breakdown of air between tungsten electrodes within the pressure range from 50 cm to 3 atmospheres. Short gaps between the electrodes were used of the order of 0.3 mm in order to reduce the gas volume between the electrodes to as small a value as possible. This was done to obtain long statistical time lags since the chance of producing electrons suitably placed for leading to breakdown will increase with the volume of the gap.

The method used was to apply to the gap a rapidly rising voltage pulse which attained a peak value of 4kV in about 10^{-4} secs. Recurrent voltage pulses were applied at rates of from 50 pulses/sec. to 400 pulses/sec. A cathode ray oscillograph connected directly across the electrode gap recorded the successive applications of voltage which were photographed on a moving film.

Each successive breakdown occurred at a different voltage which was recorded on the film and since the

shape of the applied pulse was known the statistical time lag corresponding to each breakdown of the gap could be calculated.

The value of the rate of electron emission from the cathode, N_o, was calculated from each of the following equations derived in section C.2.

$$\log \frac{n_t}{n} = -N_o t \qquad \text{C.2.7.2.}$$

$$t_s = \frac{1}{N_o} \qquad \text{C.2.5.6.}$$

Typical experimental results are shown in Fig. C.4.1. The higher electron emission and consequent lower statistical time lag in the case of the oxide layer was attributed to field emission produced by the high field across the oxide layer due to negative ions on its surface. This increase in emission due to an oxide film on tungsten is shown to be opposite to the decrease in emission due to an oxide film on copper found by Strigel 1939 as described in section C.4.2.

It was also found that the value of statistical time lag changed with time during repeated sparking. This was attributed to a change in the state of oxidation of the cathode. This effect is of great importance, and must always be guarded against during measurements of breakdown voltage or time lag.

C.5. Summary.

In conclusion it is seen that the theory of statistical time lag of static breakdown is well established and can be applied successfully to experiment.

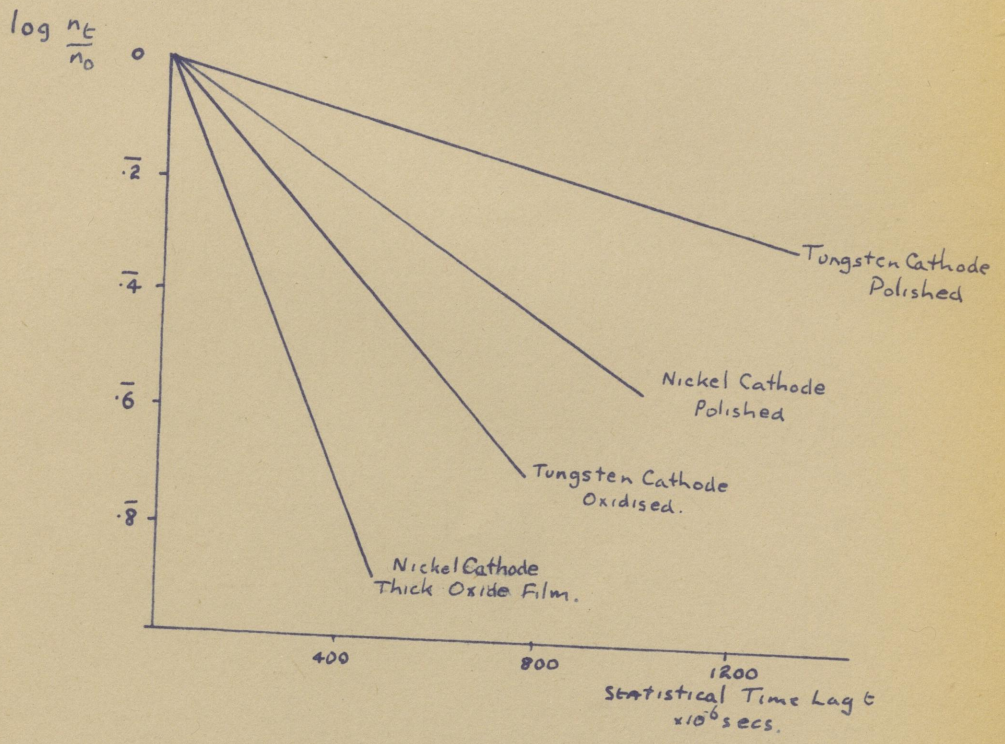

Distribution of Statistical Time Lags.
for Nickel and Tungsten

FIG C4.1

In the next sections devoted to Formative Time Lag, it will be shown in several cases that the reduction of statistical time lag by radiation of the cathode has had to be applied, and that knowledge of the causes of variations in the statistical time lag for different experimental conditions is of considerable importance.

D. FORMATIVE TIME LAG.

D.1. Introduction.

D.1.1. The formative time lag forms the second part of the delay interval. It consists of the time required for an initiatory electron (produced at the end of the statistical time lag) to produce the ionisation processes which ultimately lead to breakdown.

D.1.2. Since both statistical time lag and formative time lag are always present, the study of one is best made when the magnitude of the other is small in comparison. Hence, studies of formative time lag are usually made with strong cathode irradiation in order to reduce the statistical time lag to a minimum.

D.1.3. Several different methods are available for the study of formative time lag, the choice of method being determined by the gas pressure used and the accuracy required. The development of electronic techniques in recent years has greatly increased the accuracy of measurement. Consequently, the conclusions drawn from some early measurements have been shown to be erroneous.

D.1.4. The instant of application of the breakdown voltage is noted as the time when a switch is closed. The actual type of switch depends, of course, on the method used. Three basic techniques have been used to determine the instant of breakdown as follows:

a) observation of intense light emitted at breakdown,

b) observation of the voltage across the electrodes usually by means of a cathode ray oscillograph.

c) Measurement of the growth of current between the electrodes.

Breakdown at high gas pressure in the region of one atmosphere occurs with the emission of intense light and at high breakdown voltage which falls rapidly to a much lower value. It is therefore a suitable case for the application of methods (a) and (b). In contrast, breakdown at low gas pressure (of the order of a few mms. of mercury) does not usually involve a spark, and the fall in voltage from the breakdown voltage to the final value is much slower than in the case of high pressure. The build up of current to the final stable value is much slower at low pressure than at high pressure and method (c) has been used for this case.

Recently the improvement of electronic techniques has allowed the use of method (c) for the high pressure case and the information obtained in this way has proved of great value in the theoretical analysis of breakdown at high pressure.

D.1.5. One of the major problems of the study of formative time lag has been to determine whether or not there is an abrupt transition as the gas pressure is increased, between the long values of formative time lag found at low gas pressure, and the short values of formative time lag found at high gas pressure.

D.1.6. The measurement and theory of formative time lag at low gas pressure of the order of a few millimetres of mercury, have been shown to agree so well, that there is little doubt that breakdown, and the build-up of current, agree with Townsend's concept of a secondary ionisation process, consisting of the emission of electrons from the cathode by the bombardment of positive ions.

D.1.7. In contrast it is only recently that it has been possible to attempt to explain satisfactorily the breakdown mechanism at high gas pressure. Attempts to explain theoretically the observed values of formative time lag have evolved in step with the improvement of experimental technique. It is unfortunate that up to within six years ago proposed theories were incorrect, because they were based on insufficient experimental knowledge.

D.1.8. Briefly, early measurements of formative time lag at high gas pressure, which produced values of the order of 10^{-8} sec., were assumed to preclude the possibility of breakdown by a Townsend mechanism. Based on these measurements, the Streamer theory was proposed in 1940, but this has since been almost entirely discarded because of the contradictory evidence provided by subsequent experiments.

In the following sections, a description will first of all be given of the experimental evidence, on which the Streamer Theory was based, and this will be followed by a description of the theory itself. The next section lists some criticisms of the Streamer Theory, and is followed by descriptions of a number of experiments made recently, which indicate after all that breakdown and the formative time lag at high gas pressure can be explained by the Townsend theory for build-up of current.

D.2. Experimental Evidence of Very Short Formative Time Lags at High Gas Pressure.

D.2.1. In about 1925, it was considered that electrical breakdown in gases occurred by a Townsend mechanism in which the secondary ionising agent consisted of the emission of electrons from the cathode by the bombardment of positive

ions. Before any measurements of formative time lag had been made, Loeb 1928 and Rogowski 1928 had calculated on this basis that the value of formative time lag at atmospheric pressure should be of the order of 10^{-5} sec.

D.2.2. The first measurements of formative time lag were made in air at atmospheric pressure, by observing the voltage across the electrodes of the discharge gap on a cathode ray oscillograph via a potential divider. Such measurements were made notably by Torok 1928, Beams 1928, Taum 1928, Rogowski 1928. The values of formative time lag obtained were of the order of 10^{-8} second, and although the apparatus was crude, a discrepancy between theory and experiment in the ratio of 10^{3} : 1 was regarded as sufficient to discredit the theory of Loeb and Rogowski.

D.2.3. These experiments were quickly followed by others using method (b), which will next be described.

Measurement of time lag using light emitted by the discharge.

The production of intense light is characteristic of breakdown of gases at high pressure. Most studies have been made in air at atmospheric pressure using a Kerr Cell optical shutter. The Kerr Cell contains very pure nitro-benzene, in which are immersed two plates, across which the shutter voltage is impressed. A voltage across the plates renders the nitro-benzene doubly refracting and causes light, which has passed through a nicol prism and is therefore polarised, to be partially transmitted through a second crossed nicol on the other side of the cell.

D.2.4. In the method used by Wilson 1936, the Kerr Cell shutter was triggered at the instant of application

of the voltage across the spark gap. The voltage applied across the gap was in two parts, as shown in Fig. D.2.1. A constant stable approach voltage just below the static breakdown voltage was supplied by T_1. An overvoltage from T_2 could be applied by closing switch S, which at the same time, sent an impulse along the transmission lines W, to remove the voltage across the Kerr Cell. A finite time t, which could be calculated from the length of the wires W, elapsed between the closing of switch S, and the removal of the voltage across the Kerr Cell shutter. Whilst the voltage across the shutter was applied, any light emitted from the spark could be seen through the shutter. The value of t was reduced for each successive breakdown of the gap, until the spark could not be seen through the shutter. The formative time lag measured as the time between the application of the voltage derived from T_2, and the emission of light from the spark gap, was then equal to t, which could be calculated from the length of the wires W. The cathode was continuously illuminated by only weak ultra violet light, so that the priming current was small. Various values of voltage were applied in excess of the minimum value necessary for breakdown, and these were recorded in terms of the percentage overvoltage which is defined as follows:-

$$\text{Percentage Overvoltage} = 100 \times \frac{\text{Voltage applied minus Minimum voltage necessary for breakdown}}{\text{Minimum voltage necessary for breakdown}} \%$$

It was found that lower values of lag were obtained as the overvoltage was increased and there appeared to be no lower limit to the lags even at 200% overvoltage. Also the lowest values of formative time lag were less than the transit time across the gap of either a positive ion or electron. See Fig. D.2.2.

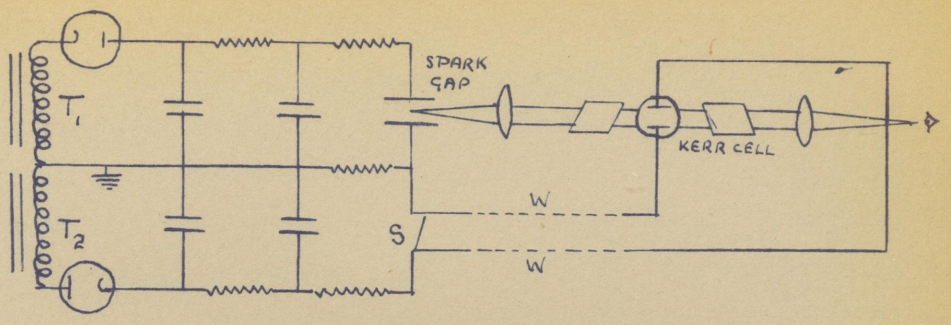

CIRCUIT DIAGRAM OF WILSON'S APPARATUS.

FIG D2·1

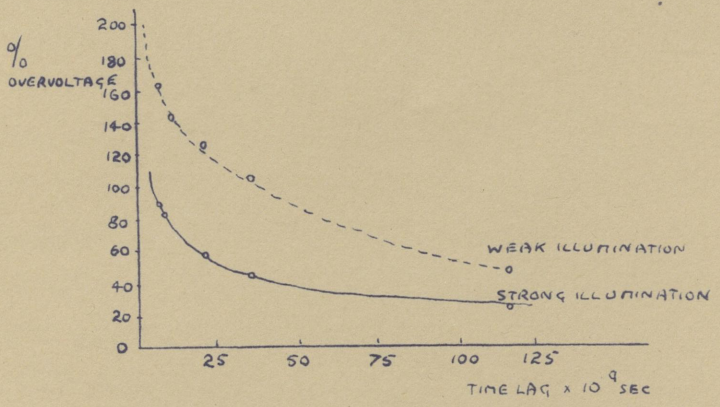

WILSON'S RESULTS

FIG D2·2.

D.2.5. White 1936 used a different technique as follows. Instead of synchronising the application of breakdown voltage with the shutter, White applied a high voltage to the gap, and triggered breakdown by illuminating the cathode from an auxiliary spark as shown in Fig. D.2.3. The additional voltage applied across the auxiliary spark gap G_1 by closing the switch S_1 and opening S_2 simultaneously, was transmitted along the wires W. When the voltage pulse reached the shutter, the light was prevented from passing through. The delay produced by the wires W could then be adjusted, by varying the wire length, to be equal to the time between the application to the main gap of sufficient light to produce breakdown, and the emission of light from the gap. Approximately 10^{-8} sec. was required for the light from G_1 to achieve sufficient intensity, so that the method was not suitable for the measurement of lags much less than 3×10^{-8} sec. Fig. D.2.4. shows the results that White obtained for three different gap lengths, and supports his conclusion that for a given overvoltage the formative time lag is greater for a 1 mm gap than for a 5 mm gap. This was explained by the assumption that breakdown occurred as the result of the build up of space charge by successive electron avalanches. Since in the shorter gap a given electron avalanche would produce less ionisation than in travelling across a larger gap, it was assumed that more avalanches would be necessary, thereby producing a longer time lag.

D.2.6. It is emphasized that the definition of formative time lag used in these methods is different from that used in methods (b) and (c). See D.1.4. Also the two methods just described are of limited accuracy. Thirdly, these measurements were made at high overvoltage only, and in neither case was it possible to measure the

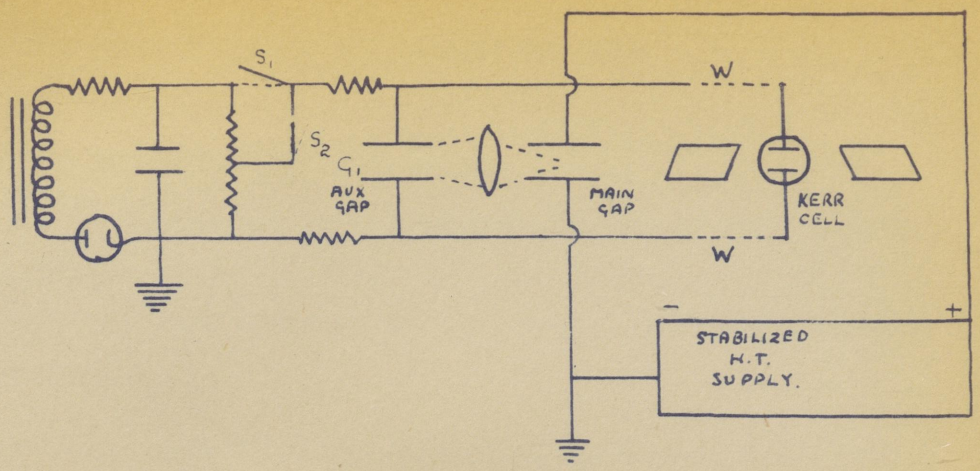

Circuit Diagram of White's Apparatus

FIG D2·3

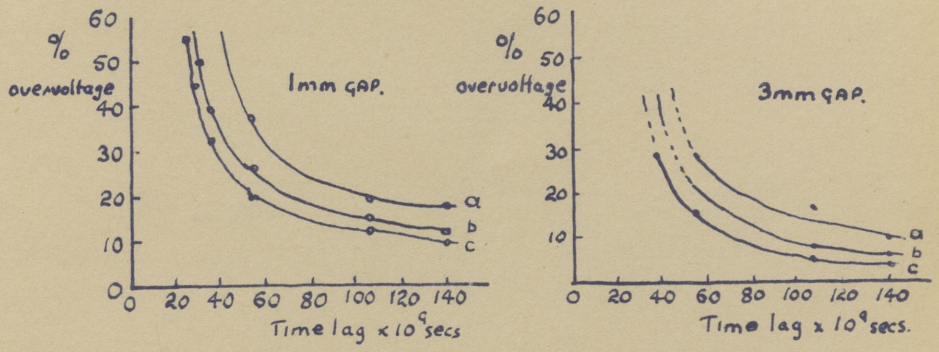

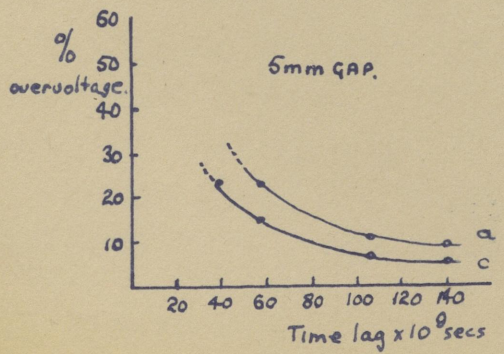

White's Results

FIG D2·4

Priming Current.

a $j_0 = 2 \times 10^{-9}$ amp/cm².

b $j_0 = 8 \times 10^{-10}$ amp/cm².

c $j_0 = 10^{-12}$ amp/cm².

formative time lag at low overvoltage.

For these reasons the methods have been discarded in favour of methods (b) and (c).

However, in spite of the lack of accuracy the values of formative time lag were of the same order of magnitude as those found in the early oscillographic measurements.

D.2.7. Measurement of time lag by monitoring the voltage across the gap.

The second principal technique for the measurement of formative time lag is the observation of the voltage across the gap during the breakdown period. The formative time lag is then defined as the interval between the application of voltage greater than the static breakdown voltage, and the beginning of the fall of voltage across the gap to the value characteristic of the second stable state.

D.2.8. The use of a cathode ray oscillograph was developed by Rogowski and his colleagues for this purpose. A resistive potential divider placed across the gap was used to apply across the y plates of the oscillograph a voltage proportional to the gap voltage. The method used to study impulse breakdown with high overvoltage which produced short formative time lags of the order of 10^{-8} sec. However, the oscillographs used in these early measurements were of crude design compared with those of today and the results were accordingly inaccurate.

D.2.9. Some measurements have already been described in section D.2.2. In addition, it was noted by other workers that the voltage across the gap as observed on the oscillograph sometimes varies with time in a peculiar manner. This was first noted by Rogowski, Flegler and

Tamm 1927 for hydrogen, air and carbon dioxide. It was observed that the voltage across the gap falls rapidly at first but then remains substantially constant for a short period and then falls again to the steady current value. As shown in Fig. D.2.5., the duration of the "step" was found to increase with decreasing pressure, which indicates a slowing up of the current build-up process as the mean free path of the electrons increases. The first part of the step was shown to correspond to the formation of a diffuse glow between the electrodes. During the rapid voltage fall after the step a concentrated filamentary discharge was observed. Buss 1933 has shown that the ratio of the step voltage to the static breakdown voltage of the gap is roughly constant. Fig. D.2.6. shows the variation of step voltage with pressure multiplied by gap width.

D.2.10. In spite of the observations of formative time lag of the order of 10^{-8} sec. during the 1930s, there were still a number of investigators, notably L.B.Loeb, 1928, who still adhered to the Townsend theory of breakdown. It was because of this faith in the Townsend theory that Tilles 1934, who was a member of Loeb's school, devised the following technique for the measurement of formative time lag at low overvoltage. If the Townsend theory could be applied it was expected that formative time lag of the order of 10^{-5} sec. should be obtained for breakdown at very low overvoltage.

On the application to the gap of an overvoltage in excess of the static breakdown voltage, a current was produced which passed through a ballistic galvanometer as shown in the circuit diagram given in Fig. D.2.7. The current was of constant magnitude until it ceased when the gap voltage fell below the static breakdown voltage. Hence the deflection of the galvonometer could be calibrated

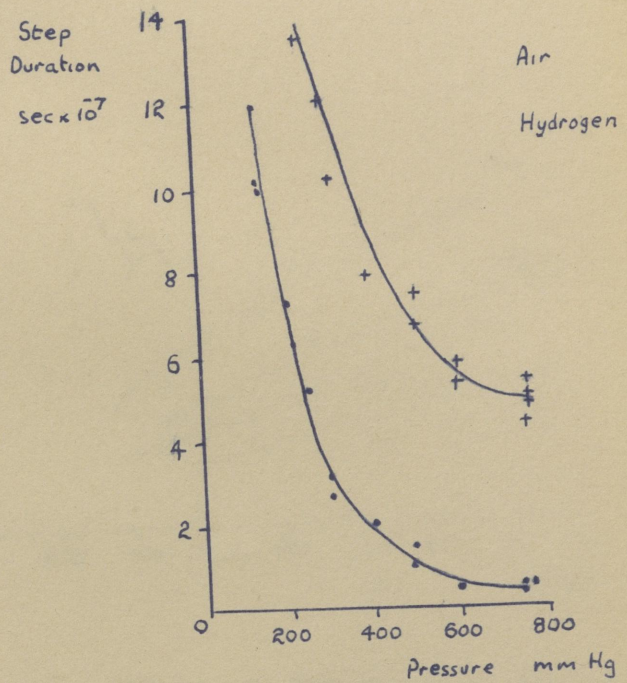

Duration of the step in the voltage collapse in Air and Hydrogen as a function of Gas Pressure.

FIG D2.5

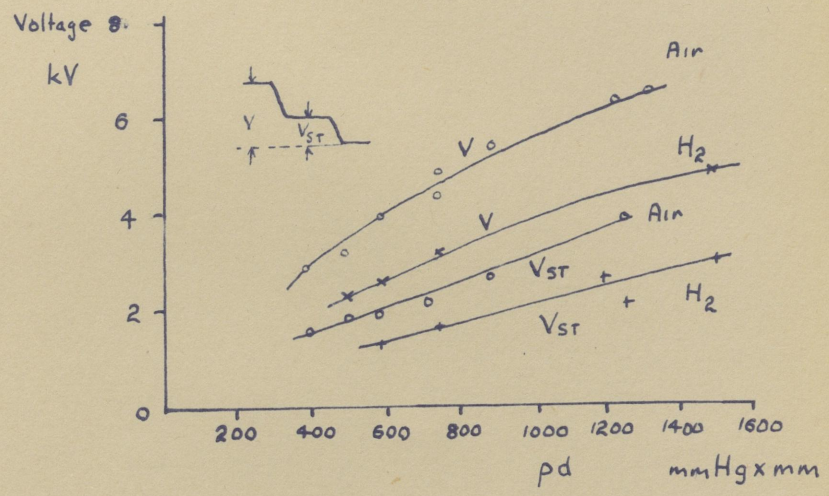

Breakdown Voltage and Step Voltage for discharges in Arr and in Hydrogen as a function of pressure multiplied by electrode separation.

FIG D2·6

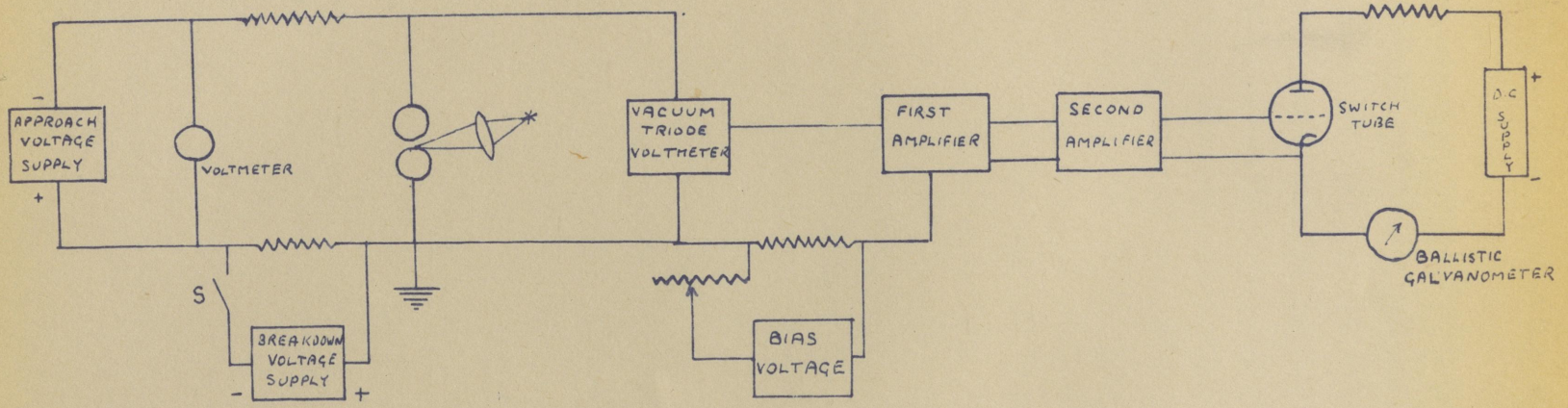

SCHEMATIC DIAGRAM OF TILLES' APPARATUS.

FIG D2·7.

directly against the duration of the current. As shown in Fig. D.2.7. a vacuum triode was placed directly across the gap and acted as valve voltmeter. The reduced voltage was applied in series with an adjustable bias to the input of a two stage resistance coupled amplifier consisting of two vacuum triodes. The bias applied to the amplifier was such that when the voltage across the gap exceeded the static breakdown voltage, the output of the amplifier swung the bias of the grid of the switch tube from a substantial negative voltage, to a substantial positive voltage. The output current of the switch tube was thereby changed from zero to a constant value equal to the anode voltage divided by the external resistance. This current ceased as soon as the voltage across the gap fell below the static breakdown voltage. The time delay was measured by the deflection of the ballistic galvanometer, which was calibrated to give directly in seconds the time that the voltage across the gap remained higher than the value for which the bias was set. The approach voltage was obtained from a synchronously driven self excited motor generator, transformer, rectifier and condenser for smoothing. The pulse was obtained by rapidly switching a bank of batteries in series with the supply.

A very short gap was used between spheres of 0.95 cm diameter separated by a gap of 0.068 cm. The object of using such a short gap was to produce long lags.

Before application of a voltage sufficient to produce breakdown, the approach voltage was adjusted to be 96% of the static breakdown voltage determined beforehand. Then on closing switch S, the pulse could be applied equal to 4% of the static breakdown voltage plus any desired overvoltage.

D.2.11. It was observed that at low values of

illumination the lags were random in length. With an increase in illumination to a value corresponding to a priming current of 5×10^{-13} amps/cm^2 it was found that 30% of the lags were of fixed length of about 10^{-4} sec and 70% were random in length. On increasing the illumination to a value equivalent to a priming current of 2×10^{-12} amps/cm^2, it was found that with approximately 5% overvoltage the lags were all of approximately the same value of 10^{-4} sec. An increase in overvoltage beyond this value produced a further decrease in formative time lag.

D.2.12. The significant feature of this experiment, was that in contrast to the earlier experiments described above, comparatively long formative time lags of the order of 10^{-4} sec. can occur even at high gas pressure, provided the overvoltage is sufficiently small.

However, although the result has since been confirmed by other workers, notably Fisher, it was concluded that the use of an approach voltage produced an accumulation of space charge in the gap before the overvoltage was applied, thereby making the result unreliable. It appears that this experiment was not given the serious attention which it deserved.

D.2.13. Although the following experiment was not performed until after the proposal of the Streamer theory and could not have been taken as evidence on which to propose it, it does show that extremely short values of formative lag are always obtained for high values of overvoltage, and does confirm the predictions of the experiments of Wilson 1936, that the formative time lag decreases with increased overvoltage.

Normal oscillographs are not suitable for the accurate measurement of delays less than 10^{-9}sec. In the experiments of Fletcher 1949, transmission lines were used to eliminate the effects of stray inductance and capacitance on the very rapid transients involved. As shown in Fig. D.2.8a. a three electrode trigger gap was arranged along the centre conductor of a co-axial transmission line and kept under nitrogen. Initially, A was at a positive potential V of the order of 20kV and point B connected to earth. When the centre electrode was triggered with a negative pulse, the trigger gap broke down, and a voltage impulse $\frac{V}{2}$ was sent down the previously earthed transmission line. The coaxial capacitor C serves to sharpen the voltage pulse so that the rise time was of the order of 4×10^{-10}secs.

The voltage across the gap was detected by a special design of oscillograph called a micro-oscillograph, which had previously been developed by G.M.Lee.

The voltage divider between the transmission line and micro-oscillograph consisted of two concentric transmission lines, the characteristic impedances of which produced a divider ratio of 100 : 1.

The spark gap used was as shown in Fig. D.2.8b., and was arranged along the centre conductor of an air dielectric coaxial transmission line. The electrode separation could be adjusted by the micrometer screw with an accuracy of ±0.0003 cm.

The brass cathode was illuminated by ultra violet light from a spark gap and the intensity adjusted by varying the diameter of an aperture placed in front of a quartz concentrator lens.

A schematic diagram of the experimental arrangement is

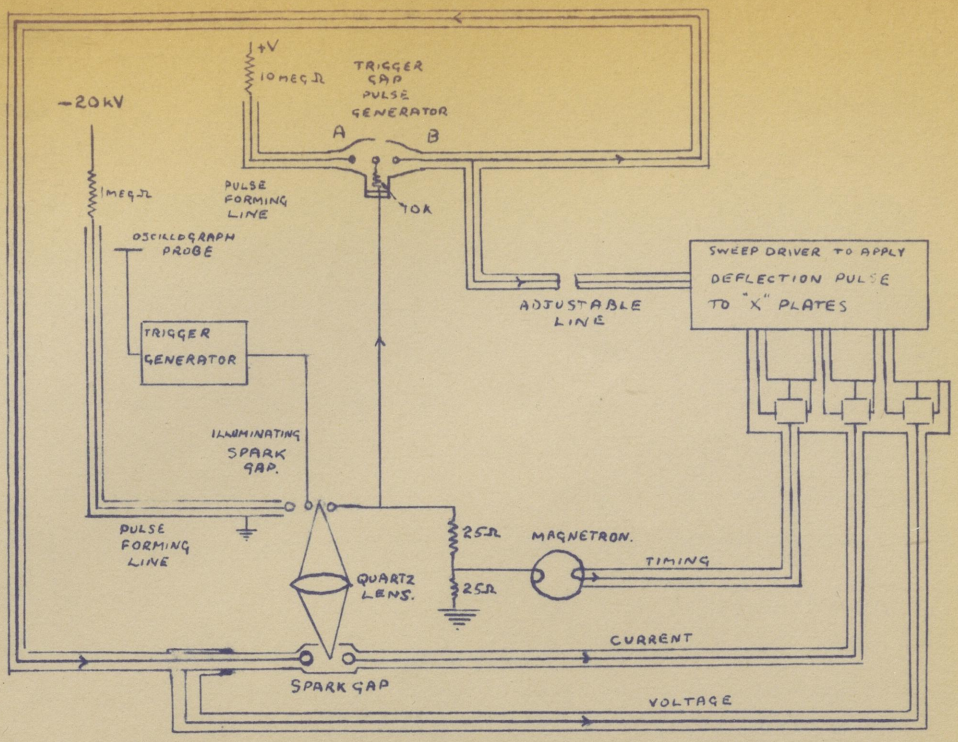

SCHEMATIC DIAGRAM OF FLETCHERS APPARATUS

FIG D2·8c

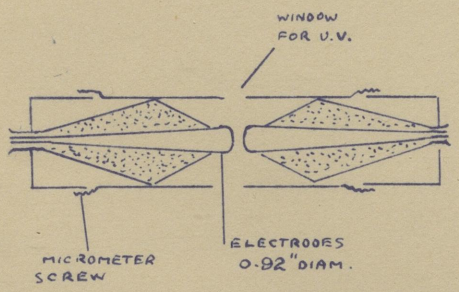

SKETCH OF SPARK GAP

FIG D2·8b

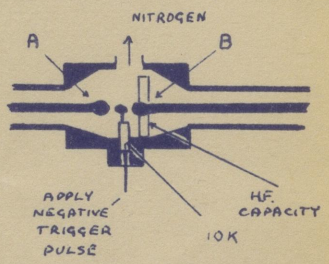

SKETCH OF TRIGGER GAP FOR GENERATING PULSE TO APPLY TO SPARK GAP

FIG D2·8a

shown in Fig. D.2.8c. When the micro-oscillograph was switched on, the trigger generator was synchronised with it to trigger off the illuminating gap. The voltage pulse produced across it triggered of the magnetron, and also triggered the ultra high speed impulse generator. When the impulse generator fired, a portion of the impulse was fed to the sweep driver, while the main part travelled down the transmission line, through the voltage divider to the spark gap. Current through the spark gap was observed by connecting the other side of the gap to the oscillograph through another transmission line. The cables from the voltage divider and the spark gap were so arranged that their signals arrived at the micro-oscillograph simultaneously. Synchronization of these with the sweep was obtained by varying the length of the line to the sweep divider.

D.2.14. The image produced on the micro-oscillograph was corrected for known reflections in the transmission lines to give a record of the variation with time of the voltage across the gap. Examples of this record for various conditions are shown in Fig. D.2.9. The end of the formative time lag was regarded as the point t_p on the figures.

At low intensity of illumination the time lags were random in length. By measuring the distribution of time lags for different values of aperture diameter A, through which the illumination passed, and by assuming that all fluctuations in time lag were due to the inadequate supply of electrons, it was possible to express the number of electrons emitted per second in terms of the aperture size. For a certain light source, the calibration equation relating the priming current i_0 and aperture diameter A was:

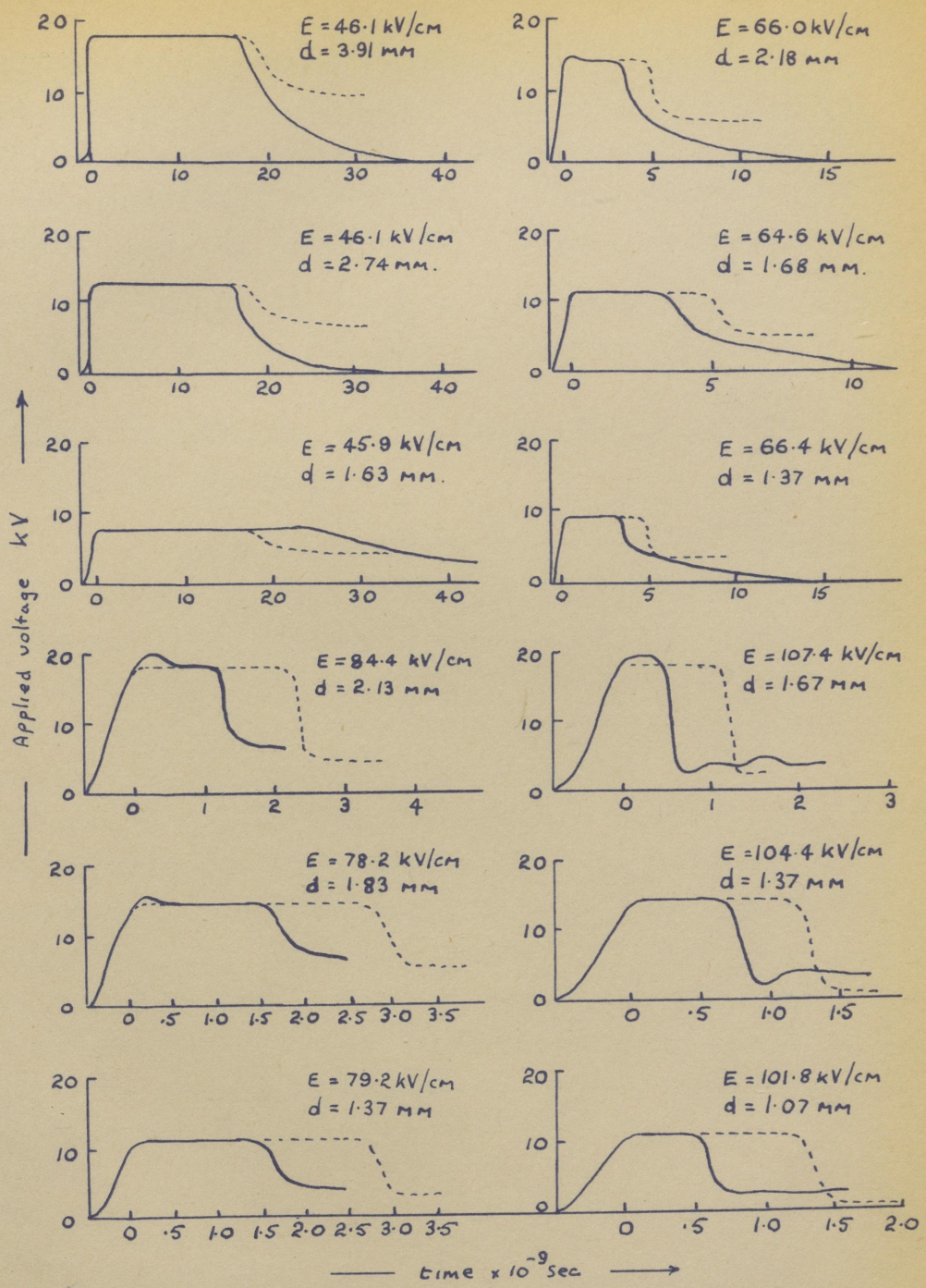

FLETCHER'S OSCILLOGRAMS ——— AND
DICKEY'S CALCUTATED CURVES - - - - - -

FIG D2·9

$$i_o = 4.3A^2 \times 10^{-8} \text{ amps/cm}^2 \qquad \text{D.2.14.1.}$$

The results are plotted in Fig. D.2.10., as a function of the applied field. For fields above 50kV/cm the formative time lag is a function of field alone, i.e. independent of gap width. Below 50kV/cm the formative time lag does depend on the gap width.

The theoretical curve shown on the graph was calculated in the manner outlined later in section D.4.12.

D.3. Introduction to the Streamer Theory of Breakdown at High Pressure.

D.3.1. It has been shown in the preceding section that the values of formative time lag at high pressure obtained in early measurements were of the order of 10^{-8} sec. In comparison, the experimental conditions were such that the transit time of a positive ion across the electrode gap was approximately 10^{-4} sec. Consequently, a secondary ionisation process consisting of the emission of electrons from the cathode by the bombardment of positive ions produced near the anode was unacceptable. At low pressure, at which the formative time lag, as will be shown later, was of the order of the positive ion transit time, it was also possible to predict the breakdown voltage from the Townsend breakdown criterion:-

$$\gamma(\exp.\alpha x - 1) = 1 \qquad \text{B.5.11.9.}$$

D.3.2. Loeb 1928 pointed out, however, that whatever the ionisation process involved, the use of this criterion is open to some doubt since a steady state expression is used to express a transitory process. Whilst the expression may apply at low pressure where space charge formation is negligible, it was considered by Loeb 1928

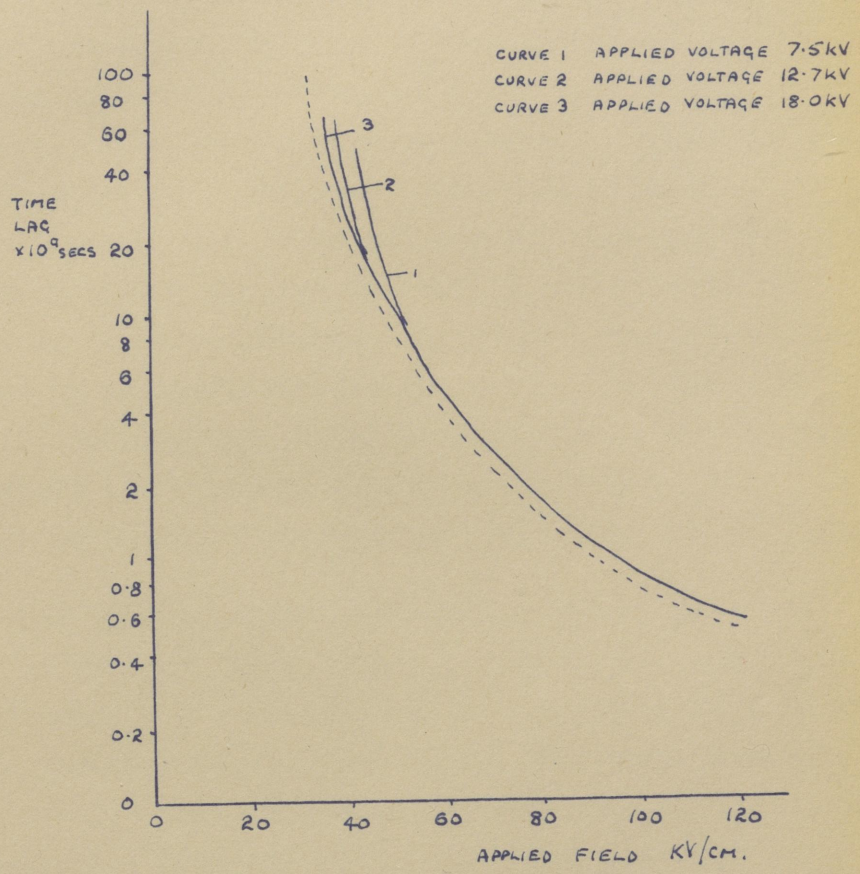

COMPARISON OF THEORY WITH EXPERIMENTAL VALUES DUE TO FLETCHER OF FORMATIVE TIME LAG IN AIR AS FUNCTION OF APPLIED FIELD FOR DIFFERENT GAP LENGTHS.

FIG D2·10

that for air at atmospheric pressure the expression is invalid. The build-up of ionic space charge during the initial current build-up would appreciably affect the potential distribution across the gap in such a way that the electric field at the cathode would be increased. Loeb 1928 calculated that in air at atmospheric pressure, fields of the order of 10^5 to 10^6 volts per cm can be expected as a result of the formation of positive ion space charge. This is due to the fact that $v_- \sim 10^3 v_+$. Loeb came to the conclusion that in the case of air at atmospheric pressure this space charge formation represents the only means by which sufficiently high values of E/p can be produced to provide the value of α required for breakdown. Basing his work on these considerations, Loeb calculated that the formative time lag at atmospheric pressure would be of the order of 10^{-4} sec.

D.3.3. The measurements described above made it necessary to change this original concept. In 1930 Loeb considered the possibility of a series of electron avalanches forming in the gap along the same narrow channel. Each avalanche would leave behind it positive ions which would diffuse radially outwards, but sufficiently slowly to distort appreciably the field along the anrrow discharge channel.

D.3.4. Using similar ideas, Franck and Hippel 1929, and Schumann 1930, calculated the general redistribution of the field in a uniform gap by positive ion space charges developed by the passage of successive avalanches. It was theoretically shown that the rate of ionization in the later avalanches is enhanced, and that breakdown in the gap may depend on the electron transit time.

D.3.5. Even if long time lags were observed in a

particular experiment, these theories assumed that their magnitude would be determined, not by the transit time of a positive ion, but by the fact that a number of electron avalanches are necessary before the optimum value of space charge is reached. It was assumed that when this particular value of space charge is achieved, breakdown occurs rapidly, as demonstrated by the rapid fall of voltage across the gap. However, it was not possible to test these theories on a quantitative basis, because they did not specify the optimum value of space charge. Also, they did not attempt to explain the actual mechanism of breakdown.

D.3.6. Before describing the principles of the Streamer Theory, it is important to note other experimental observations which were taken into consideration before it was proposed.

First of all, as described in section B.5.2., Sanders 1933 had observed that if a plot is made of $\log \frac{i}{i_0}$ against electrode separation for a fixed value of E/p, no upcurving was observed for values of E/p less than 110. See Fig. B.5.1. The absence of curvature implied that no secondary ionisation process occurred, i.e. $\gamma = 0$. Since under these circumstances it is impossible for the Townsend breakdown criterion to apply, the result was interpreted to mean that some additional process is introduced before breakdown occurs.

D.3.7. Secondly, if a Townsend mechanism involving emission of secondary electrons from the cathode by the bombardment of positive ions were the cause of breakdown it was expected that the spark would cover the entire cathode surface from which the secondary electrons are emitted. In contrast, breakdown at high gas pressure is characterised by narrow filamentary sparks. Also,

whereas by a Townsend mechanism it was expected that the spark would start from the cathode, it was frequently observed that sparks produced by a high impulse voltage started near the anode or in some cases in the middle of the spark gap and then extended rapidly towards the cathode.

D.3.8. Thirdly, at atmospheric pressure the breakdown voltage of air had been found to be virtually independent of cathode material. Townsend's theory involving a secondary ionisation at the cathode required a dependence on the cathode work function, i.e. on the value of γ.

D.4. Description of Streamer Theory.

D.4.1. With the weight of experimental evidence to discredit the Townsend theory, it was logical to search for an alternative breakdown mechanism which would be required to satisfy the following conditions:-

a) The formative time lag must be governed by electron movements and not positive ion movements.

b) The spark must follow a narrow path.

c) The spark must depend on secondary processes in the gas and must not involve the cathode.

d) Since the process is most likely at high gas pressure, it may involve space charge formation.

e) During breakdown it must be possible for the region of intense ionisation to be formed first of all near the anode and then extend towards the cathode.

These conditions were satisfied by the Streamer Theory of Loeb and Meek 1941, which extended the theories

already described in the introduction by providing a criterion for the critical space charge formation, and also a qualitative explanation of the mechanism of breakdown once the critical space charge has been formed. This was made possible by the assumption that the Townsend secondary ionisation process may be replaced by photo-ionisation within the gas as follows:-

D.4.2. Consider a particular electron emitted from the cathode. It will be accelerated toward the anode, and produce positive ions and electrons by impact with neutral atoms, in accordance with the value of the first ionisation coefficient α. As described in section B.2.3., after the swarm of positive ions and electrons has reached a distance x the distribution of positive ions is in the form of a cone as shown in Fig. B.2.2.

During and after this period, some atoms are raised to an excited state and after an excited life of approximately 10^{-8} seconds will emit electromagnetic radiation. It was assumed that this radiation is capable of producing electrons and positive ions from neutral atoms. The existence of a column of positive ions produces a radial field E_r, directed towards the avalanche axis, and consequently the electrons produced by the photons are attracted towards the centre of the avalanche. It was assumed that if this radial field E_r produced by space charge is high enough, new electrons can be accelerated to the energy required to produce more positive ions and electrons. Thus little avalanches were assumed to be formed as shown in Fig. D.4.1a. As more and more positive ions are produced in the beam, a high density of positive ions and electrons is produced within it. This region is

formed first near the anode and then extends towards the cathode as shown in Fig. D.4.1b. When it reaches the cathode a conducting filament of positive ions and electrons has been produced and breakdown is complete. This latter process was assumed to occur very rapidly. The formative time lag was regarded as the time required for a critical space charge field E_r to be built up at which sufficient photo-ionisation exists to multiply the ionisation.

The process should be most efficient when the absorption of photons is high, as in the case of high gas pressure. At low gas pressure the mean free path would be too long for the positive ion swarm to form.

D.4.3. It is at once obvious that this proposal satisfies many of the conditions. Breakdown will be governed by electron movement. Since the spark channel follows the course of the single initiatory electron avalanche, it will be narrow, and the emission of light would be expected to appear first of all at the anode.

D.4.4. The need to be able to calculate the critical space charge for breakdown to commence was satisfied by Meek (see Loeb and Meek 1941), who assumed that the critical space charge has been formed when the space charge field becomes equal to the applied field.

The calculation of the space charge field presented many mathematical difficulties and it was necessary to simplify the space charge distribution. Briefly the method of analysis was as follows:-

Consider an electron avalanche as shown in Fig. D.4.2., and let the distance of the centre of the head of the avalanche from the cathode be denoted by x. At this point, let the radius of the avalanche be denoted by r. Actually, there will not be a sharp edge to the avalanche

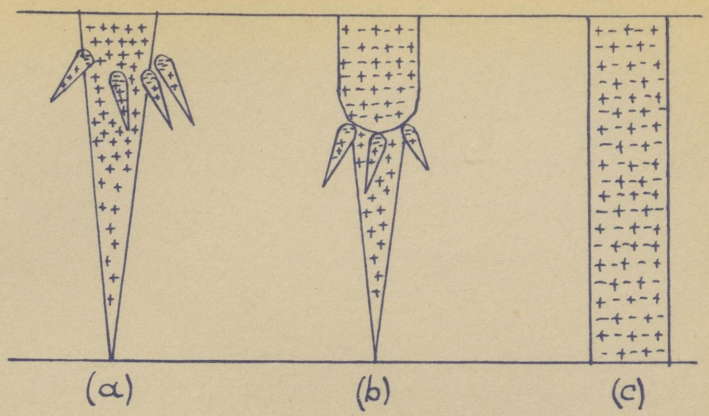

TRANSITION FROM AN AVALANCHE TO A STREAMER ACCORDING TO MEEK

FIG D4.1

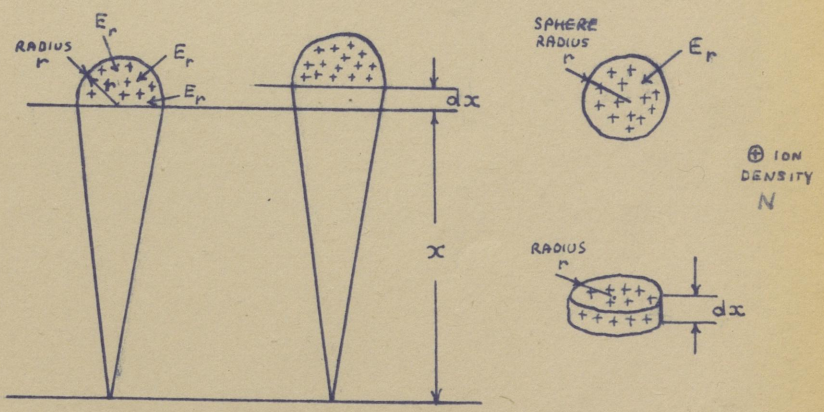

SKETCHES OF APPROXIMATIONS USED IN STREAMER THEORY

FIG D4.2

but a gradual decrease in positive ion and electron density radially outwards from the avalanche axis. The broadening of the avalanche as it proceeds towards the anode is due to diffusion. The radius r was defined as the average distance of positive ions from the avalanche axis. From the theory of diffusion, it was calculated that t secs. after the avalanche started at the cathode, the radius r may be expressed by $\sqrt{2D_+ t}$.

D.4.5. In order to calculate the electric field at the head of the avalanche, it was assumed to be equal to the field at the surface of a sphere of radius r containing the density of positive ions present in the head of the avalanche. Of course, the distribution of positive ions was not actually in the form of a sphere. The density of positive ions in the head of the avalanche was calculated as follows:-

At distance x from the cathode, the avalanche radius was r. When the centre of the head of the avalanche has moved to a distance $x + \Delta x$ from the cathode, the number of additional positive ions produced is given by

$$\frac{d\,(\exp.\alpha x)}{dx}\,\Delta x \qquad \text{D.4.5.1.}$$

$$= \alpha \exp.\alpha x\, \Delta x \qquad \text{D.4.5.2.}$$

Hence the number of additional positive ions produced per unit volume is:

$$N = \frac{\exp.\alpha x\, \Delta x}{\Delta x \pi r^2} = \frac{\alpha \exp.\alpha x}{\pi r^2} \qquad \text{D.4.5.3.}$$

N was regarded as the charge density in the hypothetical sphere of charge at the head of the avalanche.

The field E_r across the surface of a sphere radius r

containing N ions per unit volume is:-

$$E_r = \frac{4}{3}\pi r\, Ne = \frac{4}{3}\frac{e\alpha \exp.\alpha x}{r} \qquad \text{D.4.5.4.}$$

D.4.6. The next step was to convert this expression into terms which could be measured by experiment. The value substituted for r was $\sqrt{2D_+ t}$, where D_+ could be determined by independent experiment; α was obtained from the experimental values of Sanders 1933, for the particular value of E/p considered; the time t required for the avalanche to move to a distance x from the cathode was deduced from the cloud chamber measurements of avalanche velocity made by Raether 1941.

D.4.7. A comparison was made between the experimental values of breakdown voltage and the value predicted by the Streamer theory. The method was to take various values of E/p and the appropriate values of α, D_+ and avalanche velocity and calculate the value of E_r. The value of E/p for which $E = E_r$ was then regarded as the breakdown voltage.

In practice, it was found that better agreement between theory and experiment was obtained by using as the breakdown criterion

$$E_r = KE \qquad \text{D.4.7.1.}$$

where $K = 0.1$

D.4.8. It must be remembered that the theory is only approximate because of the simplifications necessary to allow mathematical treatment. Therefore, agreement or lack of agreement with experiment does not necessarily prove or disprove the fundamental principles. Bearing this in mind, the Streamer theory did represent a major advance in theory and although it had many limitations, at the time, it seemed to give the best explanation of

breakdown processes at high pressure.

D.4.9. The application of the above principles to the calculation of formative time lag was developed first by Loeb and Meek 1941.

They assumed that when the formative time lag was less than the transit time of an electron avalanche, the critical space charge developed before the avalanche reached the anode, and that the spark produced on breakdown was in the form of a "mid gap streamer": i.e. the spark started at a point between the anode and cathode and then proceeded rapidly towards the cathode.

D.4.10. When the formative time lag exceeded the transit time of an electron avalanche, they assumed that more than one avalanche was necessary before breakdown occurred. Each successive avalanche leaves behind it a swarm of positive ions which they assumed to distort the applied field. Hence, after a given avalanche the next avalanche occurred by virtue of a value of α enhanced by the residual positive ion space charge. Loeb and Meek 1941 assumed that if for the first electron avalanche the value of K does not exceed 0.1, the positive ions produced a modified field, as shown in Fig. D.4.3. At the anode the field is decreased by ΔE and at the cathode the field is increased by ΔE. Then by application of Poissons equation:

$$2\Delta E = \int_0^d 4\pi \rho \, dx = 4\pi N e d \qquad \text{D.4.10.1.}$$

where N represents the positive ion density.

If the current density of electrons leaving the cathode is j_0, then the current density of positive ions

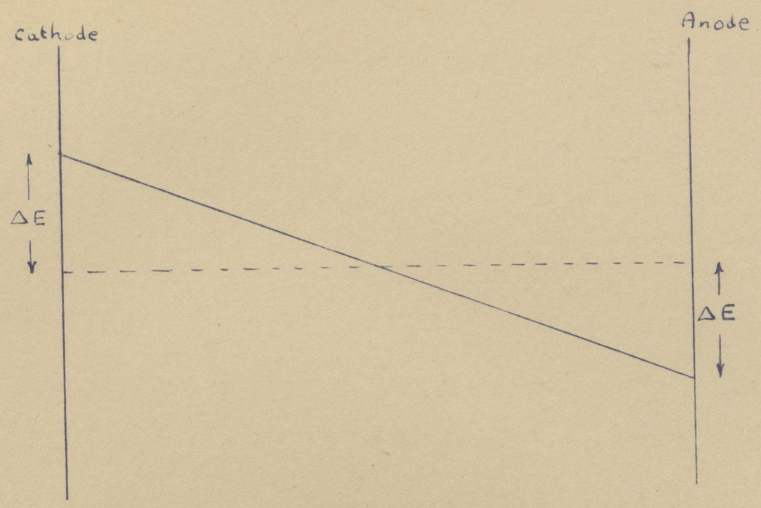

Change in Field across Gap due to Space Charge Formation

FIG D4·3

leaving the anode is:

$$j_0 \exp.\int_0^d \cdot \exp.\alpha\, dx \qquad \text{D.4.10.2.}$$

The time of transit of these ions across the gap is $\frac{d}{v} = \frac{d}{K_+ E}$ where K_+ is the positive ion mobility.

Then the density of positive ions in the gap at any instant is

$$N = j_0 \exp.\int_0^d \alpha\, dx \frac{d}{K_+ E} \frac{1}{d} \qquad \text{D.4.10.3.}$$

If equation D.4.10.1. is combined with equation D.4.10.3., to eliminate N the value of ΔE is given by

$$\Delta E = 18\pi(j_0 d \exp.\int_0^d \alpha\, dx) \qquad \text{D.4.10.4.}$$

The determination of the formative time lag was then made for any particular value of j_0 and applied field E. After the first "wave" of positive ions, which fills the gap, the new field across the gap could be calculated from equation D.4.10.4. From this could be calculated the variation of α across the gap. From such a curve for α the new value of $\int_0^d \alpha\, dx$ was calculated and substituted in Meeks equation for E_r.

The calculation was repeated until the value of E_r after a certain number of positive ion transit times became equal to KE. Then the formative time lag was assumed to be equal to the number of positive ion transit times required.

D.4.11. The analyses of Loeb and Meek cannot be regarded as complete. Firstly, no attempt was made to correlate quantitatively the Streamer theory with experimental values of formative time lag of the order of 10^{-8} secs.

Secondly, the prediction of long formative time lags of the order of 10^{-4} secs. depends on the value of K assumed in the Meek breakdown criterion which was only based on correlation of the Streamer theory and experimental values of breakdown voltage.

D.4.12. The only attempt known to explain formative time lags of the order of 10^{-8} secs. on the basis of the Streamer theory was made by Fletcher 1949, to explain his experimental results described in section D.2.13.

Fletcher 1949 modified Meeks analysis by considering the distribution of electrons and the distribution of positive ions in the electron avalanche and obtained two equations, which represented respectively, the variation with distance from the cathode of the number of electrons and number of positive ions. Because of their greater mobility, the centre of mass of the electrons preceded the centre of mass of the positive ions and their mutual separation increased as the electron avalanche proceeded towards the anode. Fletcher 1949 was forced to simplify greatly the picture of the charge distribution, and regarded the electrons and positive ions as distributed in two mutually independent spheres of charge, separated by an ever increasing distance as the avalanche proceeded. He calculated the field along the avalanche axis between the two charge centres and assumed that breakdown occurred when the axial field became equal to the applied field.

D.4.13. As shown in Fig. D.3.10. the correlation between theory and experiment was quite good. However, Fletcher's 1949 analysis did not explain the stepped nature of the voltage across the gap during breakdown, as demonstrated in Fig. D.2.9.

D.4.14. In conclusion, although the Streamer theory does overcome a number of objections to the Townsend theory, it does not provide a very satisfactory quantitative explanation of short formative time lags at high gas pressure.

D.5. Contradictory evidence subsequent to the proposition of the Streamer Theory.

D.5.1. Fisher's Measurement of Formative Time Lag at High Pressure.

As already described, one of the principal reasons for the proposal of the Streamer Theory was the failure to explain the very short time lags obtained at high gas pressure on the basis of the Townsend theory. It was believed that values of 10^{-8} sec. were typical of breakdown under all conditions at high gas pressure.

However, in 1950 Fisher and Bederson showed that this is not the case and that the experimental results of Tilles 1934 previously discredited were probably correct.

D.5.2. The object of Fisher and Bederson 1950 and 1951 was to measure the formative time lag over a wide range of overvoltage and gas pressure, in order to detect a transition from breakdown by the Streamer theory mechanism at high gas pressure, to the Townsend theory mechanism at low gas pressure as the gas pressure was reduced. The experimental technique used made possible for the first time, the accurate measurement of formative time lag at low overvoltage, and the results obtained provided a major contribution to the understanding of the breakdown process.

D.5.3. The apparatus used was as shown in Fig. D.5.1. By the application of a pulse at A, the stable d.c. bias

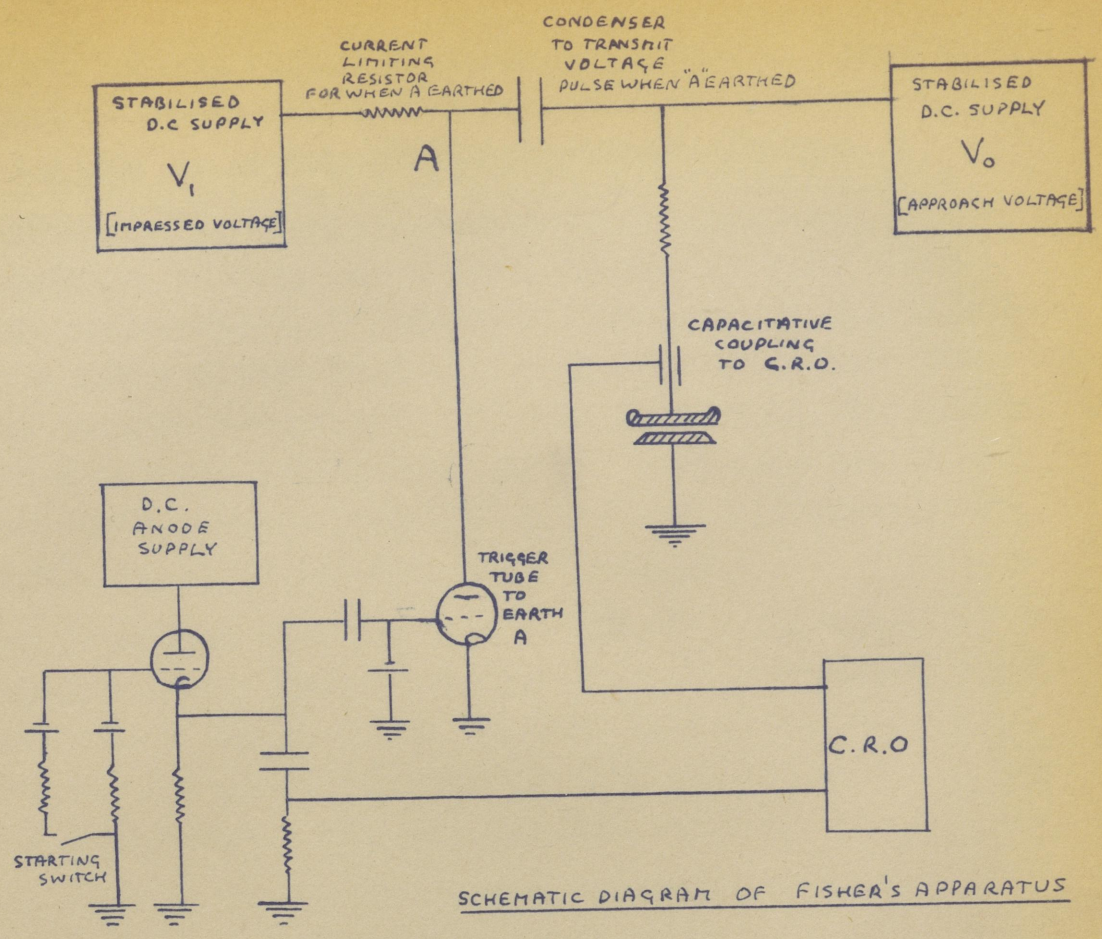

SCHEMATIC DIAGRAM OF FISHER'S APPARATUS

FIG D5·1

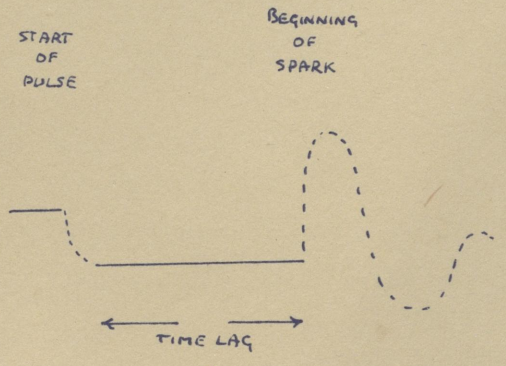

TYPICAL OSCILLOGRAPH TRACE

FIG D5·2

supply was connected to earth potential. Thereby, a pulse of magnitude V_1 was impressed upon the d.c. potential V_o of the plates via condenser C.

First of all, accurate measurements were made of the breakdown voltage for various values of pxd. For each measurement of formative time lag, V_o was adjusted to a value either 2000 volts or 4000 volts less than the breakdown voltage. It was found that the results obtained were independent of the bias used and it was therefore assumed that the space charge formation due to the approach voltage was negligible.

The formative time lag was observed on the oscilloscope capacitatively coupled to the lead to the plates and the actual value of the lag was defined as the time between the attainment of the peak pulse amplitude and the beginning of the voltage fall as shown in Fig.D.5.2.

For most of the measurements, the ultra violet illumination of the cathode was adjusted to provide a priming current i_o sufficient to eliminate statistical time lags but not large enough to distort the applied field by the formation of space charge as confirmed by measurements with different approach voltage.

D.5.4. Fig. D.5.3. shows the variation of formative time lag with percentage overvoltage for a 1 cm gap over a range of pressure from 291 mm Hg to 756 mm Hg. The result is significant in that virtually no variation of formative time lag with pressure for a given overvoltage was observed and so no transition point was apparent, although at the lowest pressure the Townsend criterion applied.

For different gap lengths the variation of formative time lag with overvoltage followed a similar but displaced curve as shown in Fig. D.5.4. Fig. D.5.5.

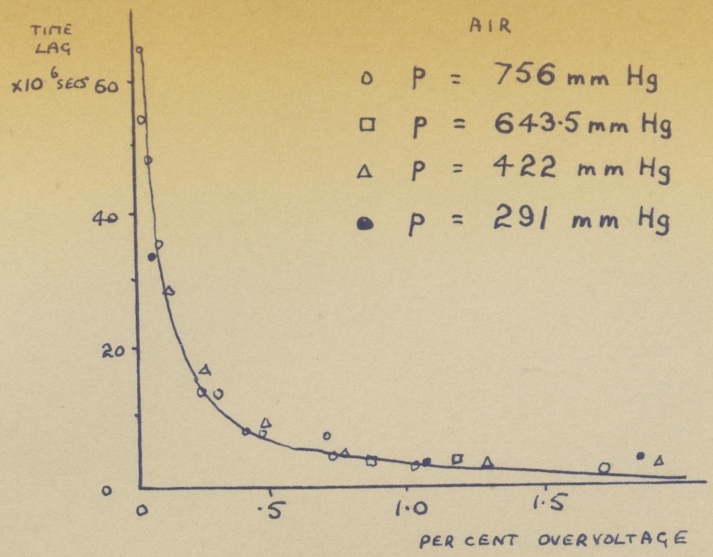

FORMATIVE TIME LAG AS A FUNCTION OF OVERVOLTAGE FOR A 1cm GAP IN AIR AT VARIOUS PRESSURES

FIG D5·3

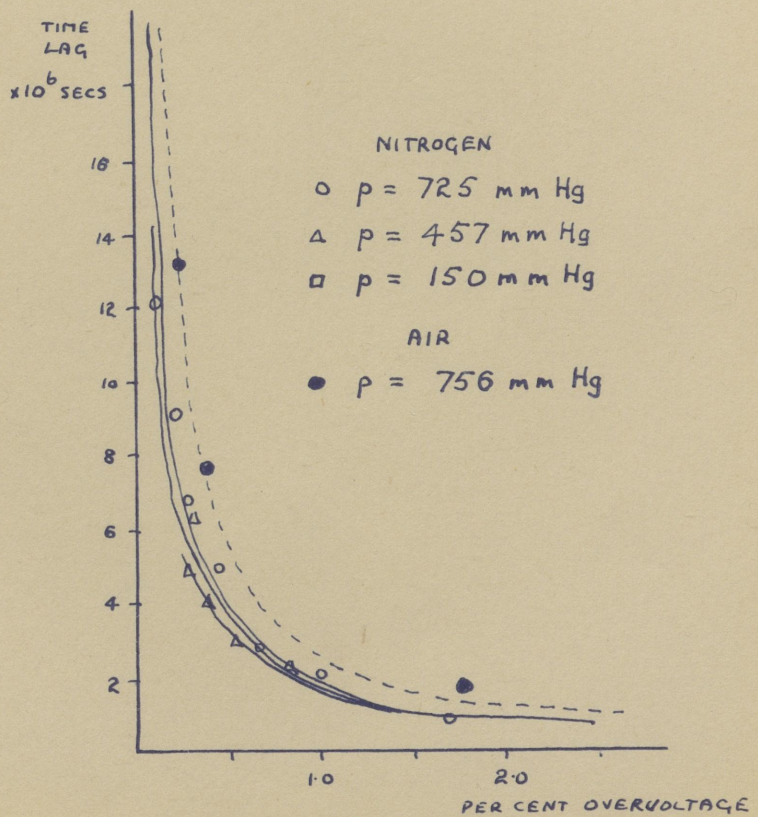

FORMATIVE TIME LAG AS A FUNCTION OF OVERVOLTAGE FOR A 1cm GAP IN NITROGEN AT VARIOUS PRESSURES COMPARED WITH VALUES FOR AIR

FIG D5·6

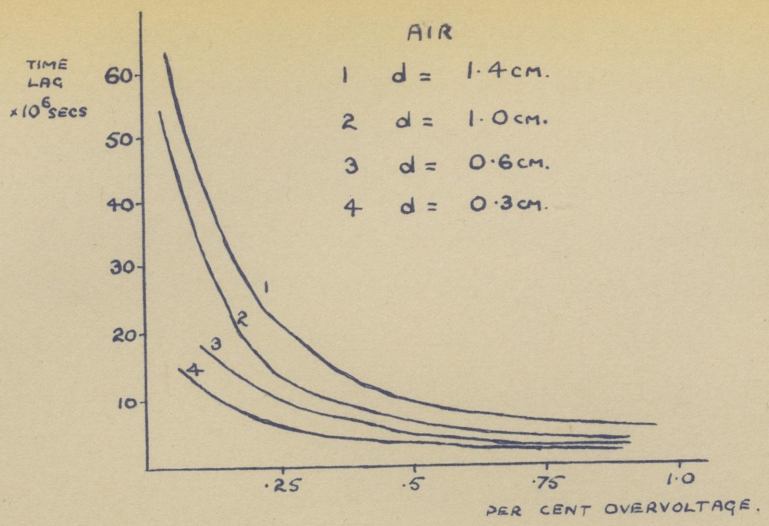

FORMATIVE TIME LAG AS A FUNCTION OF OVERVOLTAGE FOR FOUR GAP LENGTHS

FIG D5·4

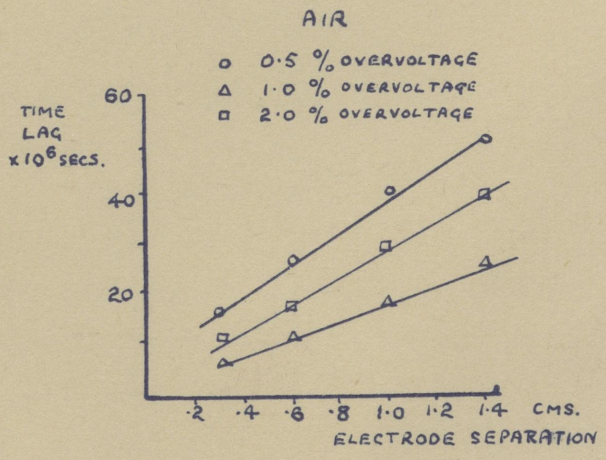

FORMATIVE TIME LAG AS A FUNCTION OF ELECTRODE SEPARATION FOR THREE VALUES OF PER CENT OVERVOLTAGE

FIG D5·5

demonstrates that to a first approximation the lag was found to be proportional to the gap length for a given overvoltage. Hence, it seems that the overvoltage and not the pressure is the critical parameter and any worthwhile experimental apparatus must provide a very accurate control and knowledge of the overvoltage applied. This is one of the principal reasons why earlier results described in sections D.2.1. - D.2.13. must be treated with caution.

The variation of formative time lag with priming current was very small. For instance, the curve shown in Fig. D.5.3. was obtained both for a priming current of 1.3 electrons/sec. and a priming current of 20 electrons per sec. This result tended to conflict with the concept of breakdown produced by the growth of space charge.

D.5.5. Using similar apparatus and experimental procedure, Fisher and various collaborators have measured lags in other gases as follows:-

Kachickas and Fisher 1952 described measurements of formative time lag of breakdown of a uniform field in nitrogen as a function of overvoltage, at gas pressures within the range 150 to 700 mm Hg and for gap lengths of from 0.3 mm to 1.4 mm. The curves relating formative time lag to overvoltage were almost the same as those for air, as shown by Fig. D.5.6. The time lags were unaffected by changes in priming current ranging from 20 to 200 electrons/sec.

It was found that dependence on the priming current was different for the two cases of (a) tank nitrogen and (b) "pure" nitrogen which had in addition been passed over red hot copper and through a liquid nitrogen trap.

D.5.6. Using the same apparatus as in their

investigations of the breakdown of air and nitrogen Kachickas and Fisher 1953 measured the formative time lags in argon as a function of overvoltage from about 5% to 100% within the pressure range 100-700 mm Hg and with electrode separations of from 0.3 to 3.0 cm. It was found that the formative time lag at a given overvoltage in argon is much longer than in the case of air or nitrogen and lags corresponding to overvoltages less than 5% could not be measured on the equipment. Values of formative time lag for the two gases air and argon are compared in Fig. D.5.7., from which it is seen that in the case of argon an overvoltage of 100% must be applied before the time lags decrease below 10^{-6} sec. The variation of formative time lag with overvoltage for various values of electrode separation is shown in Fig. D.5.8.

In view of the much longer values of time lag than those found in air, it was concluded that the breakdown mechanisms were different. This will be discussed in section D.6.7.

D.5.7. The most important feature of the results was that they could not be reconciled with the Streamer theory but as will be shown in section D.6.13. agreed quite well with the assumption of a Townsend mechanism incorporating the emission of electrons from the cathode by the impact of photons.

D.5.8. Llewellyn Jones Study of Photoionisation.

The Streamer theory was based on photoionisation in the gas because it was thought that a Townsend breakdown process was impossible. However, there was no experimental evidence at the time to prove photoionisation in the gas was possible either. In fact,

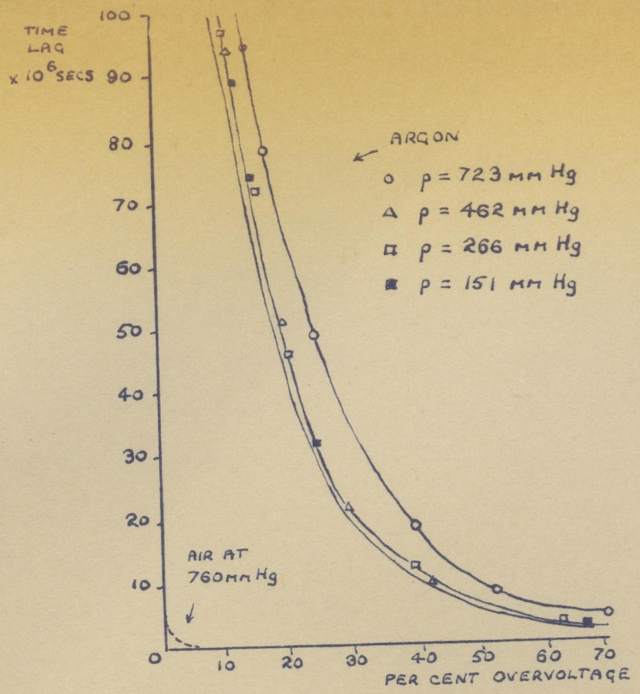

FORMATIVE TIME LAG AS A FUNCTION OF OVERVOLTAGE FOR A 1 CM GAP IN ARGON AT VARIOUS PRESSURES COMPARED WITH CURVE FOR AIR

FIG D5·7

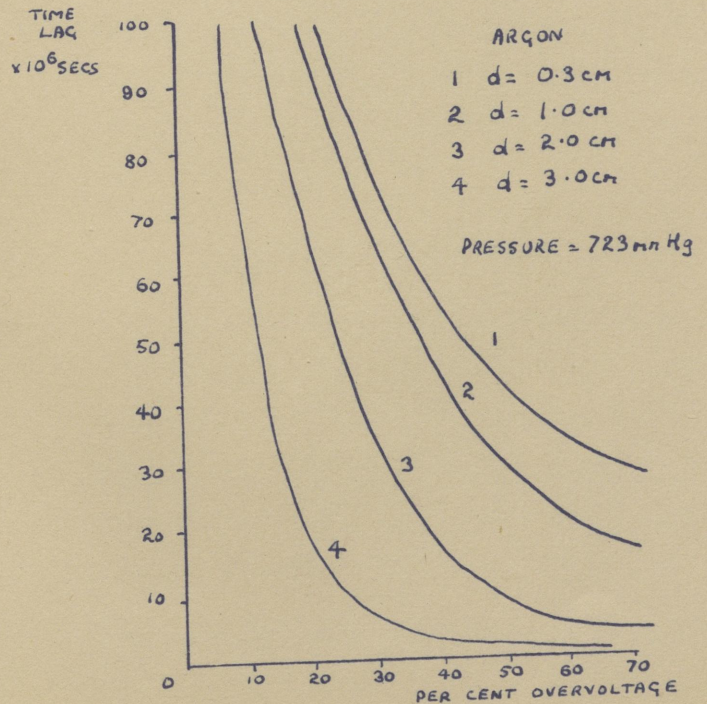

FORMATIVE TIME LAG AS A FUNCTION OF PER CENT OVERVOLTAGE FOR FOUR VALUES OF ELECTRODE SEPARATION

FIG D5·8

this process was difficult to explain for the case of a pure gas because the energy of the photon must be at least as great as the energy required to raise the energy of the neutral atoms to the ionisation energy. Unless a large number of excited atoms exist, which can be further excited by the photons, the probability of ionisation by photons for a pure gas will be very small. On the other hand, in the case of a gas mixture such as air, the energy of a photon from one gas atom A may be greater than the ionisation energy of the other B. The atom B may then be ionised by the absorption of a photon.

In 1953 J. Dutton, S.C. Haydon, F. Llewellyn Jones and P.M. Davidson reached the conclusion that photo-ionisation within the gas is possible only under certain conditions. Known valves of the relevant absorption coefficients and atomic cross sections for photons in air were applied and it was concluded that photoionisation does not contribute appreciably to breakdown in air.

D.5.9. Llewellyn Jones study of $\log \frac{i}{i_0}$ versus d.

The need to assume photoionisation in the gas was based mainly on Sanders 1933 failure to detect any curvature of the graphs of $\log \frac{i}{i_0}$ versus d for values E/p less than 110, i.e. the experimental observation that breakdown occurred without a Townsend secondary ionisation mechanism at high gas pressure.

The work of Sanders 1933 has recently been reviewed and repeated by Llewellyn Jones and Parker 1952, who demonstrated that the apparatus used by Sanders was not sufficiently accurate to detect any upcurving of the $\log \frac{i}{i_0}$ versus d graph.

D.5.10. In the method used by Sanders 1933, the spark gap was connected in series with a condenser so that the flow of current across the gap charged the condenser. For an applied voltage below the breakdown voltage, the current flowing was constant. Hence, the magnitude of the current could be determined by allowing it to flow for a fixed time, e.g. 10 secs. and measuring the potential to which the condenser became charged using a Dolazalek electrometer.

D.5.11. We must now consider the experimental conditions under which a secondary ionisation coefficient γ could be detected.

From

$$i_1 = i_o \frac{\exp. \alpha d}{1 - \gamma(\exp. \alpha d - 1)} \qquad \text{D.5.11.1.}$$

$$i_2 = i_o \exp. \alpha d \qquad \text{D.5.11.2.}$$

where i_1 denotes the current produced when a secondary ionisation coefficient exists and i_2 denotes the current in the absence of a secondary ionisation coefficient.

Then

$$\frac{i_1 - i_2}{i_2} = \gamma(\exp. \alpha d - 1) \qquad \text{D.5.11.3.}$$

Thus, if i_1 is to be detected $\gamma(\exp. \alpha d - 1)$ must not be negligible compared to unity.

The conditions used by Sanders were as follows:-

At E/p = 36V/cm/mm Hg it was found that $\frac{\alpha}{p}$ was 0.0082. From the measurements of Whitehead, the value of pd at breakdown for this value of E/p is 5000 mm Hg.cm.

At breakdown

$$\gamma(\exp.\alpha d - 1) = 1 \qquad \text{D.5.11.4.}$$

or
$$\gamma = (1-\gamma)\exp.(-\frac{\alpha}{p} \times pd) \qquad \text{D.5.11.5.}$$

$$\therefore \gamma = \exp.(-\frac{\alpha}{p} \times pd) \qquad \text{D.5.11.6.}$$

$$\therefore \gamma = \exp.(-0.0082 \times 5000) \qquad \text{D.5.11.7.}$$

$$\therefore \gamma = \exp.(-41) \qquad \text{D.5.11.8.}$$

The gas pressure used was 380 mm Hg.

The largest value of d used was 2.5 cm., when

$$\alpha d = \frac{\alpha}{p} \times p \times d \qquad \text{D.5.11.9.}$$

$$= 0.0082 \times 380 \times 2.5$$

$$= 7.8 \qquad \text{D.5.11.10.}$$

Hence,

$$\frac{i_1 - i_2}{i_2} = \exp.(-41) \times \exp.(7.8) \qquad \text{D5.11.11.}$$

which was so small as to lie outside the possibility of measurement.

It should be noted that for breakdown pd = 5000 mm Hg.cm. at p = 380 mm., so that the gap separation would have had to be increased from 2.5 cms. to $\frac{5000}{380}$ = 13 cms. before breakdown occurred.

Consequently, it is imperative that the current be measured at an electron separation close to that at which the spark would occur if a secondary ionisation coefficient is to be detected. Llewellyn Jones calculated that the measurements must be made for

electrode separations in a range within 20% of the sparking distance.

D.5.12. The apparatus used is shown diagrammatically in Fig. D.5.9. The cathode was illuminated by ultra violet light passed through holes in the anode and the electrode separation could be adjusted by a micrometer screw. Great care was taken to exclude mercury vapour from the chamber and it was necessary to use very stable sources of voltage supply because it should not vary during the charging of the condenser in series with the gap which in Llewellyn Jones apparatus was part of an electrostatic balance.

D.5.13. It was found that variations in current occurred during the time used to charge the condenser, due to variations in the condition of the cathode surface. But with great care, sufficiently repeatable results were obtained which are shown in Fig. D.5.10. for the case of air. It will be observed that for each value of E/p there was a definite upcurving of the graph from which it was possible to calculate the value of γ assuming the value of α obtained from the linear part.

The crucial test was made by introducing these values of α and γ in the Townsend breakdown criterion $\gamma(\exp.\alpha d - 1) = 1$. Excellent agreement was obtained.

D.5.14. A repeat of these experiments for nitrogen by J. Dutton, S.C. Haydon and F. Llewellyn Jones 1952 also showed the existence of a Townsend secondary ionisation coefficient which provided a good theoretical prediction of the breakdown voltage by substitution in the Townsend breakdown criterion.

D.5.15. A further feature of these investigations

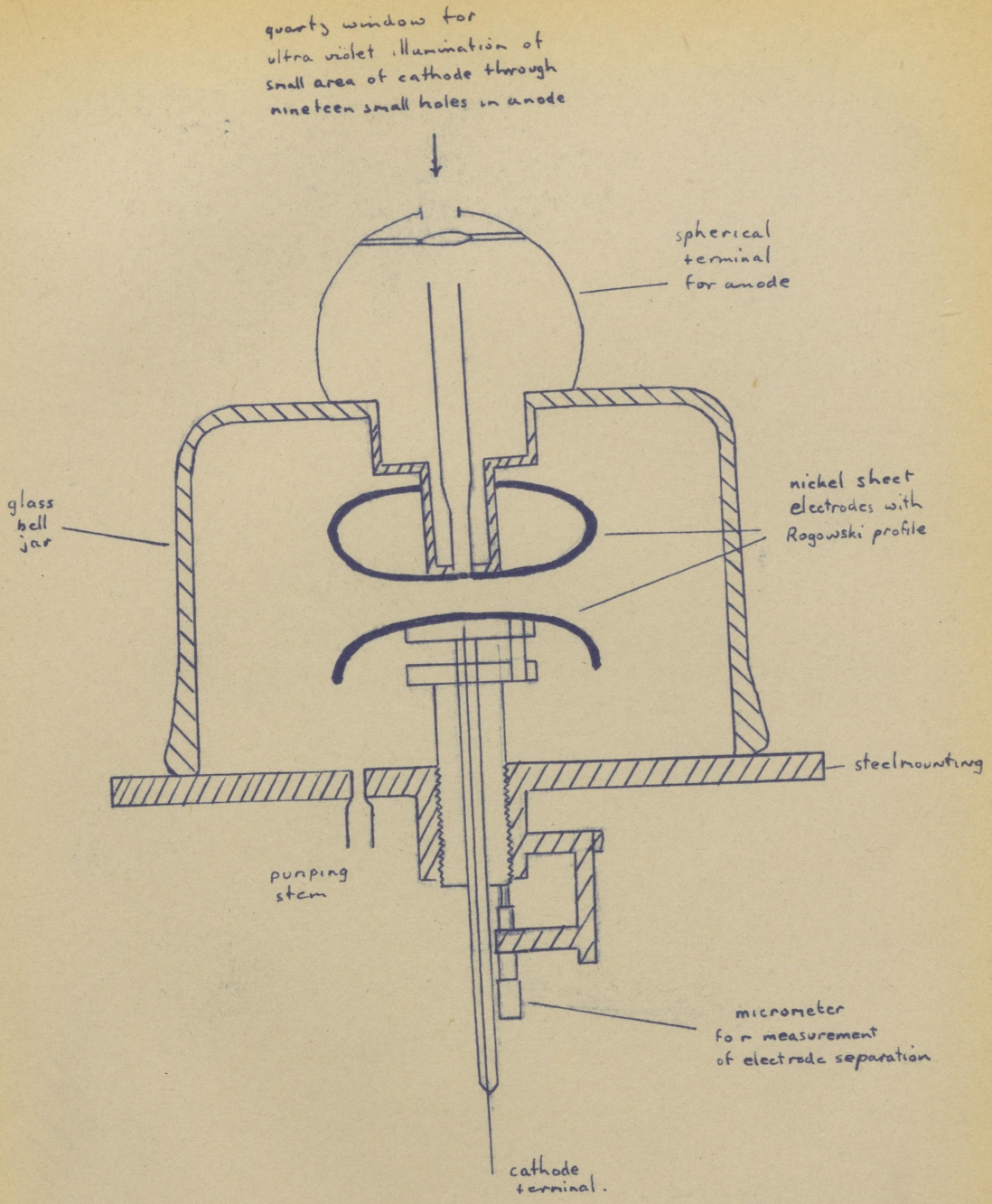

Diagram of apparatus used by Llewellyn Jones and Parker

Fig D5·9

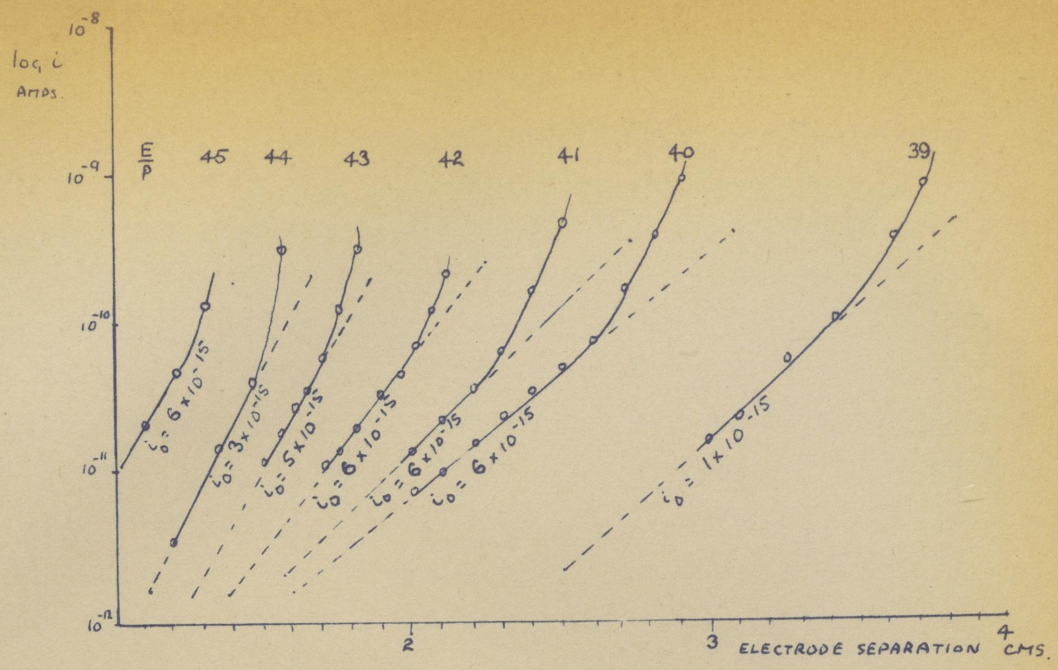

Log i VERSUS d FOR VALUES OF E/p FROM 39 TO 45 V/CM/MM Hg IN AIR

FIG D5·10

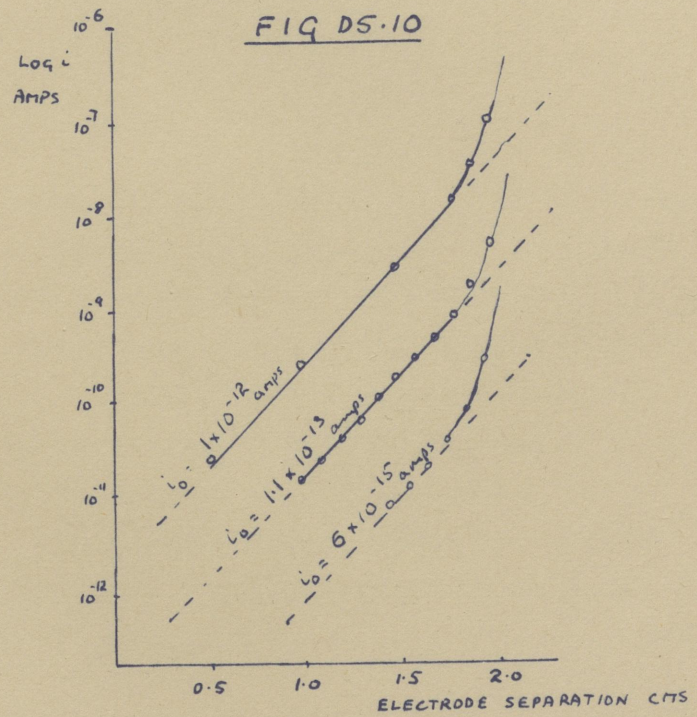

Log i VERSUS d GRAPHS OBTAINED OVER A LARGE RANGE OF i_0

FIG D5·11

was the variation of the curve of $\log \frac{i}{i_0}$ versus d for various values of i_0. Previously Posin 1936 had reported his conclusion that the formation of space charge occurs for currents in excess of 10^{-8} amp. Consequently, at first very low values of i_0 were used to ensure that i did not exceed this value. However, at the end of the investigation, larger values of i_0 were used and the effect of variation of i_0 which was found is shown in Fig. D.5.11., which was obtained for nitrogen. The graph shows that the initial stages of the curves are all linear and parallel and that the final curvatures are also the same. In fact, curves show that the values of γ and α were the same within experimental error throughout the whole range of current from 6×10^{-15} amp to 10^{-7} amp, and it was concluded that space charge effects were not so important as had often been assumed.

D.5.16. Finally, the observation of a secondary ionisation process in nitrogen cannot be due to photo-ionisation in the pure gas and since the results in air and nitrogen were very similar it was concluded that photoionisation does not occur in air either. From a study of the effect of the nature of the cathode surface it was concluded that the secondary ionisation coefficient γ is partly due to the bombardment of the cathode by photons. No information could be obtained about the relative magnitude of the two effects.

D.5.17. The Measurement of the Temporal Growth of Current at High Pressure by Bandel.

In the experiments of Llewellyn Jones the gas was not allowed to breakdown, but instead the pre-breakdown current was allowed to reach a fixed stable value

which was maintained for several seconds. In contrast, Fisher and his associates measured the very short time between the start of the build-up current and the instant of breakdown.

Ideally, in order to obtain the true picture of events, the current should be measured at each stage during the build-up to breakdown lasting only 10^{-8} seconds, and this remarkable feat has been achieved by Bandel 1954. Any method of measurement, which uses a mechanical means of indicating the current, e.g. the pointer of a galvanometer, is impracticable because of the high inertia of the instrument. An electron beam is virtually inertialess and therefore the cathode ray oscilloscope is a very convenient tool. Not until recent years have electronic techniques become sufficiently advanced to investigate current build-up at high pressure and as will be seen the measurements of Bandel 1954 made a significant contribution to theory. An additional difficulty is introduced because of the need for high voltage sources of the order of thirty thousand volts to produce breakdown. For reliable measurement, such sources must produce an extremely stable voltage output, which can be varied to within a fraction of one per cent of the breakdown voltage.

D.5.18. The method used by Bandel 1954 was to apply an overvoltage suddenly to the electrode gap and to measure the current flowing in the gap while the discharge built up to a spark. With reference to Fig. D.5.12., the high voltage supply Va obtained from a transformer, rectifier and smoothing circuit was applied to the gap via a 20MΩ current limiting resistor. The trigger circuit supplied a bias of 1000 volts negative with respect to earth to the .005μF condenser. Thus the

voltage across the condenser was Va + 1000. The voltage across the gap could then be very rapidly increased to Va + 1000 by closing switch S_1, which triggered the pulse generator which in turn rapidly returned the negative plate of the condenser to earth potential. Since the removal of the bias on the negative plate of the condenser increased rapidly the potential of the positive side by 1000 volts, the voltage across the gap was also increased by 1000 volts. The high voltage supply was variable from 0-50 kV and extremely well stabilised. In fact, the ripple was less than 0.5 volt at 32kV except for thermal drifts which could not be controlled or measured. This was a remarkable achievement and the stability was greatly superior to that used in the earlier measurements.

The beginning of the formative time lag, regarded as the instant of application of the breakdown voltage, coincided with the beginning of the horizontal sweep of the trace of the oscillograph.

The build-up of current produced a potential difference across a resistor R (see Fig. D.5.12.), which was amplified by a non-overloading amplifier and applied to the y plates of the oscillograph. By adjusting the amplification it was possible to vary the sensitivity from 2.5×10^{-4} to 2.5×10^{-1} volts (across R) per cm (y deflection).

It was not possible to observe the current immediately after the application of the breakdown pulse because of the charge current of the order of 10^6 times the discharge current , which had to flow to the cathode when the pulse was applied. Therefore, a switch was devised whereby the negative electrode of the spark gap was connected to earth until 3μ secs after the closing

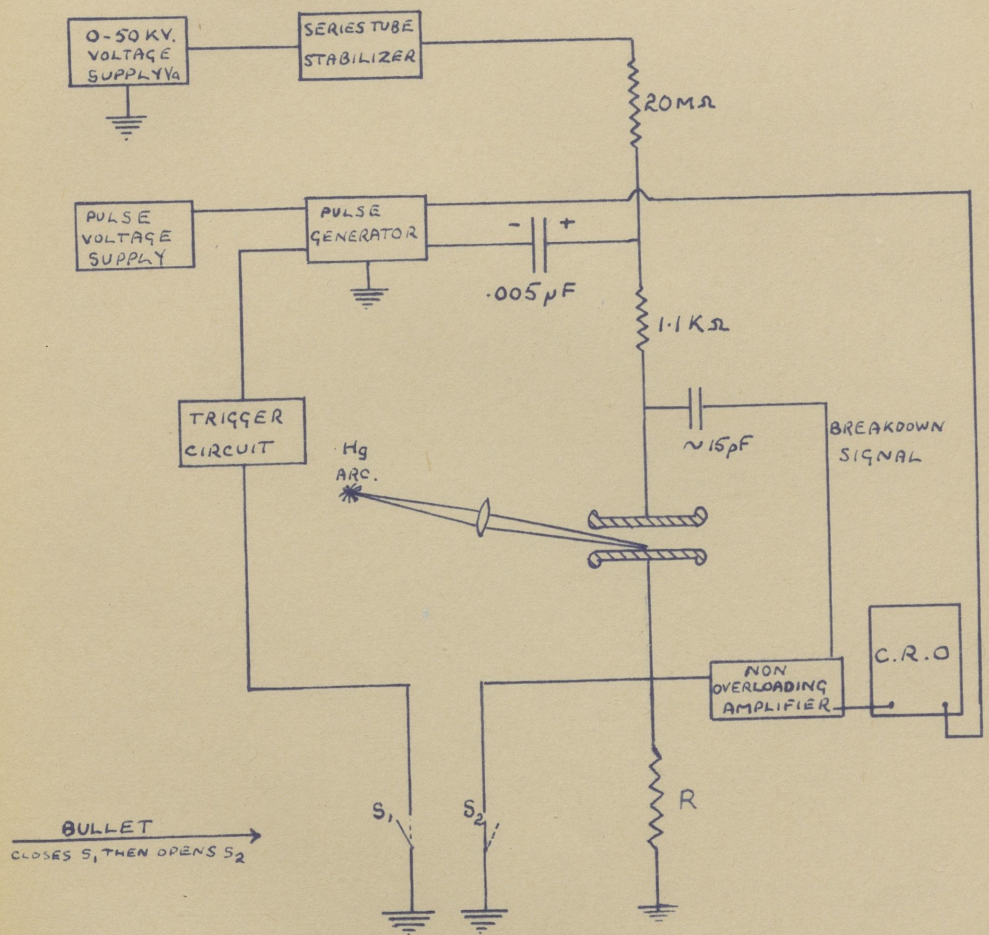

Schematic drawing of Bandel's apparatus.

FIG D5·12

of switch S_1. The best method was to operate the switches with a rifle bullet whose transit time from closing S_1 to opening S_2 was 3μsecs.

The instant of breakdown was recorded on the oscilloscope trace by taking a signal capacitatively from the high voltage lead-in insulator and coupling it to the amplifier circuit so that when breakdown occurred the sudden drop by thousands of volts drove the amplifier output to full negative signal and the trace had superimposed on it a negative pulse.

B.5.19. Cleanliness of the electrode surfaces and purity of the air used were essential. The electrodes were enclosed in a brass chamber with a Dural lid and quartz windows. All gaskets were of neoprene. The chamber was thoroughly cleaned before assembly and a trap cooled by dry ice and alcohol used to exclude mercury and tap greases. The air used was drawn from the room through glass wool and then a trap consisting of a long narrow glass tube cooled by dry ice in alcohol. The light from the quartz mercury arc was focussed on the cathode through the side windows via a quartz lens and its intensity adjusted by moving screens into or out of the beam.

As in the work of Fisher and Bederson 1951 i_o was determined by measuring the multiplied current i at 10% below the breakdown voltage and Sanders 1932 values of α were used in $i = i_o \exp.\alpha d$. The method of finding i_o is poor, although the best available, and the values of i_o quoted must be treated only as approximate. The observation by the above authors that the cathode photosensitivity changed considerably on repeated sparking was also confirmed. Bandel was not able to make measurements at short successive intervals as Fisher and Bederson had done, because of

the time required to set up the apparatus and consequently some variation up to 10% did occur in i_o.

D.5.20. The experimental procedure was first of all to allow the voltage supplies and arc to stabilise and then adjust the light intensity to the desired value of i_o.

The time lag, measured as the x deflection at which the negative pulse occurred on the trace could be observed visually by tripping switch S_1 by hand. It was adjusted to any required value by adjusting the approach voltage. It is emphasised that in this case the variation of approach voltage varies the over-voltage since a fixed one thousand volts are added to the approach voltage to produce breakdown.

In order to measure the current build-up, the oscillograph trace was photographed when switches S_1 and S_2 were tripped by firing a rifle bullet through them. The y deflection of the trace was proportional to the current, but as the range of current during the build-up period was so large it was necessary to take a number of photographs of traces for a given time lag at different sensitivity settings of the amplifier. The negatives were then projected on to a screen and the deflections converted into a semi-logarithmic graph of current versus time.

D.5.21. The general form of the current build-up is shown in Fig. D.5.13., which may be explained qualitatively as follows:-

Interpretation of the measured current is made difficult by the fact that the electron velocity is much greater than the positive ion velocity so that whenever the current is increased a larger fraction of it is due to

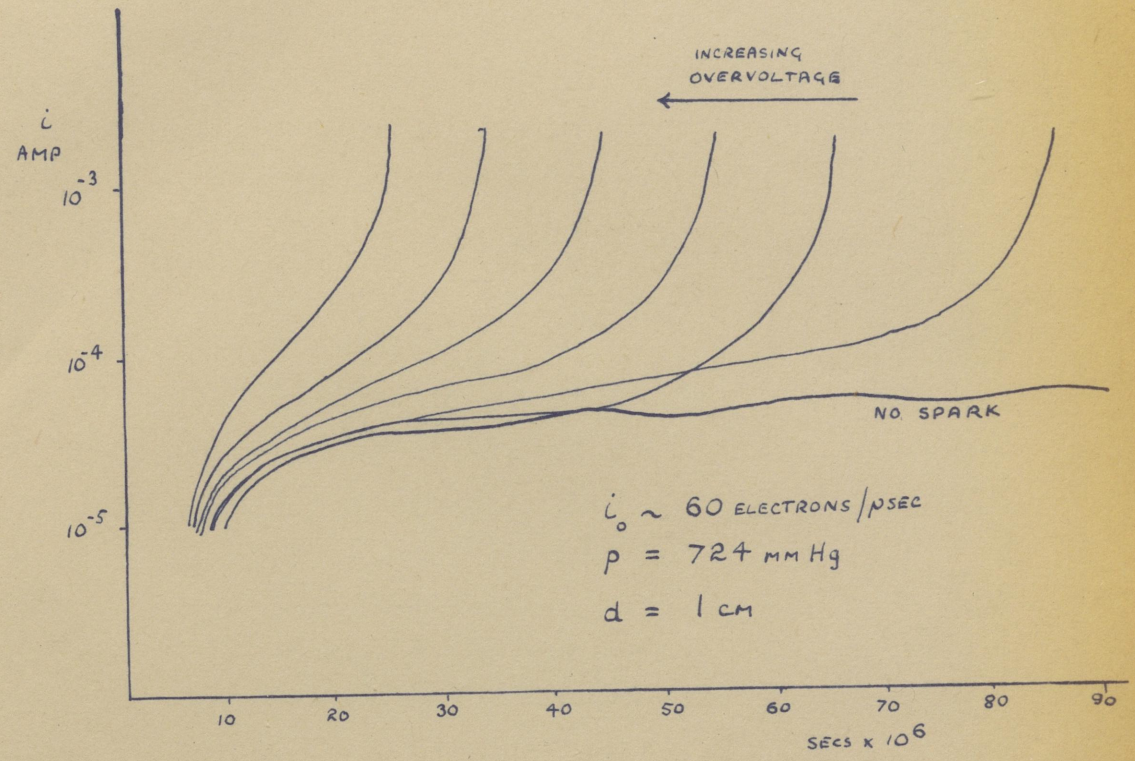

BANDEL'S MEASUREMENTS OF GROWTH OF CURRENT WITH TIME FOR VARIOUS VALUES OF OVERVOLTAGE.

FIG 05.13

electrons than would be the case for steady state conditions; and the faster it is increasing the larger is the fraction of electrons.

The initial rise in current would in the absence of secondary mechanisms reach a constant value after about one positive ion transit time. The continued upcurving seen in Fig. D.5.13. is attributed to the action of secondary mechanisms. Just before breakdown a very rapid increase was assumed by Bandel 1954 to be due to space charge distortion.

This interpretation is of great significance. It indicates the possibility of breakdown at high pressure being due to two consecutive processes: (a) Townsend type current build-up, followed by (b) Streamer formation due to space charge build-up.

In Fig. D.5.13. an example is included of actual data for cases in which sparks just failed to develop. It is significant that the initial part of the curve is essentially the same as for the cases where sparks occurred, which indicates that the second stage (b) failed to occur.

D.5.22. It was also observed that when light was focussed on the centre of the cathode, sparks appeared to occur randomly over the entire electrode area independently of the area illuminated. This would not be expected from the Streamer Theory in which the streamer or spark would be most likely to occur at the region of greatest i_0.

Alternatively, an intermediate Townsend discharge spread over the entire electrode surface would allow the observed process to occur.

D.5.23. In section D.4.12. a brief outline was given

of the method of analysis, based on the principles of the Streamer Theory, used by Fletcher 1949 to explain the results of his measurements of the formative time lag in air at very high overvoltage.

Certain objections to this analysis have been pointed out by Dickey 1952, as follows:-

(a) The required critical value of electron density at breakdown, namely 10^8 electrons/cc, according to Fletcher 1949, is not sufficiently high. The oscillograms shown in Fig. D.2.9. obtained by Fletcher 1949 show rates of fall of anode voltage of the order of 10kV per microsecond, which correspond to a capacitative current due to discharge of the gap of the order of 200 amps. This current, together with the external current through the load, corresponds to an electron density of the order of 10^{13} electrons/cc.

(b) It is difficult to explain why the streamer itself should travel much faster than the already rapid ionisation process in the initial electron avalanche. The large space charge fields would tend to speed up the ionization only on the side of the avalanche, and would retard the ionization near the centre where both the ion and electron densities are high.

(c) The assumption of the type of charge distribution used by Fletcher 1949, as outlined in section D.4.12. is a very rough approximation.

D.5.24. Instead of dividing the positive ions and electrons into two separate groups and deriving an expression for the average field between them Dickey 1952 considered the effect of the separation by the field of individual pairs of electrons and positive ions.

As the electron avalanche proceeds towards the anode, energy is removed from the electrostatic field across the gap. If this energy is removed faster than the rate provided by the flow of current from the external circuit, the voltage across the gap falls. Dickey's interpretation was that this condition denotes the beginning of breakdown.

If the anode-cathode separation is d and the potential difference across the gap is V, then the potential of an electron situated at a distance x_- from the negative electrode is $\frac{Vx_-}{d}$.

By considering a pair of electrodes and positive ions whose distances from the cathode are x_- and x_+ respectively, it is seen that the energy associated with their separation is given by:

$$\frac{1}{2}\frac{eV}{d}(x_- - x_+) \qquad \text{D.5.24.1.}$$

Then if the subscript i denotes the i^{th} particle, the total energy of the whole system containing N electrons and N positive ions is given by:

$$W = \frac{1}{2}CV + \frac{1}{2}\frac{eV}{d}\sum_{i=1}^{i=N}(x_{-i} - x_{+i}) \qquad \text{D.5.24.2.}$$

From this expression it may be shown that the voltage across the gap at time t, i.e. V_t is given by:

$$V_t = V_o - \frac{1}{C}\sum_{i=1}^{i=N}\frac{e}{d}(x_{-i} - x_{+i}) - \int_o^t i_{ext(t)}\,dt \qquad \text{D.5.24.3.}$$

where V_o is the initial voltage across the gap, and $i_{(ext)t}$ is the current flowing through the external circuit at time t.

By differentiation:

$$C\frac{dV}{dt} = -\frac{Nev}{d} + i_{ext.} \qquad \text{D.5.24.4.}$$

This equation could be applied to Fletcher's experimental conditions as follows:-

(a) $i_{(ext)t}$ is equivalent to the current produced by the decrease in voltage across the gap across two resistances equal to the characteristic impedance R_c of the transmission line in parallel.

$$\text{i.e. } i_{(ext)t} = \frac{V_o - V_t}{2R_c} \qquad \text{D.5.24.5.}$$

(b) N the number of electrons at time t was assumed to be produced by a Townsend avalanche only.

$$\text{i.e.} \qquad N = N_o \exp. \int_o^t \alpha v \, dt \qquad \text{D.5.24.6.}$$

where N_o is the initial number of electrons.

This is of course equivalent to the conventional Townsend build-up equation.

$$i = i_o \exp. \int_o^x \alpha \, dx \qquad \text{D.5.25.7.}$$

By substituting equation D.5.24.5. and equation D.5.24.6. in equation D.5.24.4.:

$$C\frac{dV}{dt} = -\frac{evN_o}{d} \exp. \int_o^t \alpha v \, dt + \frac{V_o - V}{2R_o} \qquad \text{D.5.25.8.}$$

D.5.25. The values of α and v used were the same as those used by Meek, see section D.4.6.

By using successive approximations, solutions of equation D.5.24.8. were obtained, which are superimposed on the results of Fletcher in Fig. D.2.8.

The significant feature is the stepped form of the solution, which agreed quite well with experiment.

The initial rapid fall of voltage is explained by a capacitative current. The flattening off of the curve is explained by the condition when the ionisation rate falls to such a low value that the number of electrons in the gap is substantially constant. Under these conditions the gap has an almost constant resistance.

D.6. A Comparison of the theories of formative time lag based on the Townsend mechanism for different types of ionisation agent.

D.6.1. From the experimental results described in the last section, there is evidence that the Townsend current build-up mechanism applies both at high pressure and low pressure. The formative time lags at given overvoltage may be very different provided the difference in pressure at the two measurements is high enough. This may be explained by assuming that more than one type of Townsend secondary ionisation agent may occur in a given breakdown. At high gas pressure high speed secondary ionisation agents such as photons may predominate, whereas at low gas pressure breakdown may be due to the action of comparatively slow ionisation agents, e.g. positive ions. First of all the secondary process will be considered, which is accepted for the case of low gas pressure.

D.6.2. Secondary ionisation process consisting of positive ion bombardment of the cathode.

It will be assumed that the formation of positive ion

space charge is negligible.

Then an equation for the growth of current with time may be derived as follows:-

Let i_o = priming current

$i_-(0,t)$ = total electron current from the cathode at t seconds

$i_-(d,t)$ = total electron current at the anode at t seconds

$i_+(0,t)$ = total positive ion current from the cathode at t seconds

$i_+(d,t)$ = total positive ion current at the anode at t seconds

γ_+ = time required for positive ions to travel from anode to cathode

Then

$$i_-(0,t) = i_o + \gamma_p\, i_+(0,t) \qquad \text{D.6.2.1.}$$

$$i_+(0,t) = i_+(d, t - \gamma_+) \qquad \text{D.6.2.2.}$$

$$i_+(d,t) = i_-(d,t) - i_-(0,t) \qquad \text{D.6.2.3.}$$

$$i_-(d,t) = i_-(0,t) \text{ exp. } \alpha\, d \qquad \text{D.6.2.4.}$$

α_o is the value of α at the breakdown voltage.

By combining equations D.6.2.1. and D.6.2.2.:

$$i_-(0,t) = i_o + \gamma_p i_+(d, t - \gamma_+) \qquad \text{D.6.2.5.}$$

$$= i_o + \gamma_p \left[i_-(d, t - \gamma_+) - i_-(0, t - \gamma_+) \right] \qquad \text{D.6.2.6.}$$

$$= i_o + \gamma_p \left[\text{exp. } \alpha\, d - 1 \right] \left[i_-(0,t) - \frac{di_-(0,t)}{dt} \gamma_+ \right] \qquad \text{D.6.2.7.}$$

At the breakdown threshold:

$$\gamma_p \text{ (exp. } \alpha_o d - 1) = 1 \qquad \text{B.5.11.9.}$$

Let

$$\gamma_p(\exp.\alpha d - 1) = M \qquad \text{D.6.2.8.}$$

Then by substitution

$$M \tau_+ \frac{di_-(0,t)}{dt} = (M-1) \times i_-(0,t) - i_o \qquad \text{D.6.2.9.}$$

By integration

$$\int_0^{t=t} \frac{dt}{M \tau_+} = \int_{i_o}^{i_-(0,t)} \frac{di_-(0,t)}{i_o + (M-1) \times i_-(0,t)} \qquad \text{D.2.6.10.}$$

Hence,

$$\frac{t}{M \tau_+} = \frac{1}{M-1} \log \frac{1 + (M-1)\frac{i_-(0,t)}{i_o}}{M} \qquad \text{D.6.2.11.}$$

Let $\epsilon = \gamma_p \exp.(\alpha d - 1) - 1$ D.6.2.12.

Then $M = 1 + \epsilon$ D.6.2.13.

$$t = \tau_+ \left(\frac{1+\epsilon}{\epsilon}\right) \log \frac{1 + \frac{\epsilon\, i_-(0,t)}{i_o}}{1 + \epsilon} \qquad \text{D.6.2.14.}$$

Near the threshold where ϵ is small

$$t \doteq \frac{\tau_+}{\epsilon} \log\left(1 + \epsilon \frac{i_-(0,t)}{i_o}\right) \qquad \text{D.6.2.15.}$$

If a value for τ_+ is assumed, this equation may be used to calculate the variation of $i_-(0,t)$ with t for various values of ϵ. This is shown in Fig. D.6.1., for which τ_+ was taken as 5×10^{-6} secs.

For $\epsilon = o$ the current rises linearly with time.

In practice, this will not continue indefinitely, because the field between the electrodes will eventually be distorted by the formation of positive ion space charge.

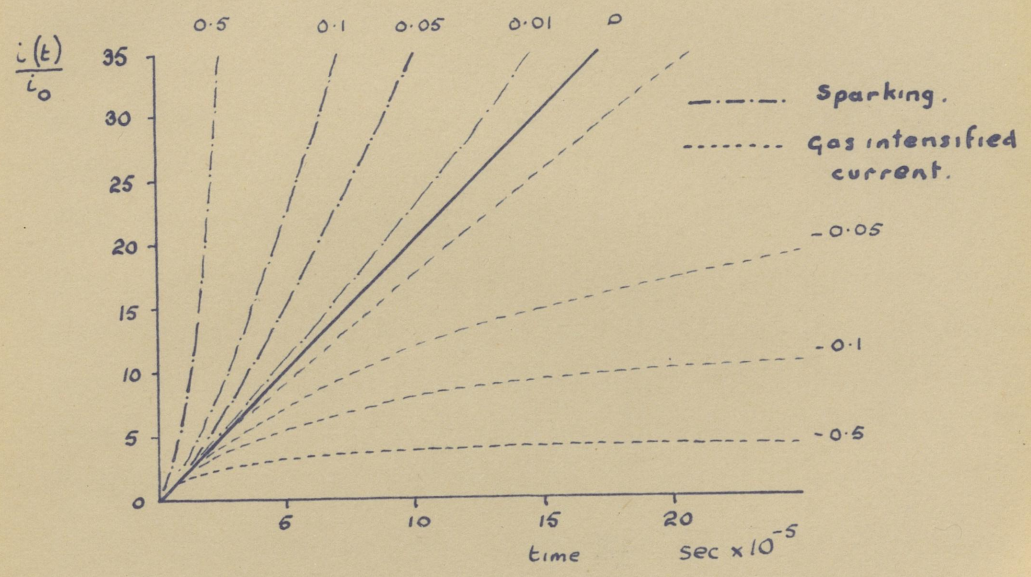

Variation of $i(t)/i_0$ with Time.

Fig D6·1

For $\epsilon < 0$ the current rises first of all almost linearly with time and then tends towards a limiting finite value as t approaches infinity.

For $\epsilon > 0$ the current rises at an ever increasing rate.

D.6.3. The above analysis was made by Schade 1937, who applied it to his investigations of the growth of current in Neon at low gas pressure of the order of a few millimetres of mercury. The discharge tube was as shown in Fig. D.6.2. The plane parallel electrodes were 1 cm. apart. The cathode was barium coated and the priming current enhanced by irradiation of the cathode by visible light. The magnitude of i_o could then be controlled by the light intensity.

For a given applied voltage and cathode irradiation the current was measured at successive time intervals, after the application of the voltage, until it reached a stable value of the order of milliamps. This was repeated for various values of i_o.

If t_f is taken as the time when the second stable state is reached, i.e. t_f is the formative time lag, the value of $i_-(0,t)$ in Schade's experimental apparatus was of the order of milliamps.

Let this value of $i_-(0,t)$ be denoted by i_e.

Then $\frac{i_e}{i_o} \gg 1$ in equation D.6.2.15.

Therefore,

$$t_f = \frac{\tau_+}{\epsilon} \log \epsilon \frac{i_e}{i_o} \qquad \text{D.6.3.1.}$$

D.6.4. Schade's 1937 experimental relation between t_f and $\log i_o$ is shown in Fig. D.6.3. The linear part is in agreement with equation D.6.3.1. The departure

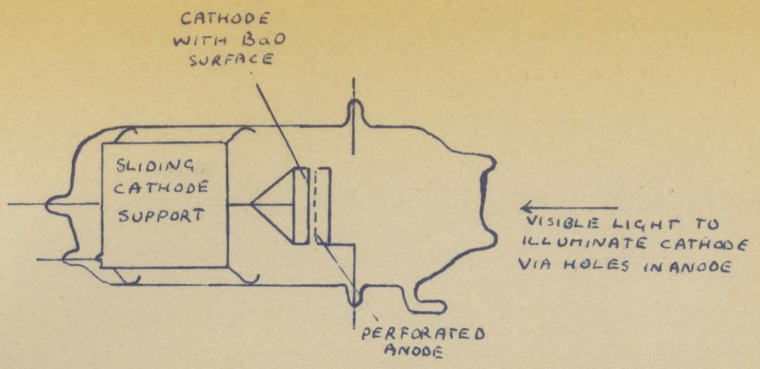

SCHADE'S DISCHARGE TUBE WITH NICKEL ELECTRODES

FIG D6·2

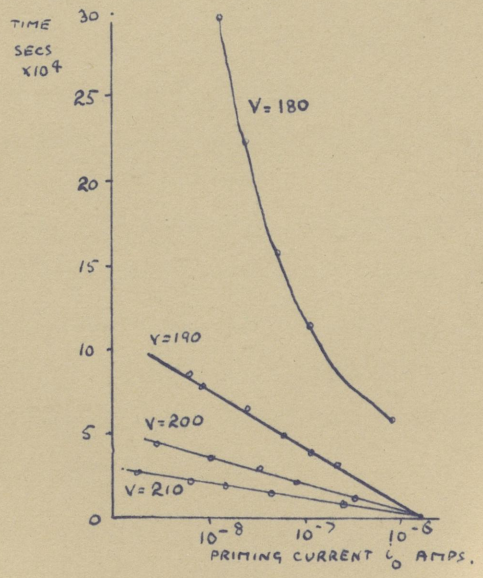

DEPENDENCE OF TIME REQUIRED FOR CURRENT TO RISE FROM i_0 TO ie ON VALUE OF i_0 FOR VARIOUS VALUES OF V

FIG D6·3

from linearity when V approaches the breakdown voltage V_s is not predicted by equation D.6.3.1., since the approximations of equation D.6.2.15. are no longer valid.

D.6.5. Secondary ionisation process consisting of photon bombardment of cathode.

The analysis of the previous section would equally well apply to the case of photon action at the cathode if were replaced by γ_r and the transit time τ_+ were γ_p replaced by the transit time of an electron from anode to cathode.

In their analysis of their experiments on nitrogen, Kachikas and Fisher 1952 rejected the possibility of positive ion action at the cathode because of the short values of formative time lag observed. Instead, they assumed that emission of electrons occurred at or near the cathode by the action of photons which had been produced near the anode. In contrast to Schade, they also assumed that space charge deformation of the field across the gap was necessary before breakdown occurred.

D.6.6. In the following analysis it was assumed that each electron avalanche starts from the cathode as its predecessor reaches the anode, i.e. the photons are produced near the anode and the transit time of the photons is neglected in comparison with the transit time of the electron avalanche.

If one electron starts toward the anode at t = 0:-

At $t = \tau_-$ $\gamma_r(\exp.\alpha d-1)$ electrons exist at the cathode.

At $t = 2\tau_-$ $\gamma_r^2(\exp.\alpha d-1)^2$ electrons exist at the cathode.

At $t = n\tau_-$ $\gamma_r^n(\exp.\alpha d-1)^n$ electrons exist at the cathode.

where τ_- is the transit time of the electron avalanche, and γ_r is the number of electrons produced by photons at the

cathode per positive ion in the gap (see section B.5.13.).

It was assumed that the effect of space charge formation was negligible until N_c electrons had been formed, whereupon the distortion of the field produced breakdown in the form of a filamentary streamer.

i.e.:

$$\gamma_r^n(\exp.\alpha d - 1)^n = N_c \qquad \text{D.6.6.1.}$$

Also

$$\gamma_r \exp.\alpha_c d = 1 \qquad \text{D.6.6.2.}$$

since this is a special case of the Townsend breakdown criterion.

Since $\exp.\alpha d$ is of the order of 1000, equation D.6.6.1. may be written:-

$$\gamma_r^n \exp.n\alpha d = N_c \qquad \text{D.6.6.3.}$$

Hence by combining equations D.6.6.3. and D.6.6.2., and remembering that = $_c$ + :

$$\exp.nd\,\Delta\alpha = N_c \qquad \text{D.6.6.4.}$$

Now,

$$nd = vt_f \qquad \text{D.6.6.5.}$$

where v is the electron velocity.

Therefore, by combining equations D.6.6.5. and D.6.6.4.:

$$t_f = \frac{\log N_c}{v\,\Delta\alpha} \qquad \text{D.6.6.6.}$$

Mesch's 1932 values of α were used and Nielsen's 1936 measurements of electron mobility in nitrogen were extrapolated.

The value $N_c = 10^5$ was chosen to fit the observed time lag at one overvoltage at atmospheric pressure and at an

electrode separation of 1 cm. using equation D.6.6.6. The value based on one experimental result was used to predict the formative time lag under different experimental conditions.

D.6.7. In the case of nitrogen good agreement between theory and experiment was obtained. In contrast, poor agreement was obtained for oxygen and argon, where the observed lags were longer than predicted by the above theory. It was suggested that in oxygen, the mobility of the negative charge carriers is reduced by the formation of negative ions. In argon, it was suggested that the transit time of photons was increased by their absorption and re-emission in the gas.

D.6.8. Secondary ionisation process consisting of both photon and positive ion bombardment of the cathode.

As mentioned in section D.5.17. Llewellyn Jones and Parker 1952 concluded from the studies of $\log \frac{i}{i_o}$ versus d that both photons and positive ions are effective in producing secondary electrons at the cathode at high gas pressure.

D.6.9. The following analysis discussed by J. Dutton, S.C. Haydon, F. Llewellyn Jones and P.M. Davidson 1953 is essentially a rigorous extension of Schade's theory in which both γ_p and γ_r are taken into account.

It was assumed that ionisation by both positive ions and photons in the gas was negligible and that the only electron generation in the gas is by impact between electrons and neutral atoms.

The continuity equations for the gas volume are then:

$$\frac{\partial}{\partial t}\left\{i_-(x,t)\right\} = -\frac{\partial}{\partial x}\left\{i_-(x,t)\right\} + \alpha\, i_-(x,t) \quad \text{D.6.9.1.}$$

$$\frac{\partial}{\partial t}\left\{i_+(x,t)\right\} = +\frac{\partial}{\partial x}\left\{i_+(x,t)\right\} + \alpha\, i_-(x,t) \quad \text{D.6.9.2.}$$

In order to solve the equations the two following boundary conditions were applied:-

(a) At t = 0 the current in the gas is zero,

(b) At x = 0 t = t $i_-(0,t)$ is represented by the sum of the currents due to the incidence of photons and positive ions.

Further, it was assumed that there is no absorption of radiation in the gas.

With these conditions it was found that the solution of equations D.6.9.1. and D.6.9.2. could be expressed by:

$$i_-(0,t) = \frac{i_o(1-\exp.\lambda t)}{1-(\gamma_p+\gamma_r)(\exp.\alpha d-1)} \quad \text{D.6.9.3.}$$

λ could be calculated from a complicated expression involving the values of γ_p, γ_r, α, and the electron and positive ion mobilities.

D.6.10. In order to apply this expression to a practical example, it was decided to choose i_o as 10^{-12} amp. which is often used experimentally to eliminate statistical time lag. An electron separation of 1 cm. at 760 mm Hg was considered for which the value of $\frac{E}{p}$ for breakdown was known. Then the value of α was deduced from the experiments of Sanders and the value of γ calculated from the breakdown criterion.

For a given value of γ values of γ_p and γ_r were

chosen to satisfy the equation

$$\gamma = \gamma_p + \gamma_r \qquad \text{D.6.9.4.}$$

and substituted in equation D.6.9.3.

In this way the electron current at the cathode could be calculated for various values of t and various values of $\frac{\gamma_p}{\gamma_r}$ for a given value of γ.

This calculation was then repeated for various values of overvoltage by assuming that γ remained the same, but that α was that value corresponding to $\frac{E}{p}$, at the overvoltage applied.

D.6.11. The normal criterion for the end of the formative time lag is the instant when the voltage across the gap starts to fall. In this case, as in the case of Schade's theory, it was necessary to assume that the formative time lag ends when $i_-(0,t)$ reaches a certain value. Schade 1937 found good agreement with experiment by regarding the critical value of $i_-(0,t)$ for breakdown as the current when light was emitted. For the case of high gas pressure a visible discharge is usually observed within the current range 10^{-7} - 10^{-5} amp.

D.6.12. Fig. D.6.4. shows the calculated variation of formative time lag for various values of $\frac{\gamma_r}{\gamma}$ and $i_-(0,t)$. A very marked dependence on the value of $\frac{\gamma_r}{\gamma}$ is shown together with an appreciable variation, due to the value of $i_-(0,t)$ used.

Fig. D.6.5. shows the calculated variation of formative time lag with $\frac{\gamma_r}{\gamma}$ for the particular case of $i_-(0,t) = 10^{-7}$ amp. These curves indicate that it should be possible to determine the nature of the secondary ionisation process operating from the shape of the

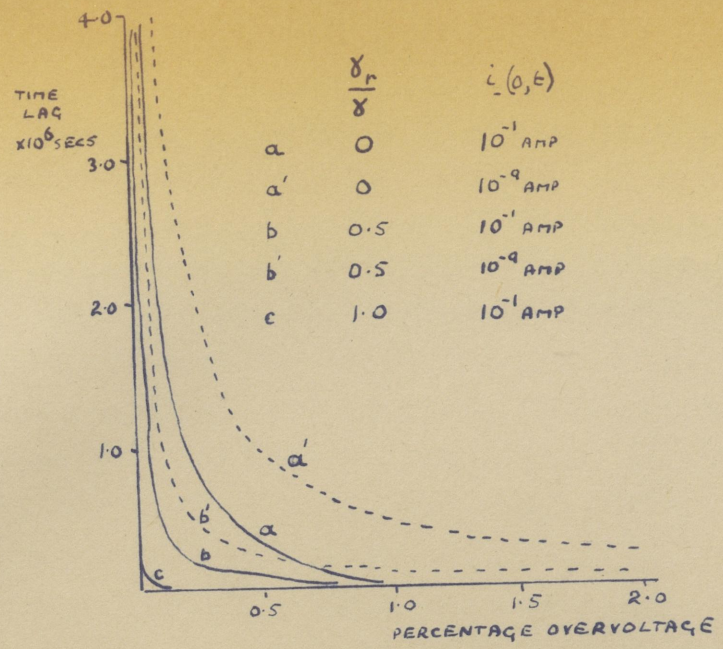

COMPARISON OF THE THEORETICAL CURVES OF FORMATIVE TIME LAG AGAINST PERCENTAGE OVERVOLTAGE FOR VARIOUS VALUES OF $i_-(0,\epsilon)$ AND $\frac{\gamma_r}{\gamma}$.

FIG D6·4

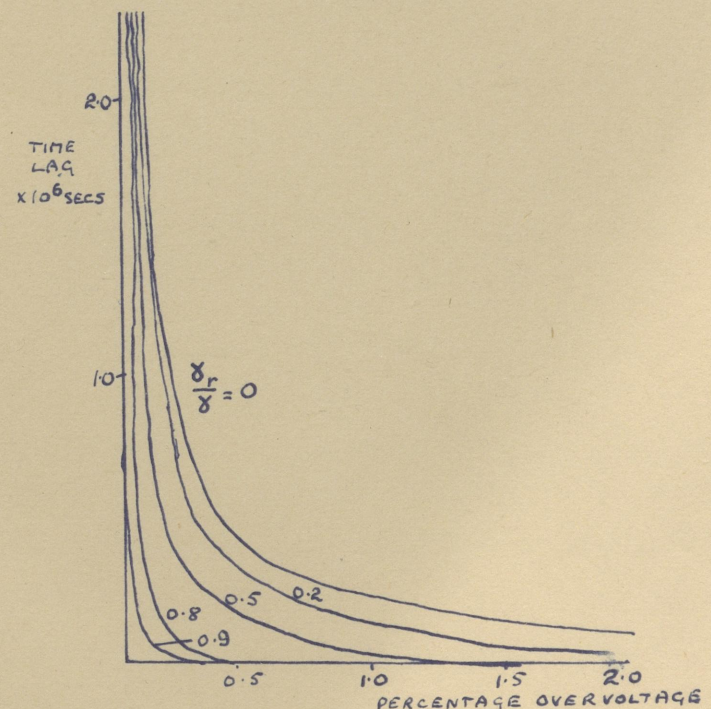

THEORETICAL CURVES SHOWING THE VARIATION OF THE FORMATIVE TIME LAG WITH PERCENTAGE OVERVOLTAGE FOR A VALUE OF $i_-(0,\epsilon) = 10^{-7}$ AMP AND VARIOUS VALUES OF $\frac{\gamma_r}{\gamma}$

FIG D6·5

curve. However, an unknown error is introduced because it is not known which is the correct value of $i_-(0,t)$ to use.

D.6.13. Fig. D.6.6. represents an attempt to analyse the results obtained by Kachickas and Fisher 1952. The full lines represent the case of secondary emission from the cathode due entirely to the impact of photons calculated for various values of $i_-(0,t)$. The closest agreement is then obtained by a value of $i_-(0,t)$ of 10^6 amps. which is unreasonably large. Hence, it would seem that the assumption of $\gamma = \gamma_r$ as made by Kachickas and Fisher 1952 (see section D.6.6.) is not good enough. For the more reasonable case of $i_-(0,t) = 10^{-1}$ amp., quite good agreement was obtained by assuming $\frac{\gamma_r}{\gamma} = 0.9$, as shown by the dotted line in Fig. D.6.6.

D.6.14. Whilst a comparison between theory and experiment must not be carried too far in view of the dependence on the assumed critical value of $i_-(0,t)$ for breakdown, the results of the analyses are significant in view of the two following points:-

(a) The same primary and secondary ionisation processes which produce the observed growth of pre-breakdown current given by equation D.6.9.3. lead under non-steady state conditions $V \gg V_s$ to a rapid increase of the formative time lag with increasing over-voltage.

(b) When photo-electric emission from the cathode exists, time lags as low as 10^{-6} sec. can be obtained with an overvoltage as low as 2%.

Hence, the low values of formative time lag at high pressure can after all be explained by the same ionisation processes which produce breakdown at low pressure.

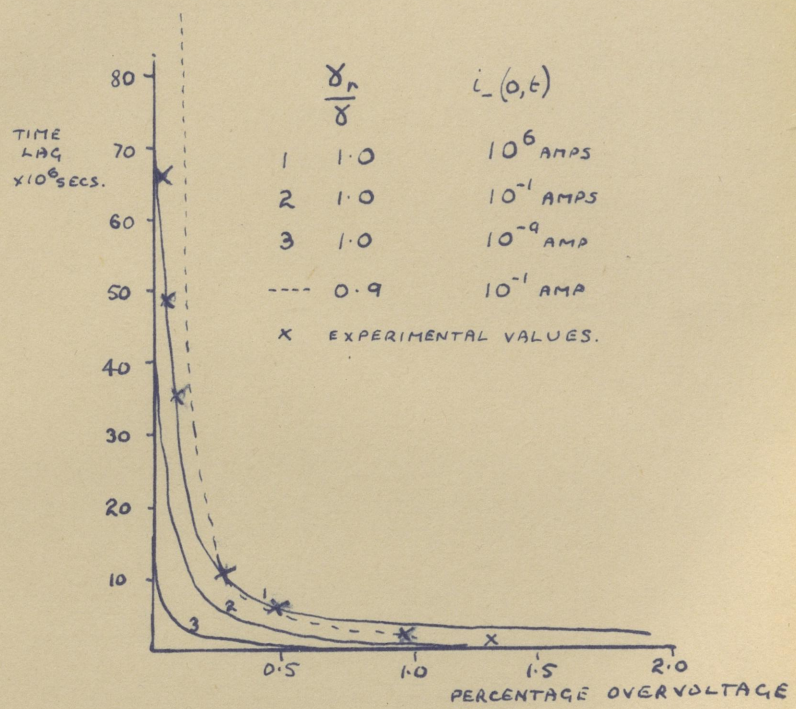

COMPARISON OF THE THEORETICAL CURVES OF FORMATIVE TIME LAG AGAINST PERCENTAGE OVERVOLTAGE WITH MEASUREMENTS OF FISHER AND BEDERSON

FIG D6·6

From the foregoing, it seems likely that the reduction in formative time lag observed as the pressure is increased from the order of a few mms of mercury to approximately atmospheric pressure, is due to the increased proportion of photon ionisation in the secondary ionisation process.

However, although the predicted values of formative time lag agree well with experiment, the theory does not explain the filamentary nature of the spark at high pressure. To do this, more must be known of the significance of the attainment of a critical value of N_c in Fisher's theory or a critical value of $i_-(0,t)$ in Llewellyn Jones' theory.

D.7. The formation of space charge during the formative time lag and its dependence on i_0.

D.7.1. Whilst the observations of Bandel 1954 and Llewellyn Jones and Parker 1952 both support the assumption of current growth by a Townsend mechanism, they differ in as much as Bandel found a strong dependence on i_0 whereas Llewellyn Jones and Parker showed that their curves for $\log \frac{i}{i_0}$ versus d predicted the same values of α and γ for the range of i_0 from 6×10^{-15} amp. to 1×10^{-7} amp.

D.7.2. This discrepancy has since been explained by Crowe, Bragg and Thomas 1954, as follows:

It must be remembered that as far as the formation of space charge is concerned, it is the current density and not the current which is important. Bearing this in mind, the effect of the formation of space charge on the distribution of electric field across the gap, and therefore the value of α at different points

across the gap can be calculated thus:

$$j_-(x) = j_-(0) \frac{\exp.\alpha x}{1 - \gamma(\exp.\alpha x - 1)} \qquad \text{D.7.2.1.}$$

if the field is uniform across the gap.

When space charge has formed $\exp.\alpha x$ must be replaced by $\exp. \int_0^x \alpha \, dx$, since $\frac{\alpha}{p}$ is a function of $\frac{E}{p}$.

Let
$$u = \int_0^x \alpha \, dx \qquad \text{D.7.2.2.}$$

$$\bar{u} = \int_0^d \alpha \, dx \qquad \text{D.7.2.3.}$$

Then
$$\frac{du}{dx} = \alpha \qquad \text{D.7.2.4.}$$

Hence, equation D.7.2.1. may be replaced by

$$j_-(x) = j_-(0) \frac{\exp.u}{1 - \gamma(\exp.\bar{u} - 1)} \qquad \text{D.7.2.5.}$$

The variation of the field across the gas is given by Poisson's equation

$$\frac{\partial E}{\partial x} = - 4\pi e (N_+ - N_-) \qquad \text{D.7.2.6.}$$

Since $j = NKE$ when K is the mobility, D.7.2.7.

$$\frac{\partial E}{\partial x} = - \frac{4\pi}{E}\left(\frac{j_+(x)}{K_+} - \frac{j_-(x)}{K_-}\right) \qquad \text{D.7.2.8.}$$

Since K_- is about 300 time K_+, $\frac{1}{K_-}$ may be neglected.

Hence,
$$\frac{\partial E}{\partial x} = - \frac{4\pi}{E} \frac{j_+(x)}{K_+} \qquad \text{D.7.2.9.}$$

$$= - \frac{4\pi}{E} \frac{j(x) - j_-(x)}{K_+} \qquad \text{D.7.2.10.}$$

Now $j(x) = j_-(d)$, since $j_+(d) = 0$ D.7.2.11.

Therefore, by substitution

$$\alpha\,\delta E = -\frac{4\pi}{EK_+}\, j_0\, \frac{\exp.u - \exp.u}{1 - \gamma(\exp.u - 1)}\, du \qquad \text{D.7.2.12.}$$

To enable equation D.7.2.12. to be integrated, it was assumed that

$$\frac{\alpha}{p} = A \exp.\left(\frac{Bp}{E}\right) \qquad \text{D.7.2.13.}$$

as applied to nitrogen where the constants A and B are known with considerable accuracy.

D.7.3. The conditions chosen were

$p = 700$ mm Hg $d = 1.0$ mm

$\gamma = 3.19 \times 10^{-4}$ $B = 260$ volts/cm/mm Hg

$A = 7.0$ (cm x mm Hg)$^{-1}$ $K_+ = 3.0 \times \frac{760}{p}$ cm^2/volt.sec.

$j_0 = 6.36 \times 10^{-11}$ amps/sq.cm.

Under these conditions the space charge fields were calculated and shown to be important at an applied voltage 1% below breakdown.

Fig. D.7.1. shows the variation across the gap of N_+, E and α for various applied voltages.

Whereas the Townsend equation predicts $i \longrightarrow \infty$ the effect of space charge formation is to produce a negative characteristic in the plot of log i versus V as shown in Fig. D.7.2.

In practice, the negative characteristic would correspond to an unstable state and may correspond to breakdown in in the form of a filamentary streamer.

Provided the various curves deduced from the Townsend

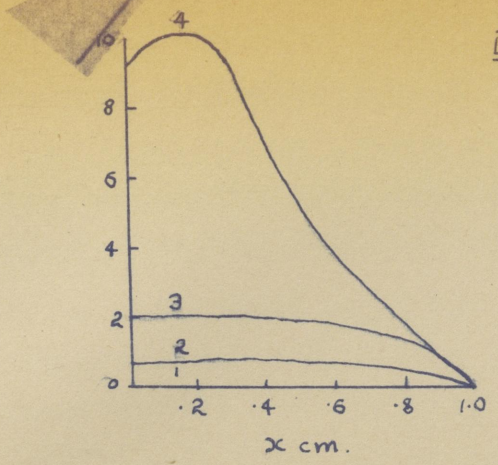

Distribution of

a) positive ions

b) electric field $\bar{E}$

c) α

across gap for various voltages near threshold.

INDEX TO CURVES

1 $\bar{U}$ = 8·0 V = 28·257 kV

2 $\bar{U}$ = 8·04 V = 28·348 kV

3 $\bar{U}$ = 8·047 V = 28·130 kV

4 $\bar{U}$ = 8·0495 V = 25·781 kV

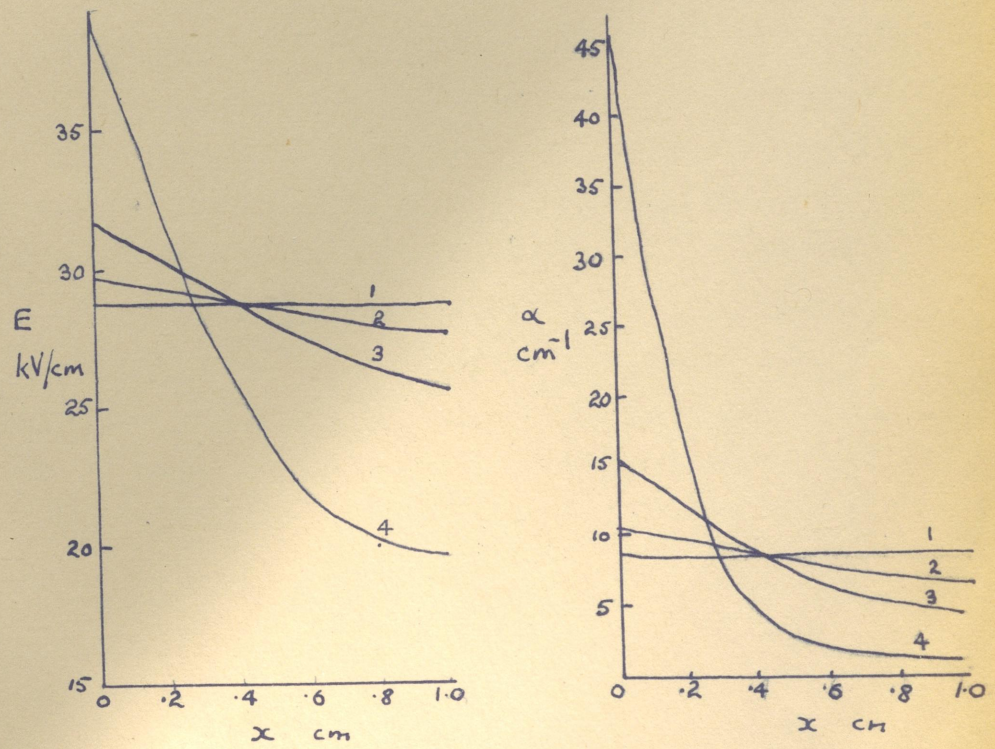

FIG D7·1

formula for different values of j_o, as shown in Fig.D.7.3., meet this theoretical curve below the start of the negative characteristic, the breakdown voltage and formative time lag will not be influenced by the value of j_o.

γ may be determined from the slope of the log j versus d curve just before breakdown. Since the space charge formation alters the slope of the log j versus d curve, it will affect the value of γ as determined by this method.

D.7.4. The above theory was applied to the conditions used by Llewellyn Jones and Parker 1952 in their experiments described in section D.5.9.

i.e. p = 300 mm Hg d = 2.09 mm Hg

and the values of A, B, K_+ and γ given in section D.7.3.

The calculated curves showing the growth of current are given in Fig. D.7.2. It will be seen that a negative characteristic due to the existence of space charge should not exist for values of j_o less than 10^{-11} amps/cm^2.

The area of cathode from which the priming current was emitted was 0.5 cm^2, and therefore the range of j_o studied by Llewellyn Jones and Parker 1952 was 5.6×10^{-15} to 2×10^{-12} amps/cm^2, which is clearly outside the range in which the formation of space charge would occur.

D.7.5. It is probable that Bandel 1954 used values of j_o sufficient to produce space charge distortion. Dependence of the rate of growth of current on i_o was found which the priming current was changed from 6 electrons/μsec. to 60 electrons/μsec. This corresponds to i_o ranging from 3.7×10^{-11} amps to 37×10^{-11} amps. Unfortunately, the area of illumination was not specified but since the illumination of the cathode was focussed

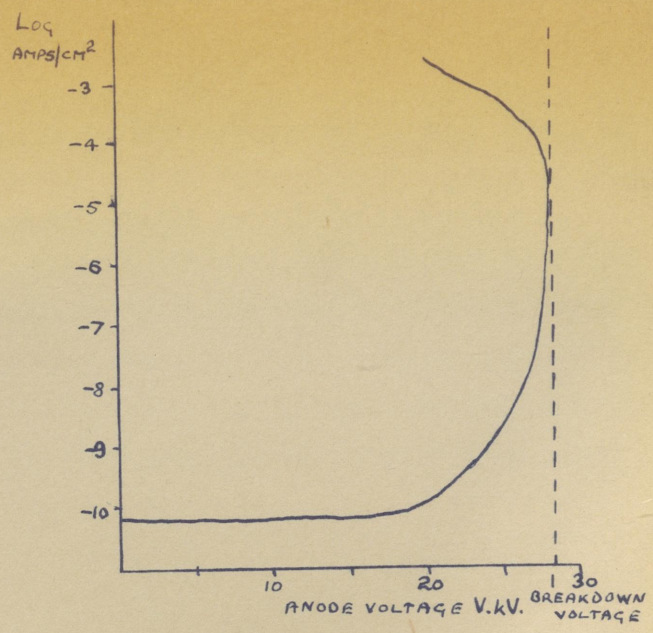

VARIATION OF STEADY STATE CURRENT WITH VOLTAGE

FIG D7·2

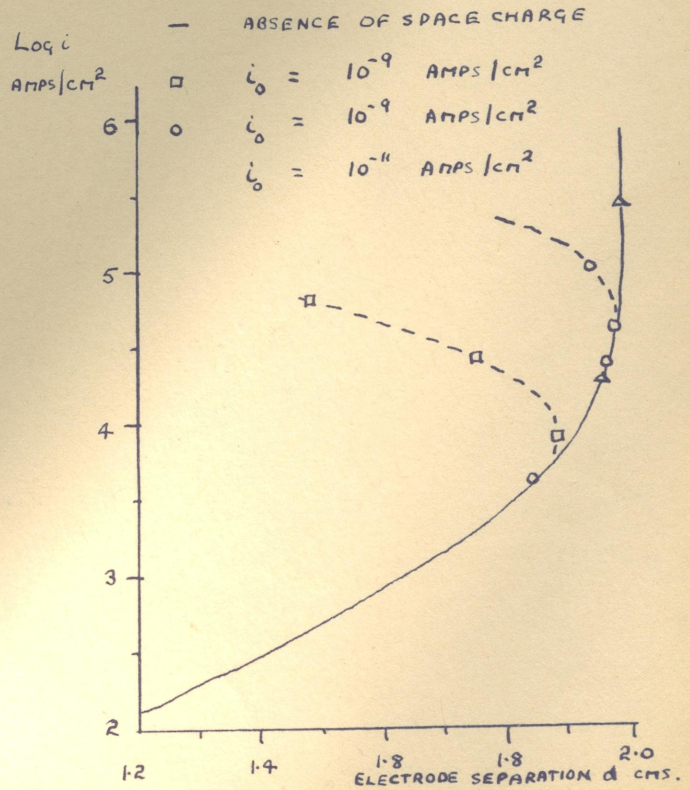

THE INFLUENCE OF SPACE CHARGE ON THE CURVATURE OF LOG i VERSUS ELECTRODE SEPARATION AT CONSTANT $\frac{V}{d}$

FIG D7·3

by a quartz lens, it is unlikely that the area of the cathode exceeded 1 cm^2, and therefore space charge effects probably occurred.

D.7.6. This analysis cleared up a discrepancy between experimental observations, both of which suggested that the formative time lag at high pressure can be calculated by consideration of the growth of current in the gap by a Townsend mechanism.

D.8. Summary and Recent Developments.

It has been shown in sections D.6.2 - D.6.4. that at low gas pressure of the order of a few mms of mercury the formative time lag may be explained in terms of the Townsend theory of breakdown involving first ionisation coefficient α and second ionisation coefficient γ_p.

During the 1930's the failure by Sanders 1933 to detect any secondary ionisation coefficient at high pressure described in sections B.5.2. and D.5.10., coupled with the early measurements of formative time lag by optical and oscillographic methods described in sections D.2.2. - D.2.9., made it appear that the Townsend theory was untenable at high pressure.

This led to the proposition of the Streamer theory described in sections D.4.1. - D.4.7., which was based on the assumption of photoionisation in the gas. The limitations of this theory were discussed in sections D.4.8. - D.4.14. and sections D.5.1. - D.5.25. were devoted to description of a number of subsequent experimental investigations, made possible by improvements in experimental techniques, all of which tended to discount the possibility of the Streamer theory mechanism.

Thus in recent years, the Townsend theory has gained more acceptabce and the final sections D.6.1. - D.6.14. are devoted to a survey of the dependence of the Townsend theory on different types of ionisation agent. The apparently anomalous dependence of current build-up on priming current i_o obtained by Bandel 1954 and Llewellyn Jones and Parker 1952 was explained by Crowe Bragg and Thomas 1954, as

described in section D.7.1. - D.7.6.

It would appear in the light of the above evidence that the Streamer theory is not necessary to derive the magnitude of the formative time lag which can be explained by a Townsend current build-up.

On the other hand, the Townsend breakdown theory does not explain the filamentary nature of the spark at high pressure, whereas the Streamer theory does at least attempt to do so.

Is it possible that breakdown at high pressure is due to a Townsend build-up, which at a critical stage attains the filamentary nature of a spark? The experiments described in section D.2.9., which indicate two stages in the breakdown interval certainly suggest it, and recently Raether 1953 has proposed the following mechanism:-

The sequence of events proposed is shown in Fig. D.8.1. Photons and positive ions, produced in an initiatory electron avalanche which obeys Townsend's laws of primary and secondary ionisation, travel back to the cathode and there produce additional electrons each of which starts its own avalanche as shown in Fig. D.8.1a. This is the normal Townsend concept, where the number of initial avalanches depends on the priming current. As shown in Fig. D.8.1c., a swarm of positive ions is left near the anode thus deforming the field across the gap. Then at a certain stage in this Townsend build-up one of the avalanches reaches a critical size and breakdown occurs. Raether 1949 has succeeded in photographing an electron avalanche at the stage of critical multiplication, a reproduction of which is given in the reference.

On the basis of this evidence, Raether has

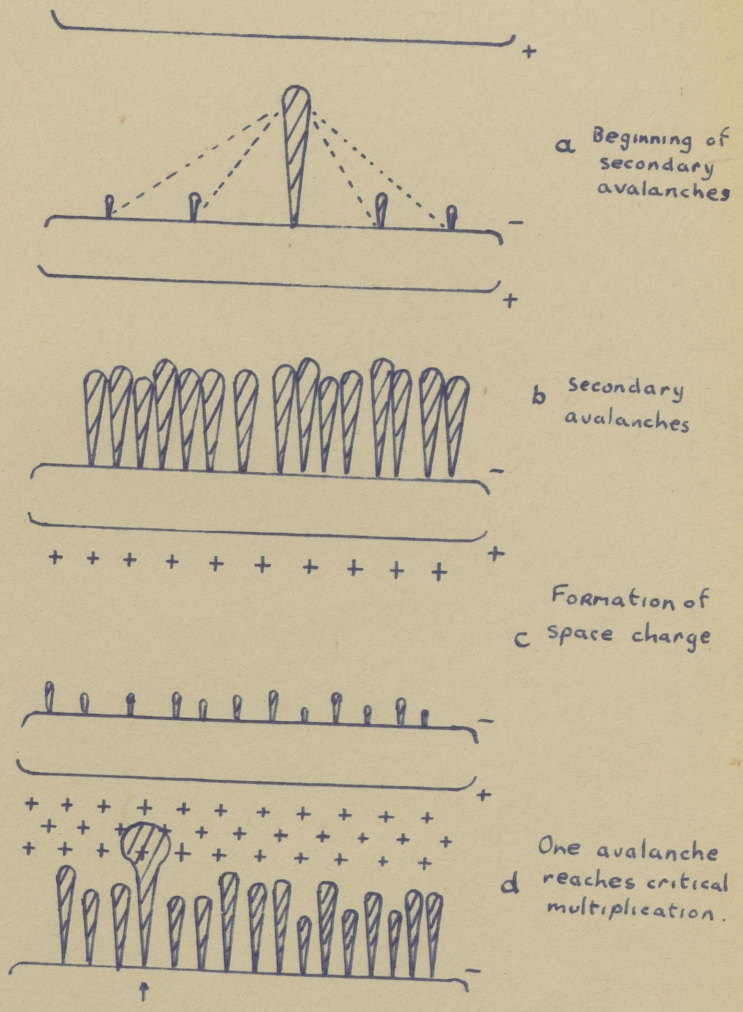

Raether's Schematic Picture of Spark Formation at Static Breakdown

FIG 08-1

attempted to represent a generalized picture of the breakdown interval over a wide range of gas pressure and overvoltage for air. He assumed that the transition from Townsend build-up to a filamentary breakdown channel occurs when the value of αd exceeds a critical value αd given by $(\alpha d)_{crit.} = 17 + \log_e d$.

Fig. D.8.2. shows this critical curve superimposed on the values of αd calculated from recent measurements of breakdown voltage in air. The dotted lines represent roughly the values of overvoltage. From this diagram it can be seen that breakdown conditions represented by points below the $(\alpha d)_{crit.}$ curve represent breakdown in accordance with the Townsend breakdown criterion and the points above the line correspond to breakdown where space charge distortion produces a narrow filamentary breakdown channel or streamer.

This first complete picture predicts that static breakdown in air occurs by a Townsend mechanism for values of pd up to at least 1500 mm Hg cm. As the overvoltage is increased, the value of pd decreases for which the critical condition for streamer breakdown occurs before the Townsend criterion for breakdown.

This suggests that it should be possible, at a given pressure, to observe a transition from one breakdown mechanism to the other as the overvoltage applied is progressively increased.

This evidence has recently been supplied by Kohrmann 1954, who demonstrated a discontinuity in the curve relating formative time lag and overvoltage as shown in Fig. D.8.3.

Although the delay interval of electrical

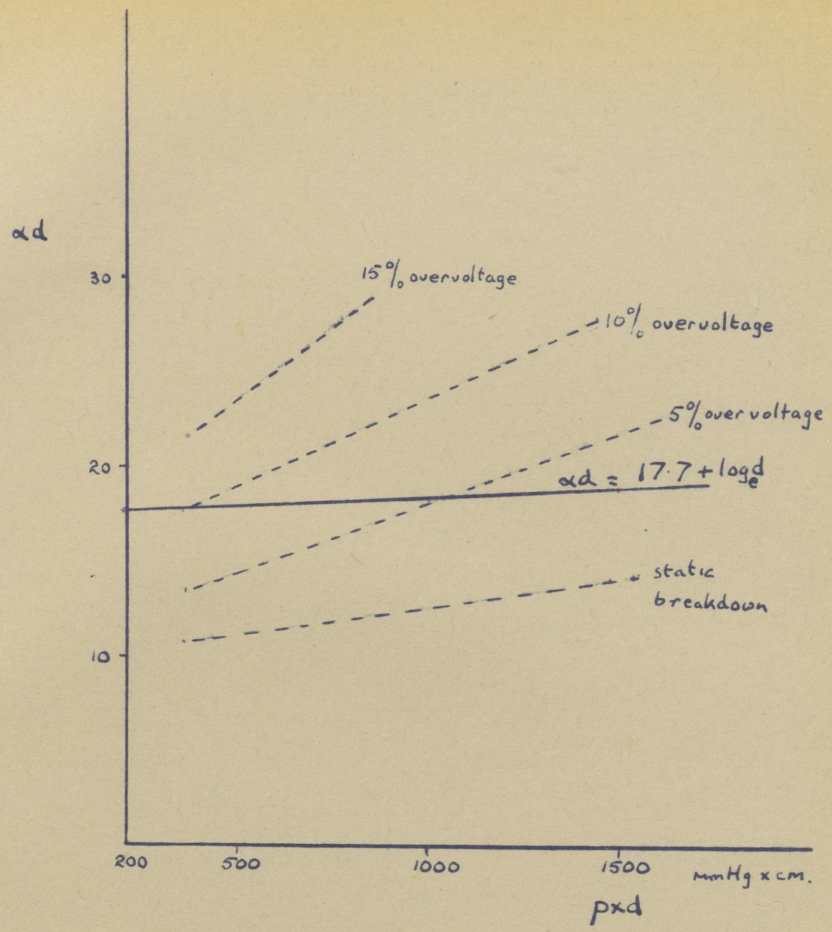

The values of αd at static breakdown and at different overvoltage compared with Raether's value of αd for the onset of critical avanlanche multiplication

Fig D8·2

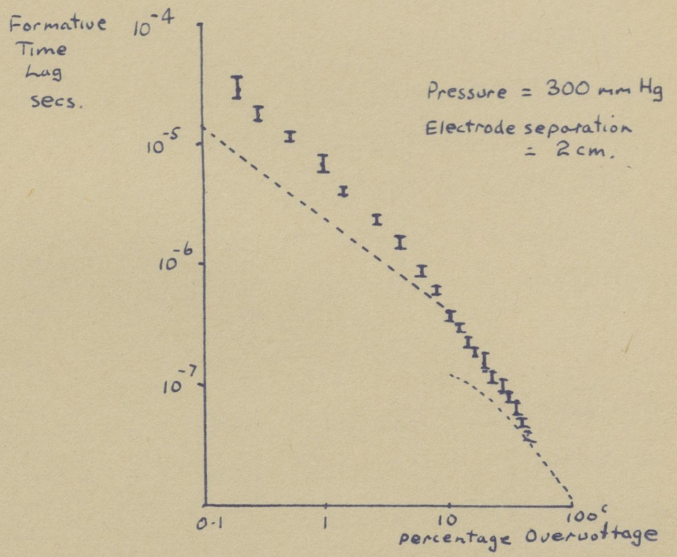

Formative Time Lag as a function of Overvoltage.

(Showing spread of measured values)

FIG D8·3

breakdown in gases is by no means fully understood, it has been shown that during recent years a considerable advance in knowledge has been made. It would appear that the initial current build-up is by a Townsend process involving first and second ionisation coefficients α and γ.

At low pressure the Townsend breakdown criterion is achieved. At high pressure αd may reach a critical value shown on a curve, such as Fig. D.8.2. before the fulfilment of the Townsend criterion. In that case, a narrow filamentary streamer is formed. The form of the curves shown in Fig. D.8.2. may well depend on the nature of the gas since it depends on the relative values of α and γ, which are different for different gases.

By the use of this type of representation of experimental results for various gases, it seems possible that in the near future formative time lags should be capable of prediction for various values of gas, pressure, electrode spacing and overvoltage.

Further studies of the avalanches themselves using for instance the cloud chamber are necessary to provide a physical interpretation of the critical value of αd, of which the Streamer theory was a first attempt.

REFERENCES

		Vol.	Page	Year
Bandel H.W.	Phys.Rev.	95	1117	1954
Beams J.W.	Journ.Franklin Inst.	206	809	1928
Berkey W.E. & Slepian J.	Journ.Appl.Phys.	11	765	1940
Bowls W.E.	Phys.Rev.	53	293	1938
Buss K.	Arch.Elektrotech.	27	35	1933
Crowe R.W. Bragg J.K. & Thomas V.G.	Phys. Rev.	96	10	1954
Dickey F.R.	Journ.Appl.Phys.	23	1336	1952
Dutton J., Haydon S.C., Llewellyn-Jones F. & Davidson P.	Proc.Roy.Soc.A.	218	206	1953
Ditto	Proc.Roy.Soc.A.	213	203	1952
Fisher L.H. & Bederson B.	Phys.Rev.	76	1501	1949
Ditto	Phys.Rev.	78	331	1950
Fisher L.H. & Kachikas G.A.	Phys. Rev.	79	232	1950
Fisher L.H. & Bederson B.	Phys.Rev.	81	109	1951
Fisher L.H. & Kachikas G.A.	Phys.Rev.	88	878	1952
Ditto	Phys.Rev.	91	775	1953
Fletcher R.C.	Phys.Rev.	76	1501	1949
Franck J. & von Hippel A.	Z.f.Physik	57	695	1929
Hale D.H.	Phys.Rev.	54	241	1939
Heymann F.G.	Proc.Phys.Soc.B.	63	25	1950

		Vol.	Page	Year.
Kohrmann W.	Naturwissenschaft	41	400	1954
Lee G.M.	Proc.Inst.Rad.Engrs.	34	121W	1946
Legler W.	Z.Physics	140	221	1955
Llewellyn Jones F.	Proc.Phys.Soc.B.	62	366	1949
Llewellyn Jones F. & Parker A.B.	Proc.Roy.Soc.A.	213	185	1952
Loeb L.B.	Journ.Franklin Inst.	205	305	1928
Loeb L.B. & Meek J.M.	Mechanism of the Electric Spark Stanford University Press			1941
Masch K.	Arch.Elektrotech.	26	587	1932
Mayr O.	Arch.Elektrotech.	24	15	1930
Nielsen R.A.	Phys.Rev.	50	950	1936
Paetow H.	Zeit.F.Phys.	111	770	1939
Posin P.Q.	Phys.Rev.	50	650	1936
Raether H.	Zeit.F.Phys.	107	91	1937
Raether H.	Elektrotech.Z.	63	101	1942
Raether H.	Erg. ex Naturw.	22	73	1949
Raether H.	Z.angew.Phys.	5	211	1953
Raether H.	Z.angew.Phys.	7	50	1955
Rogowski W. Flegler E. & Tamm R.	Arch.Elektrotech.	18	506	1927
Rogowski W.	Arch.Elektrotech.	20	99	1928
Sanders F.H.	Phys.Rev.	44	1020	1933
Schade R.	Z.Phys.	104	487	1937
Schmidt K.J.	Z.Phys.	139	251	1954
Schumann W.O.	Z.Tech.Phys.	11	195	1930
Strigel R.	Elektrische Stosstestigheit J.Springer. Berlin			1939

		Vol.	Page	Year.
Tamm R.	Arch.Elektrotech.	20		1928
Tilles A.	Phys.Rev.	46	1015	1934
Torok J.J.	Trans. A.I.E.E.	47	177	1928
Townsend J.S.	Electricity in Gases Oxford Press			1915
Varney R.N. White H.J. Loeb L.B. & Posin D.Q.	Phys.Rev.	48	818	1935
White H.J.	Phys.Rev.	46	99	1934
Wijsmann	Phys.Rev.	75	833	1949
Wilson R.R.	Phys.Rev.	50	1082	1936

ADDITIONAL NOTES

P.10. Line 8. — For "is" read "should be" (diagram is merely schematic).

P.13. Line 10. — Add "As discussed in section D.5.23. onwards, this representation is of little value for quantitative analysis."

P.25. Line 16 etc. — Replace "ionisation agent - electron volts" by "ionisation agents obey the following rules:-

For photons $h\nu \geqslant e\phi$

For metastable atoms $\frac{1}{2}mv^2 + eV_m \geqslant e\phi$

For positive ions $\frac{1}{2}mv^2 + eV_i \geqslant 2e\phi$

The cathode work function ϕ is usually in the range 4-7 electron volts."

P.26. Line 19. — Omit P.

P.27. Line 22. — For γ_p^{ν} read γ_p.

P.33. Line 11. — For "N and dN" read "N and N + dN".

P.34. Line 16. — For "by an initial electron" read "by the products of an avalanche started by one initial electron".

P.54. Eq.B.5.11.9. — For "x" read "d".

P.65. Line 2. — For "does" read "did appear to"

Fig. D.5.8. — Reverse order of 1,2,3,4. on graph.

P.80. Line 12. — For "electrodes" read "electrons".

Eq.D.5.24.2. — For "+" read "-".

Eq.D.5.24.3. — Add brackets to enclose terms after $\frac{1}{C}$.

P.81. Line 8. — For "parallel" read "series".

P.84. Eq.D.6.2.9. — For "$-i_o$" read "$+i_o$".

Eq.D.6.2.14. — Add ϵ to read: " $\dfrac{1 + \dfrac{\epsilon\, i_-(o,t)}{i_o}}{1 + \epsilon}$ "

P.86. Line 6. — For "The analysis" read "The result of the analysis, i.e. equation D.6.2.15."

P.87. Eq.D.6.6.2. — For = read $\doteq$.

Eq.D.6.6.3. — For = read $\doteq$.